REPORT NO.
UCB/EERC-91/08
AUGUST 1991

EARTHQUAKE ENGINEERING RESEARCH CENTER

A RESPONSE SPECTRUM METHOD FOR MULTIPLE-SUPPORT SEISMIC EXCITATIONS

by

ARMEN DER KIUREGHIAN

ANSGAR NEUENHOFER

Report to the National Science Foundation

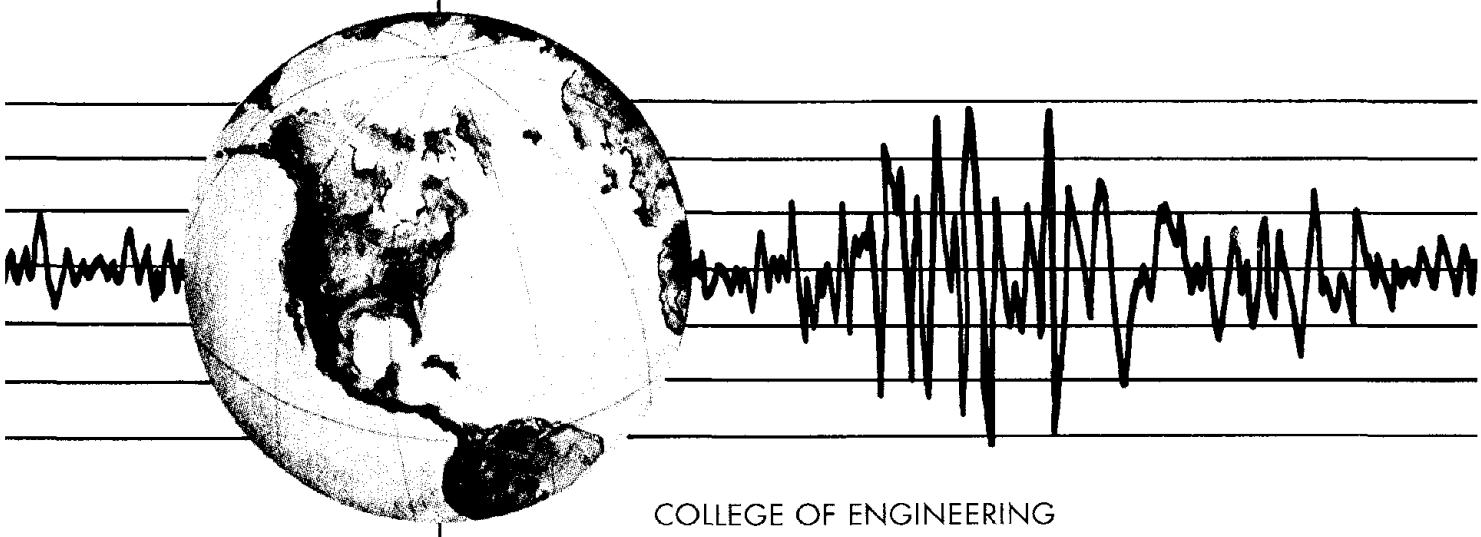

COLLEGE OF ENGINEERING

UNIVERSITY OF CALIFORNIA AT BERKELEY

For sale by the National Technical Information Service, U.S. Department of Commerce, Springfield, Virginia 22161

See back of report for up to date listing of EERC reports.

REPORT DOCUMENTATION PAGE	1. REPORT NO. NSF/ENG-91010	2.	PB93-114536

4. Title and Subtitle

A Response Spectrum Method for Multiple-Support Seismic Excitations

5. Report Date: August 1991

6.

7. Author(s): Armen Der Kiureghian and Ansgar Neuenhofer

8. Performing Organization Rept. No.: UCB/EERC-91/08

9. Performing Organization Name and Address

Earthquake Engineering Research Center
University of California, Berkeley
1301 So. 46th Street
Richmond, Calif. 94804

10. Project/Task/Work Unit No.

11. Contract(C) or Grant(G) No.

(C)

(G) BCS-9011112

12. Sponsoring Organization Name and Address

National Science Foundation
1800 G. Street, N.W.
Washington, D.C. 20550

13. Type of Report & Period Covered

14.

15. Supplementary Notes

16. Abstract (Limit: 200 words)

A new response spectrum method is developed for seismic analysis of linear multi-degree-of-freedom, multiply-supported structures subjected to spatially varying ground motions. Variations of the ground motion due to wave passage, loss of coherency with distance, and variation of local soil conditions are considered. The method is based on fundamental principles of random vibration theory and properly accounts for the effects of correlation between the support motions as well as between the modal responses of the structure.

In the proposed method, the peak response is given in terms of a combination rule involving the peak ground displacements and mean response spectra associated with the support degrees of freedom, and a set of cross-support and cross-mode correlation coefficients that are determined in terms of the individual spectra and the coherency function describing the nature of the spatial variability of the ground motion. Contributions of the pseudo-static and dynamic components of the response, as well as their covariance, are explicitly included in the combination rule. The new method is applied to an example structure with three supports.

A comprehensive analysis of the required cross-correlation coefficients is carried out to investigate the influences of the wave passage and loss of coherency effects, as well as the effect of local site conditions.

17. Document Analysis a. Descriptors

b. Identifiers/Open-Ended Terms

c. COSATI Field/Group

18. Availability Statement: Release Unlimited	19. Security Class (This Report): unclassified	21. No. of Pages: 74
	20. Security Class (This Page): unclassified	22. Price

(See ANSI-Z39.18) *See Instructions on Reverse*

OPTIONAL FORM 272 (4-77)
(Formerly NTIS-35)
Department of Commerce

A RESPONSE SPECTRUM METHOD FOR MULTIPLE-SUPPORT SEISMIC EXCITATIONS

By

Armen Der Kiureghian
and
Ansgar Neuenhofer

A report on research supported by
the National Science Foundation under
Grant No. BCS-9011112

Report No. UCB/EERC-91/08
Earthquake Engineering Research Center
College of Engineering
University of California at Berkeley

August 1991

ABSTRACT

A new response spectrum method is developed for seismic analysis of linear multi-degree-of-freedom, multiply-supported structures subjected to spatially varying ground motions. Variations of the ground motion due to wave passage, loss of coherency with distance, and variation of local soil conditions are considered. The method is based on fundamental principles of random vibration theory and properly accounts for the effects of correlation between the support motions as well as between the modal responses of the structure.

In the proposed method, the peak response is given in terms of a combination rule involving the peak ground displacements and mean response spectra associated with the support degrees of freedom, and a set of cross-support and cross-mode correlation coefficients that are determined in terms of the individual spectra and the coherency function describing the nature of the spatial variability of the ground motion. Contributions of the pseudo-static and dynamic components of the response, as well as their covariance, are explicitly included in the combination rule.

A comprehensive analysis of the required cross-correlation coefficients is carried out to investigate the influences of the wave passage and loss of coherency effects, as well as the effect of local site conditions. It is found that the cross-correlation coefficients involved in the covariance between the pseudo-static and dynamic components of the response are generally small, whereas the cross-correlation coefficients involved in the terms representing the individual components can be significant even for distant supports and well spaced modes.

The new method is applied to an example structure with three supports. The example demonstrates the influence of the spatial variability of the ground motion on selected responses of the structure, and examines the relative contributions of the pseudo-static, dynamic, and their covariance terms to the total response. It is found that in most cases the spatial variability tends to reduce the response (in relation to the case with uniform support motions), often by a significant amount (e.g., by close to 30 percent). However, this rule cannot be generalized since, under certain conditions (i.e., stiff structures and rapid loss of coherency) the response may actually amplify due to an increase in the pseudo-static component of the response. Therefore, a proper accounting of the spatial variability effect in seismic analysis of multiply-supported structures is essential. The response spectrum method developed offers a simple and accurate alternative for this purpose.

ACKNOWLEDGMENT

This study was supported by the National Science Foundation Grant No. BCS-9011112 with Dr. S-C. Liu as Program Director. The second author was supported in part by the German Academic Exchange Service (DAAD) during his studies at the University of California at Berkeley. This support is gratefully acknowledged.

TABLE OF CONTENTS

	page
ABSTRACT	i
ACKNOWLEDGEMENT	ii
TABLE OF CONTENTS	iii
LIST OF TABLES	iv
LIST OF FIGURES	v
1. INTRODUCTION	1
1.1 Background	1
1.2 Objectives and Scope	3
1.3 Organization of Report	4
2. RESPONSE OF MULTIPLY-SUPPORTED STRUCTURE TO DIFFERENTIAL SUPPORT MOTIONS	5
2.1 Introduction	5
2.2 Equations of Motion	5
2.3 Mean-Square of Stationary Response	7
2.4 The Coherency Function	8
3. SIGNIFICANCE OF CROSS-MODAL AND CROSS-SUPPORT CORRELATIONS	12
3.1 Introduction	12
3.2 Cross-Correlation Coefficient Between Ground Displacements at Stations k and l	13
3.3 Cross-Correlation Coefficient Between Ground Displacement at Station k and Oscillator Response at Station l	14
3.4 Cross-Correlation Coefficient Between Responses of Oscillator at Stations k and l	15
3.5 Concluding Remarks	17
4. DEVELOPMENT OF THE RESPONSE SPECTRUM METHOD	31
4.1 Introduction	31
4.2 Mode-and-Support Combination Rule	32
4.3 Power Spectral Density Consistent with Given Mean Response Spectrum	33
4.4 Numerical Example	36
5. EXAMPLE APPLICATION	41
5.1 Introduction	41
5.2 Description of the Example Structure	41
5.3 Description of Support Excitations	42
5.4 Results	43
5.5 Concluding Remarks	45
6. SUMMARY AND CONCLUSIONS	53
6.1 Summary	53
6.2 Conclusions	54
REFERENCES	56
APPENDIX A	59

LIST OF TABLES

		page
Table 3.1	PSD Filter Parameters for Model Soil Types	18
Table 5.1	Modal Frequencies	46
Table 5.2	Effective Influence Factors a_k	46
Table 5.3	Effective Modal Participation Factors b_{ki}	47
Table 5.4	Cross-Correlation Coefficients $\rho_{u_k u_l}$	47
Table 5.5	Cross-Correlation Coefficients $\rho_{u_k s_{lj}}$	48
Table 5.6	Cross-Correlation Coefficients $\rho_{s_{ki} s_{lj}}$	49
Table 5.7	Mean Peak Responses of the "Flexible" Beam	50
Table 5.8	Mean Peak Responses of the "Stiff" Beam	51

LIST OF FIGURES

		page
Figure 2.1	Pair of Oscillators	11
Figure 3.1	PSD's of Ground Acceleration for Three Soil Conditions	19
Figure 3.2	PSD's of Ground Displacement for Three Soil Conditions	19
Figure 3.3	Cross-Correlation Coefficient Between Ground Displacements at Stations k and l	20
Figure 3.4	Cross-Correlation Coefficient Between Ground Displacement at Station k and Response of Oscillator at Station l for Similar Soil Conditions and Wave Direction k to l	21
Figure 3.5	Cross-Correlation Coefficient Between Ground Displacement at Station k and Response of Oscillator at Station l for Similar Soil Conditions and Wave Direction l to k	22
Figure 3.6	Cross-Correlation Coefficient Between Ground Displacement at Station k and Response of Oscillator at Station l for Dissimilar Soil Conditions and Wave Direction k to l	23
Figure 3.7	Cross-Correlation Coefficient Between Ground Displacement at Station k and Response of Oscillator at Station l for Dissimilar Soil Conditions and Wave Direction l to k	24
Figure 3.8	Cross-Correlation Coefficient Between Responses of Oscillators at Stations k and l for Similar Soil Conditions and $d_{kl}^{L}/v_{app} = 0\ sec.$	25
Figure 3.9	Cross-Correlation Coefficient Between Responses of Oscillators at Stations k and l for Similar Soil Conditions and $d_{kl}^{L}/v_{app} = 0.5\ sec.$ with Wave Direction from k to l	26
Figure 3.10	Cross-Correlation Coefficient Between Responses of Oscillators at Stations k and l for Similar Soil Conditions and $d_{kl}^{L}/v_{app} = 0.5\ sec.$ with Wave Direction from l to k	27
Figure 3.11	Cross-Correlation Coefficient Between Responses of Oscillators at Stations k and l for Dissimilar Soil Conditions and $d_{kl}^{L}/v_{app} = 0\ sec.$	28
Figure 3.12	Cross-Correlation Coefficient Between Responses of Oscillators at Stations k and l for Dissimilar Soil Conditions and $d_{kl}^{L}/v_{app} = 0.5\ sec.$ with Wave Direction from k to l	29
Figure 3.13	Cross-Correlation Coefficient Between Responses of Oscillators at Stations k and l for Dissimilar Soil Conditions and $d_{kl}^{L}/v_{app} = 0.5\ sec.$ with Wave Direction from l to k	30

Figure 4.1	Design Relative Displacement Response Spectrum	38
Figure 4.2	Successive Approximations of the Response-Spectrum-Consistent PSD of Ground Acceleration	38
Figure 4.3	First-Order Approximations of the Response-Spectrum-Consistent PSD for Different Values of the Parameter p: (a) Acceleration PSD; (b) Displacement PSD	39
Figure 4.4	Cross-Correlation Coefficient Between Ground Displacements at Stations k and l for Different Values of the Parameter p	40
Figure 5.1	Example Structure	52
Figure 5.2	First Four Mode Shapes of Example Structure	52
Figure 5.3	Influence Vectors for Vertical Support Motions	52

CHAPTER 1
INTRODUCTION

1.1 Background

Observations during recent earthquakes, notably the Loma Prieta earthquake of October 17, 1989, have clearly demonstrated that seismic ground motions can vary significantly over distances which are of the same order of magnitude as the dimensions of some extended structures, such as bridges (Housner et al., 1990). Three phenomena are responsible for these variations: (1) the difference in the arrival times of seismic waves at different stations; (2) the loss of coherency of the motions due to reflections and refractions of the waves in the heterogeneous medium of the ground, as well as due to the difference in the manner of superposition of waves arriving from an extended source at various stations; and (3) the difference in the local soil conditions at each station and the manner in which they influence the amplitude and frequency content of the bedrock motion. Recent analyses with array recordings have shed light on the nature of these effects and their relative importance (Bolt et al., 1982; Loh et al., 1982; Abrahamson and Bolt, 1985; Hao et al., 1989; Harichandran and Vanmarcke, 1986; Loh and Yeh, 1988; Abrahamson et al., 1991).

The effects of differential support motions on the response of extended structures have been investigated for a long time (e.g., Bogdanoff et al., 1965; Johnson and Gallety, 1972; Masri 1976; Werner et al., 1979; Abdel-Ghaffar and Rubin, 1982). It is known that, under realistic conditions, the variations in the support motions can significantly influence the internal forces generated in the structure (e.g., see Abdel-Ghaffar and Rubin, 1982). While in most cases the magnitudes of these forces are reduced, there are situations where the variations in the support motions may result in larger internal forces. The failure of several bridges during the Loma Prieta earthquake has highlighted the need for a better understanding of this phenomenon, and for the development of practical analysis methods that can accurately account for its effects.

Presently, dynamic analysis with spatially varying input motions is performed either by the time history approach, or by the method of random vibrations. For the former approach, one is required to define the input accelerations at the various support points in terms of their complete time histories. These are usually specified by one of three means: (1) selection of a ground motion array previously recorded in a setting similar to the design situation at hand; (2) generation of time histories based on modeling of the seismic source and propagation of waves in an elastic medium; and (3) simulation of time histories based on the random vibration approach. The chief disadvantage of the time history approach is that the results produced from the analysis are specific to the set of selected time histories. Often the results vary significantly when an alternative set of records with equal validity is considered. A further disadvantage is that the analysis requires extensive amounts of computation, thus precluding the possibility of analysis with alternative sets of records.

The random vibration approach is based on a statistical characterization of the set of motions at the support points (Abdel-Ghaffar and Rubin, 1982; Harichandran and Wang, 1988; Zerva, 1990). Typically, stationary analysis is performed and the set of motions are specified in terms of a matrix of auto- and cross-power spectral density functions that define the amplitudes and frequency contents of the motions. The cross-power spectral density for any pair of support motions, which characterizes the cross-correlation between them, is usually defined in terms of the respective auto-power spectral densities and a coherency function. Various theoretical and empirical models of the coherency function have been developed in recent years (Harichandran and Vanmarcke, 1986; Luco and Wong, 1986; Loh and Yeh, 1988; Hao et al., 1989; Abrahamson et al., 1991). The chief advantage of the random vibration approach is that it provides a statistical measure of the response which is not controlled by an arbitrary choice of the input motions. This approach is particularly appealing from the viewpoint of design, where consideration should be given to entire families of potential ground motions at the stations of interest.

While the random vibration approach is appealing for its statistical nature, it is not yet accepted as a method of analysis by practicing engineers. Furthermore, most seismic design codes specify the earthquake motion in terms of the response spectrum and not the power spectral density. Therefore, it is desirable to develop a method of analysis that is based on the response spectrum specification of the input motions, and which accurately accounts for the effects of variation between the support motions. It should be noted that the response spectrum itself is a statistical characterization of the ground motion and, if properly used, it can provide the same level of rigor and accuracy as the random vibration approach with power spectral densities. Furthermore, since a response spectrum inherently includes the effect of nonstationarity of the earthquake motion, the approach with the response spectrum is superior to the conventional random vibration approach that is based on a strict assumption of stationarity.

Several attempts have been made at developing a response spectrum method for multiply supported structures. In one study several ad hoc combination rules have been investigated by comparing with time-history results (Dong and Wieland, 1988). In another study, the support motions have been grouped into independent subgroups with perfect correlation between the members of each subgroup (Yamamura and Tanaka, 1990). A more refined method has been suggested by Berrah and Kausel (1989), where the spectrum at each support point is adjusted in account of the spatial variability effect arising from the incoherence alone. However, they do not consider the contribution of the pseudo-static component and its cross-correlation with the dynamic response.

1.2 Objectives and Scope

In this report, a new response spectrum method is developed, which properly accounts for the effects of variability in the support motions that arises from the wave passage effect, the incoherence effect, as well as the effects of the local soil conditions. The method is based on the principles of random vibration theory and accurately accounts for the cross-correlations between the support motions as well as the modes of vibration of the structure. The combination rule for the mean of the peak response is of the form

$$\mathrm{E}[\max|z(t)|] = \Bigg[\sum_{k=1}^{m}\sum_{l=1}^{m} a_k a_l \rho_{u_k u_l} u_{k,\max} u_{l,\max} + 2\sum_{k=1}^{m}\sum_{l=1}^{m}\sum_{j=1}^{n} a_k b_{lj} \rho_{u_k s_{lj}} u_{k,\max} D_l(\omega_j,\zeta_j) + \sum_{k=1}^{m}\sum_{l=1}^{m}\sum_{i=1}^{n}\sum_{j=1}^{n} b_{ki} b_{lj} \rho_{s_{ki} s_{lj}} D_k(\omega_i,\zeta_i) D_l(\omega_j,\zeta_j) \Bigg]^{1/2} \tag{1.1}$$

in which a_k and b_{ki} are structure-dependent effective influence and modal participation factors, respectively, $u_{k,\max}$ denotes the peak ground displacement at station k, $D_k(\omega_i,\zeta_i)$ denotes the ordinate of the response spectrum at the support degree of freedom k for the frequency and damping of mode i, and $\rho_{u_k u_l}$, $\rho_{u_k s_{lj}}$, and $\rho_{s_{ki} s_{lj}}$ are cross-correlation coefficients between the support motions and the modes of the structure. The first term inside brackets with summations over the support degrees of freedom represents the pseudo-static component of the response, the third term with summations over the support degrees of freedom and the modes of the structure represents the dynamic component, and the second term represents the contribution arising from the covariance between the pseudo-static and dynamic components. Much of the present report is devoted to the derivation of the above formula and to a comprehensive understanding of the nature of the coefficients $\rho_{u_k u_l}$, $\rho_{u_k s_{lj}}$ and $\rho_{s_{ki} s_{lj}}$. As will be shown later, these coefficients are all computed directly in terms of the known peak ground displacements and the response spectra at the various support points, as well as an estimate of the duration of motion. No other information is necessary for the application of the proposed response spectrum method.

The response spectrum method presented here is accurate, since it is based on fundamental concepts of the random vibration theory, and it is simple since it employs a simple combination rule in terms of the peak ground displacement and the response spectrum at each support point. The method avoids costly and questionable analysis by time histories, and circumvents the random vibration approach that is not common in the engineering practice and suffers from the assumption of stationarity. Most importantly, the method is practical, since it employs information (i.e., peak ground displacements and response spectra at each support point, an estimate of the duration of motion, and the

coherency function) that is commonly available in seismic design applications.

1.3 Organization of the Report

Following this introductory chapter, Chapter 2 deals with the development of the equations of motion and the stationary random vibration analysis of multi-degree-of-freedom structures subjected to differential support motions. This chapter also includes a discussion of the coherency function and the manner in which it describes the effects of wave passage and incoherence. Chapter 3 presents a comprehensive parametric study of the coefficients $\rho_{u_k u_l}$, $\rho_{u_k s_{lj}}$ and $\rho_{s_{ki} s_{lj}}$. General trends and conclusions are derived with respect to the significance and range of applicability of these coefficients. Chapter 4 presents the development of the response spectrum method. The focus of this chapter is on deriving the combination rule in Eq. 1.1 based on the random vibration formulation of Chapter 2, and on developing a method for computing the correlation coefficients $\rho_{u_k u_l}$, $\rho_{u_k s_{lj}}$ and $\rho_{s_{ki} s_{lj}}$ in terms of the known peak ground displacements and response spectra. In the course of this development, an improved method for generating a power spectral density consistent with a given response spectrum is presented. Chapter 5 presents an application of the proposed response spectrum method for an example structure. The structure is a two span continuous beam with $50\,m$ per span and two alternative fundamental periods. Selected responses of the beam are computed for different assumptions regarding the nature of the variation between the support motions. All three components of the response, i.e., the pseudo-static, dynamic, and their cross-covariance, are separately listed, thus showing the influence of each form of spatial variability on each component of the response. General observations and conclusions are derived from this example. Finally, Chapter 6 presents a summary of the report and the main conclusions and results of the study.

CHAPTER 2
MDOF RESPONSE TO DIFFERENTIAL SUPPORT MOTIONS

2.1 Introduction

In this chapter, a formulation for the stationary response of multi-degree-of-freedom systems with multiple supports and subjected to spatially varying ground motions is developed. While such a formulation is not new, in the present analysis it is cast in a new form that permits useful interpretation of the terms involved in the expression for the mean-square response, which then allows the development of the response spectrum method in Chapter 4. The derivations in this chapter, hence, are fundamental to the response spectrum method to be developed.

2.2 Equations of Motion

The equations of motion for a discretized, n-degree-of-freedom linear system subjected to m support motions can be written in the matrix form (Clough and Penzien 1975)

$$\begin{bmatrix} \mathbf{M} & \mathbf{M}_c \\ \mathbf{M}_c^{\mathrm{T}} & \mathbf{M}_g \end{bmatrix} \begin{Bmatrix} \ddot{\mathbf{x}} \\ \ddot{\mathbf{u}} \end{Bmatrix} + \begin{bmatrix} \mathbf{C} & \mathbf{C}_c \\ \mathbf{C}_c^{\mathrm{T}} & \mathbf{C}_g \end{bmatrix} \begin{Bmatrix} \dot{\mathbf{x}} \\ \dot{\mathbf{u}} \end{Bmatrix} + \begin{bmatrix} \mathbf{K} & \mathbf{K}_c \\ \mathbf{K}_c^{\mathrm{T}} & \mathbf{K}_g \end{bmatrix} \begin{Bmatrix} \mathbf{x} \\ \mathbf{u} \end{Bmatrix} = \begin{Bmatrix} \mathbf{0} \\ \mathbf{F} \end{Bmatrix} \tag{2.1}$$

where $\mathbf{x} = [x_1, \ldots, x_n]^{\mathrm{T}}$ is the n-vector of (total) displacements at the unconstrained degrees of freedom; $\mathbf{u} = [u_1, \ldots, u_m]^{\mathrm{T}}$ is the m-vector of prescribed support displacements; $\mathbf{M}$, $\mathbf{C}$ and $\mathbf{K}$ are the $n \times n$ mass, damping and stiffness matrices associated with the unconstrained degrees of freedom, respectively; $\mathbf{M}_g$, $\mathbf{C}_g$ and $\mathbf{K}_g$ are the $m \times m$ matrices associated with the support degrees of freedom; $\mathbf{M}_c$, $\mathbf{C}_c$ and $\mathbf{K}_c$ are the $n \times m$ coupling matrices associated with both sets of degrees of freedom; and $\mathbf{F}$ is the m-vector of reacting forces at the support degrees of freedom. Both $\mathbf{x}$ and $\mathbf{u}$ may contain translational as well as rotational components.

In the analysis of such systems, it is common to decompose the response into pseudo-static and dynamic components. Following the conventional procedure (Clough and Penzien 1975), we define

$$\mathbf{x} = \mathbf{x}^s + \mathbf{x}^d \tag{2.2}$$

where the pseudo-static component, $\mathbf{x}^s$, is the solution to Eq. 2.1 when the inertia and damping terms are discarded, and is given by

$$\mathbf{x}^s = -\mathbf{K}^{-1}\mathbf{K}_c\,\mathbf{u} = \mathbf{R}\,\mathbf{u} \tag{2.3}$$

in which $\mathbf{R} = -\mathbf{K}^{-1}\mathbf{K}_c$ is denoted the influence matrix. Substituting Eqs. 2.2 and 2.3 in Eq. 2.1, the dynamic component of the response is obtained in the differential form

$$\mathbf{M}\ddot{\mathbf{x}}^d + \mathbf{C}\dot{\mathbf{x}}^d + \mathbf{K}\mathbf{x}^d = -(\mathbf{M}\mathbf{R} + \mathbf{M}_c)\ddot{\mathbf{u}} - (\mathbf{C}\mathbf{R} + \mathbf{C}_c)\dot{\mathbf{u}}$$

$$\approx -(\mathbf{MR}+\mathbf{M}_c)\,\ddot{\mathbf{u}} \tag{2.4}$$

where the right-hand side is approximated by neglecting the damping forces, which are usually much smaller than the corresponding inertia forces on the same side. This approximation is exact when the damping matrix is proportional to the stiffness matrix. It is noted that $\mathbf{M}_c = \mathbf{0}$ if a lumped mass model is used.

To formulate a response spectrum method, it is necessary to employ the normal mode approach. Let $\mathbf{\Phi}=[\boldsymbol{\phi}_1 \cdots \boldsymbol{\phi}_n]$, ω_i and ζ_i, $i=1,\cdots,n$, denote the modal matrix, natural frequencies and modal damping ratios of the structure with its support points fixed. Using the transformation $\mathbf{x}^d = \mathbf{\Phi}\,\mathbf{y}$, $\mathbf{y}=[y_1,\cdots,y_n]^{\mathrm{T}}$, in Eq. 2.4 and employing the orthogonality of the mode shapes (assuming proportional damping), the decoupled equations of motion are obtained

$$\ddot{y}_i + 2\zeta_i\omega_i\dot{y}_i + \omega_i^2 y_i = \sum_{k=1}^{m} \beta_{ki}\,\ddot{u}_k(t) \quad i=1,\cdots,n \tag{2.5}$$

where the index k denotes the degrees of freedom associated with the prescribed support motions, the subscript i denotes the mode number, and β_{ki} is the modal participation factor given by

$$\beta_{ki} = -\frac{\boldsymbol{\phi}_i^{\mathrm{T}}(\mathbf{M}\mathbf{r}_k + \mathbf{M}_c\mathbf{i}_k)}{\boldsymbol{\phi}_i^{\mathrm{T}}\mathbf{M}\boldsymbol{\phi}_i} \tag{2.6}$$

where $\mathbf{r}_k$ is the k-th column of $\mathbf{R}$ and $\mathbf{i}_k$ is the k-th column of an $m \times m$ identity matrix. It is convenient to define a normalized modal response $s_{ki}(t)$, representing the response of a single-degree-of-freedom oscillator of unit mass, frequency ω_i and damping ζ_i, which is subjected to the base motion $u_k(t)$. From Eq. 2.5, $s_{ki}(t)$ satisfies the equation

$$\ddot{s}_{ki} + 2\zeta_i\omega_i\dot{s}_{ki} + \omega_i^2 s_{ki} = \ddot{u}_k(t) \tag{2.7}$$

Obviously, $y_i(t) = \sum_{k=1}^{m} \beta_{ki}\, s_{ki}(t)$.

A generic response quantity of interest, $z(t)$ (e.g., a nodal displacement, an internal force, stress or strain component), in general can be expressed as a linear function of the nodal displacements $\mathbf{x}$, i.e.,

$$z(t) = \mathbf{q}^{\mathrm{T}}\mathbf{x}(t) = \mathbf{q}^{\mathrm{T}}[\mathbf{x}^s(t) + \mathbf{x}^d(t)] \tag{2.8}$$

where $\mathbf{q}$ is a response transfer vector which usually depends on the geometry and stiffness properties of the structure. Substituting for the pseudo-static component of $\mathbf{x}$ from Eq. 2.3 and for the dynamic component in terms of the normalized modal responses, the generic response $z(t)$ is written as

$$z(t) = \sum_{k=1}^{m} a_k u_k(t) + \sum_{k=1}^{m}\sum_{i=1}^{n} b_{ki} s_{ki}(t) \tag{2.9}$$

in which

$$a_k = \mathbf{q}^{\mathrm{T}}\mathbf{r}_k \qquad k=1,\ldots,m \tag{2.10}$$

$$b_{ki} = \mathbf{q}^{\mathrm{T}}\boldsymbol{\phi}_i\beta_{ki} \qquad k=1,\ldots,m;\quad i=1,\ldots,n \tag{2.11}$$

are denoted effective influence coefficients and effective modal participation factors, respectivcly. It is important to note that a_k and b_{ki} are functions only of the structural properties, and that $s_{ki}(t)$ is dependent only on the i-th modal frequency and damping ratio and the k-th input motion. Clearly, the first sum on the right-hand side of Eq. 2.9 represents the pseudo-static component of the response and the double-sum term represents the dynamic component.

2.3 Mean-Square of Stationary Response

The response spectrum formulation to be developed is based on elementary notions of the random vibration theory. Towards that cnd, we assume that the support motions $u_k(t)$ are jointly stationary processes with zero means, and that the response in each mode of the structure is also stationary. These assumptions are reasonable for the intended purpose, as long as the fundamental period of vibration of the structure is short in relation to the duration of excitation. The stationarity assumption will be relaxed later when the response spectrum method is developed.

Using Eq. 2.9, the power spectral density of the generic response can be written in the form

$$G_{zz}(\omega) = \sum_{k=1}^{m}\sum_{l=1}^{m} a_k a_l G_{u_k u_l}(\mathrm{i}\omega) + 2\sum_{k=1}^{m}\sum_{l=1}^{m}\sum_{j=1}^{n} a_k b_{lj}\, H_j(-\mathrm{i}\omega)\, G_{u_k \ddot{u}_l}(\mathrm{i}\omega)$$

$$+ \sum_{k=1}^{m}\sum_{l=1}^{m}\sum_{i=1}^{n}\sum_{j=1}^{n} b_{ki} b_{lj}\, H_i(\mathrm{i}\omega)\, H_j(-\mathrm{i}\omega)\, G_{\ddot{u}_k \ddot{u}_l}(\mathrm{i}\omega) \tag{2.12}$$

in which $G_{xy}(\mathrm{i}\omega)$ denotes the cross-power spectral density of processes x and y, $\mathrm{i}=(-1)^{1/2}$ is the imaginary unit, and $H_i(\mathrm{i}\omega) = [\omega_i^2 - \omega^2 + 2\mathrm{i}\zeta_i\omega_i\omega]^{-1}$ represents the frequency response function of mode i. Integrating over the frequency domain $-\infty < \omega < \infty$, the mean-square response is obtained

$$\sigma_z^2 = \sum_{k=1}^{m}\sum_{l=1}^{m} a_k a_l \rho_{u_k u_l}\sigma_{u_k}\sigma_{u_l} + 2\sum_{k=1}^{m}\sum_{l=1}^{m}\sum_{j=1}^{n} a_k b_{lj}\, \rho_{u_k s_{lj}}\sigma_{u_k}\sigma_{s_{lj}}$$

$$+ \sum_{k=1}^{m}\sum_{l=1}^{m}\sum_{i=1}^{n}\sum_{j=1}^{n} b_{ki} b_{lj}\, \rho_{s_{ki} s_{lj}}\sigma_{s_{ki}}\sigma_{s_{lj}} \tag{2.13}$$

in which σ_{u_k} and $\sigma_{s_{ki}}$ are the root-mean-squares of the ground displacement $u_k(t)$ and the normalized modal response $s_{ki}(t)$, respectively. These are given by the integrals

$$\sigma_{u_k}^2 = \int_{-\infty}^{\infty} G_{u_k u_k}(\omega)\, d\omega \tag{2.14}$$

$$\sigma_{s_{ki}}^2 = \int_{-\infty}^{\infty} |H_i(\mathrm{i}\omega)|^2 \, G_{\ddot{u}_k \ddot{u}_k}(\omega) d\omega \tag{2.15}$$

in which $G_{u_k u_k}(\omega)$ and $G_{\ddot{u}_k \ddot{u}_k}(\omega)$ are the real-valued power spectral densities of the ground displacement and acceleration processes, respectively. The terms $\rho_{u_k u_l}$, $\rho_{u_k s_{lj}}$ and $\rho_{s_{ki} s_{lj}}$ in Eq. 2.13 are cross-correlation coefficients defined by

$$\rho_{u_k u_l} = \frac{1}{\sigma_{u_k} \sigma_{u_l}} \int_{-\infty}^{\infty} G_{u_k u_l}(\mathrm{i}\omega) d\omega \tag{2.16}$$

$$\rho_{u_k s_{lj}} = \frac{1}{\sigma_{u_k} \sigma_{s_{lj}}} \int_{-\infty}^{\infty} H_j(-\mathrm{i}\omega) G_{u_k \ddot{u}_l}(\mathrm{i}\omega) d\omega \tag{2.17}$$

$$\rho_{s_{ki} s_{lj}} = \frac{1}{\sigma_{s_{ki}} \sigma_{s_{lj}}} \int_{-\infty}^{\infty} H_i(\mathrm{i}\omega) \, H_j(-\mathrm{i}\omega) G_{\ddot{u}_k \ddot{u}_l}(\mathrm{i}\omega) d\omega \tag{2.18}$$

Each of the above integrands has an antisymmetric imaginary part and, hence, all three integrals have real values.

The correlation coefficients in Eqs. 2.16-2.18 can be interpreted in terms of a pair of oscillators, representing modes i and j of the structure, which are respectively subjected to the support motions $u_k(t)$ and $u_l(t)$, as shown in Fig. 2.1. Specifically, $\rho_{u_k u_l}$ denotes the cross-correlation coefficient between the two support displacements (at the same time instant), $\rho_{u_k s_{lj}}$ denotes the cross-correlation coefficient between the displacement at support k and the response of the oscillator at support l, and $\rho_{s_{ki} s_{lj}}$ denotes the cross-correlation coefficient between the responses of the two oscillators. These coefficients incorporate all the effects of cross-modal and cross-support correlations that arise in the response of the structure to the spatially varying ground motions. Their evaluation requires the definition of the cross-power spectral densities in Eqs. 2.16-2.18, which is described in the following section.

2.4 The Coherency Function

Three distinct phenomena are responsible for the spatial variations of seismic ground motions. The first is the finite nature of the seismic wave velocities, which leads to different arrival times of the waves at stations located apart. This effect is denoted hereafter as the "wave passage effect." The second is a result of propagation of the waves in a complex heterogeneous medium with numerous reflections and refractions, as well as the result of signals from different parts of a finite source superimposing differently at each station. This effect is denoted hereafter as the "incoherence effect." The third is the effect of the local soil conditions, which can strongly influence the propagation of the motions

from the bedrock to the ground surface at each station, as was clearly observed during the Loma Prieta earthquake of 1989. These variations in the ground motion from point to point, which in general are random in nature, are best characterized by the cross-power spectral density of ground accelerations, $G_{\ddot{u}_k\ddot{u}_l}(\mathrm{i}\omega)$. The coherency function is a normalized version of this function, defined by

$$\gamma_{kl}(\mathrm{i}\omega) = \frac{G_{\ddot{u}_k\ddot{u}_l}(\mathrm{i}\omega)}{[G_{\ddot{u}_k\ddot{u}_k}(\omega)\, G_{\ddot{u}_l\ddot{u}_l}(\omega)]^{1/2}} \tag{2.19}$$

In general, $\gamma_{kl}(\mathrm{i}\omega)$ is Hermitian with an even real part and an odd imaginary part, and it has a bounded modulus, $-1 \le |\gamma_{kl}(\mathrm{i}\omega)| \le 1$ (Lin 1967). One may write

$$\gamma_{kl}(\mathrm{i}\omega) = |\gamma_{kl}(\mathrm{i}\omega)| \exp[\,\mathrm{i}\theta_{kl}(\omega)] \tag{2.20}$$

where

$$\theta_{kl}(\omega) = \tan^{-1} \frac{\mathrm{Im}\, \gamma_{kl}(\mathrm{i}\omega)}{\mathrm{Re}\, \gamma_{kl}(\mathrm{i}\omega)} \tag{2.21}$$

It can be shown that the two terms on the right-hand side of Eq. 2.20 characterize the first two distinct phenomena mentioned above: the term $\exp[\mathrm{i}\theta_{kl}(\omega)]$ characterizes the wave passage effect with $\theta_{kl}(\omega)$ denoting the phase angle between the two stations for waves of frequency ω, whereas the real function $|\gamma_{kl}(\mathrm{i}\omega)|$ characterizes the incoherence effect. Various theoretical and empirical models of the coherency function have been developed in recent years (e.g., Luco and Wang, 1986; Abrahamson et al., 1991). For the purpose of the numerical investigations in this work, we adopt the model

$$\gamma_{kl} = \exp\left[-\left(\frac{\alpha\omega d_{kl}}{v_s}\right)^2\right] \exp\left(\mathrm{i}\,\frac{\omega d_{kl}^L}{v_{app}}\right) \tag{2.22}$$

in which α is an incoherence factor, d_{kl} denotes the horizontal distance between stations k and l, d_{kl}^L denotes the projected horizontal distance in the longitudinal direction of wave propagation, v_s is the shear wave velocity of the medium, and v_{app} is the surface apparent wave velocity. As can be seen, this model assumes increasing incoherence with increasing frequency or distance between the stations, and considers the phase angle as a linear function of the frequency. Empirical coherency functions developed from the SMART-1 array data indicate similar trends for real earthquake records (Harichandran and Vanmarcke, 1986; Abrahamson et al., 1991). While the method developed here is not restricted to any particular form of the coherency function, the above model is used throughout the study because of its simplicity and its frequent use by other investigators (Luco and Wang, 1986; Zerva, 1990, 1991).

Employing Eq. 2.19, the cross-power spectral density of the ground accelerations at stations k and l is written as

$$G_{\ddot{u}_k\ddot{u}_l}(i\omega) = \gamma_{kl}(i\omega)\,[G_{\ddot{u}_k\ddot{u}_k}(\omega)\,G_{\ddot{u}_l\ddot{u}_l}(\omega)]^{1/2} \tag{2.23}$$

Furthermore, using a well known relation for the power spectral density of a derivative process, the two remaining cross-power spectral densities required in Eqs. 2.16 and 2.17 are written as

$$G_{u_k\ddot{u}_l}(i\omega) = -\omega^{-2}\,\gamma_{kl}(i\omega)[G_{\ddot{u}_k\ddot{u}_k}(\omega)\,G_{\ddot{u}_l\ddot{u}_l}(\omega)]^{1/2} \tag{2.24}$$

$$G_{u_k u_l}(i\omega) = \omega^{-4}\,\gamma_{kl}(i\omega)[G_{\ddot{u}_k\ddot{u}_k}(\omega)\,G_{\ddot{u}_l\ddot{u}_l}(\omega)]^{1/2} \tag{2.25}$$

It is evident that once the coherency function $\gamma_{kl}(i\omega)$ is specified, the required cross-power spectral densities for computing the cross-correlation coefficients in Eqs. 2.16-2.18 are completely described in terms of the auto-power spectral densities, $G_{\ddot{u}_k\ddot{u}_k}(\omega)$ and $G_{\ddot{u}_l\ddot{u}_l}(\omega)$, of the acceleration processes at the two stations. The shapes of the latter functions, in turn, describe the influences of the local soil conditions at the two stations.

In conclusion, the set of auto-power spectral densities of the ground acceleration at each support degree of freedom and the coherency functions for each pair of stations is a complete characterization of the input motions for the analysis of multiply-supported structures. This characterization incorporates all the required information on the spatial variabilities due to the effects of wave passage, incoherence, and local soil conditions. In practice, while a different power spectral density shape may be assigned to each station consistent with its soil conditions, a single coherency model may have to be used for an entire region (regardless of the local soil conditions) because more detailed information may not be available.

It is important to note that the subscripts k and l in the above formulation refer to the support degrees of freedom and not to the support points themselves. Most generally one has three translational degrees of freedom (normally two horizontal and one vertical) and three rotational degrees of freedom at each support. The formulation presented here is general and can account for all the components of the ground motion at each support point, including their cross-correlations. While the cross-correlation between different components of ground motion at a single station have been investigated (Penzien and Watabe, 1975), unfortunately the cross-correlation between different components at different stations (e.g., the horizontal component at one station and the vertical component at another station) has not been evaluated for the available array recordings. The present work clearly demonstrates the need for such a study in the future.

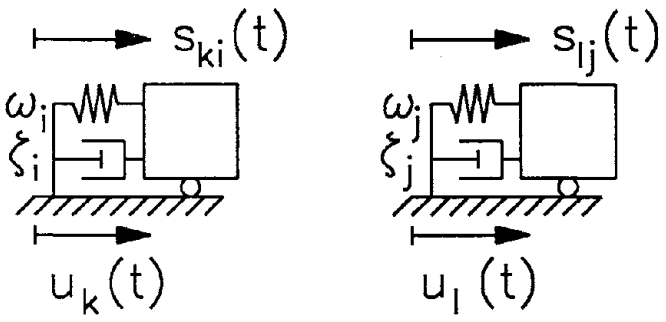

Figure 2.1 Pair of Oscillators

CHAPTER 3

SIGNIFICANCE OF CROSS-MODAL AND CROSS-SUPPORT CORRELATIONS

3.1 Introduction

In this chapter we investigate the significance of the cross-modal and cross-support correlation coefficients $\rho_{u_k u_l}$, $\rho_{u_k s_{lj}}$ and $\rho_{s_{ki} s_{lj}}$ defined by Eqs. 2.16-2.18 of Chapter 2. The purpose is to determine the influence of various model parameters on each of these coefficients, and to evaluate the significance of the cross terms involved in each of the sums in the combination rule of Eq. 2.13.

As a basic model for the power spectral density of ground acceleration, we consider the well known Kanai-Tajimi model defined by

$$G_{\ddot{u}_k \ddot{u}_k}(\omega) = G_{kk} \frac{\omega_{fk}^4 + 4\zeta_{fk}^2 \omega_{fk}^2 \omega^2}{(\omega_{fk}^2 - \omega^2)^2 + 4\zeta_{fk}^2 \omega_{fk}^2 \omega^2} \tag{3.1}$$

where G_{kk} is a scale factor and ω_{fk} and ζ_{fk} are the filter parameters respectively representing the natural frequency and damping of the soil layer at the k-th station. It is well known, however, that this model is inadequate to describe the ground displacement, as it yields infinite power for the displacement process as ω approaches zero. To correct this, Clough and Penzien (1975) suggested introducing a second filter to modify the form to

$$G_{\ddot{u}_k \ddot{u}_k}(\omega) = G_{kk} \frac{\omega_{fk}^4 + 4\zeta_{fk}^2 \omega_{fk}^2 \omega^2}{(\omega_{fk}^2 - \omega^2)^2 + 4\zeta_{fk}^2 \omega_{fk}^2 \omega^2} \frac{\omega^4}{(\omega_{gk}^2 - \omega^2)^2 + 4\zeta_{gk}^2 \omega_{gk}^2 \omega^2} \tag{3.2}$$

where ω_{gk} and ζ_{gk} are the parameters for the second filter. For $\omega_{gk} \ll \omega_{fk}$, the second filter influences the power spectral density shape only in the region of very low frequencies, since the second quotient quickly approaches unity with increasing ω. For $\omega \to 0$, the above power spectral density is of order ω^4, which implies a finite power for the ground displacement.

To investigate sites with "firm", "medium" and "soft" soils, we consider the values of the filter parameters listed in Table 3.1. These values produce reasonable power spectral density shapes of the ground acceleration for the three different soil conditions, as shown in Fig. 3.1. For example, the power spectral density for the soft soil indicates a relatively narrow-band process with a predominant period of 1.25 seconds, which might be representative of deep alluvium sites, such as parts of Mexico City. The spectral shape for the firm ground is broad banded and contains significant contributions from higher frequencies. The corresponding power spectral densities for the ground displacement are shown in Fig. 3.2. As expected, the power in the displacement process is concentrated in the low frequencies. These spectral shapes are strongly influenced by the parameters of the second filter.

For the coherency function, we assume the model in Eq. 2.22, with the assumption that v_s and v_{app} are some kind of "average" values for each pair of stations k and l or for the entire region. For the parametric studies, we consider ranges of values of the quantities $\alpha d_{kl}/v_s$ and d_{kl}^L/v_{app}. Based on reported values of α and α/v_s (Luco and Wong, 1986; Zerva, 1990), and considering a reasonable range of distances between stations that might be of engineering interest, the parameter $\alpha d_{kl}/v_s$ is varied between 0 and $0.5\,s$ (in some cases up to $2.0\,s$), and d_{kl}^L/v_{app} is varied between 0.0 and $1.0\,s$. The physical significance of these ranges will be discussed shortly.

In the following sections, we investigate each of the three cross-correlation coefficients required in Eq. 2.13 for the auto-power spectral density and coherency models described above.

3.2 Cross-Correlation Coefficient Between Ground Displacements at Stations k and l

Figure 3.3 shows plots of the cross-correlation coefficient $\rho_{u_k u_l}$ for the ground displacements at two stations k and l for sites with firm, medium and soft soil conditions and for $0 \le \alpha d_{kl}/v_s \le 2$ and $d_{kl}^L/v_{app} = 0.0$, 0.5 and 1.0. The curves in Figs. 3.3a-c are for identical soil conditions at the two stations, whereas those in Figs. 3.3d-f are for dissimilar soil conditions. The cases with $\alpha d_{kl}/v_s = 0$ neglect the incoherence effect, whereas the cases with $d_{kl}^L/v_{app} = 0$ neglect the wave passage effect.

In Figs. 3.3a-c with identical site conditions, it is clear that the correlation coefficient is consistently smaller for firmer soil conditions. This is because for firmer grounds the displacement process is richer in the higher frequency components, and waves with such frequencies tend to lose coherency faster than long-period waves do. Both the incoherence and the wave passage effect reduce the value of the correlation coefficient. As will be shown shortly, this is not necessarily the case with the effect of wave passage on cross-correlation coefficients $\rho_{u_k s_{lj}}$ and $\rho_{s_{ki} s_{lj}}$.

The behavior in Figs. 3.3d-f for dissimilar soil conditions at the two sites is similar to those observed in Figs. 3.3a-c. One noteworthy point is that in this case even with $\alpha d_{kl}/v_s = 0$ and $d_{kl}^L/v_{app} = 0$ (Fig. 3.3d) there is lack of perfect correlation between the two motions. This is due to the difference in the power spectral density shapes of the motions at the two sites with different soil conditions.

The results in Fig. 3.3 which include the wave passage effect (i.e., Figs. 3.3b, c, e and f) are for the waves arriving first at station k and then station l. Reversing this direction (i.e., replacing d_{kl}^L by $-d_{kl}^L$) only changes the sign of the imaginary part of the coherency function (Eq. 2.22) or the cross-power spectral density function $G_{u_k u_l}(i\omega)$ in Eq. 2.16. Since the imaginary part of this function is anti-symmetric, this change does not affect the integral in Eq. 2.16 and $\rho_{u_k u_l}$ remains unchanged with the reversal in the direction of wave passage. This lack of dependence on the direction of wave passage does not apply to the coefficients $\rho_{u_k s_{lj}}$ and $\rho_{s_{ki} s_{lj}}$, due to the presence of the complex frequency

response function $H_i(i\omega)$ in Eqs. 2.17 and 2.18.

In typical applications the value of $\alpha d_{kl}/v_s$ is usually quite small, e.g., for $\alpha = 0.5$, $d_{kl} = 500\,m$ and $v_s = 500\,m/s$, $\alpha d_{kl}/v_s = 0.5$. Also the parameter d_{kl}^L/v_{app} describing the wave passage effect can be small; for example, it is zero for vertically propagating waves where $v_{app} = \infty$. It follows that, for realistic values of the parameters, the correlation between the ground displacements can be large. Thus, under typical conditions, one cannot neglect the contributions of the cross terms in the first sum of Eq. 2.13, which represents the pseudo-static component of the response.

3.3 Cross-Correlation Coefficient Between Ground Displacement at Station k and Oscillator Response at Station l

The cross-correlation coefficient $\rho_{u_k s_{lj}}$ is a function of the oscillator frequency ω_j and damping ratio ζ_j and the parameters defining the coherency function and the site conditions at stations k and l. Figs. 3.4-3.7 show plots of this function against ω_j for $\zeta_j = 0.05$, when the two stations have firm or soft soil conditions. For the medium soil condition, $\rho_{u_k s_{lj}}$ has values in between the values for the firm and soft sites, and for the sake of brevity the curves are not shown. Figs. 3.4 and 3.5 are for identical soil conditions at the two sites, whereas Figs. 3.6 and 3.7 are for dissimilar soil conditions. Furthermore, Figs. 3.4 and 3.6 are for the waves arriving first at station k and then at station l, whereas Figs. 3.5 and 3.7 are for the waves traveling in the opposite direction. The pairs of curves from top to bottom in each figure are for increasing values of the wave passage effect as defined by the parameter d_{kl}^L/v_{app}, whereas each pair of curves are for values $\alpha d_{kl}/v_s = 0$ and 0.5, representing cases without and with the effect of incoherence. As indicated earlier, the ranges of parameter values considered include the values of interest in most applications.

For $\omega_j \to 0$, i.e., for an infinitely flexible oscillator, $s_{lj} \to -u_l$, since the oscillator then has zero absolute displacement. Thus, $\rho_{u_k s_{lj}} = -\rho_{u_k u_l}$ at $\omega_j = 0$. Furthermore, if the soil conditions are identical and the incoherence and wave passage effects are absent (i.e., the cases with $\alpha d_{kl}/v_s = 0$ and $d_{kl}^L/v_{app} = 0$ in Figs. 3.4 and 3.5), the ground motions at the two stations are perfectly correlated and, hence, $\rho_{u_k s_{lj}} = -1$. For this reason $\rho_{u_k s_{lj}}$ has a relatively large negative value for ω_j near zero even when the effects of incoherence and wave passage are included. However, for values of ω_j that are of engineering interest, say $\omega_j/2\pi > 0.5\ Hz$, $\rho_{u_k s_{lj}}$ is small, particularly in presence of incoherence and for soft soils, where most of the power in the ground displacement is in low frequencies.

For $\omega_j \to \infty$, i.e., for an infinitely stiff oscillator, $s_{lj} \to -\ddot{u}_l/\omega_j^2$, since the inertia and damping forces are negligible in relation to the restoring force. Hence, $\rho_{u_k s_{lj}} \to -\rho_{u_k \ddot{u}_l}$ for large ω_j, which is independent of ω_j. In general, the cross-correlation between the ground displacement and acceleration

for seismic motions is small and negative. Therefore, for increasing ω_j, the curves in Figs. 3.4-3.7 asymptotically approach small positive values which are only dependent on the site conditions and the coherency function.

Figs. 3.4 and 3.5 show the results for identical soil conditions at the two stations but with opposite directions of wave passage. Specifically, Fig. 3.4 is for the waves arriving first at station k and then at station l where the oscillator is attached, and Fig. 3.5 is for the opposite direction of wave passage. As can be seen, the direction of wave passage has a significant influence on the coefficient $\rho_{u_k s_{lj}}$. Similar results are observed in Figs. 3.6 and 3.7 for the dissimilar soil conditions. Note in the latter figures that $\rho_{u_k s_{lj}}$ does not go to -1 for $\omega_j = 0$ because of the dissimilar soil conditions at the two sites.

It is clear from Figs. 3.4-3.7 that for the models considered the cross-correlation coefficient $\rho_{u_k s_{lj}}$ is significant only for modes with very low frequencies, say below 0.5 Hz. Hence, when the fundamental frequency of a structure is higher than this limit, the second summation in Eq. 2.13, which represents the cross-covariance between the pseudo-static and dynamic components of the response, may be neglected without a significant loss of accuracy. This includes terms for $k = l$, as can be seen in Figs. 3.4 and 3.5 for $d_{kl} = d_{kl}^L = 0$.

3.4 Cross-Correlation Coefficient Between Responses of Oscillators at Stations k and l

The cross-correlation coefficient $\rho_{s_{ki} s_{lj}}$ is a function of the frequencies and damping ratios of the two oscillators, ω_i, ω_j and ζ_i, ζ_j, respectively, and the parameters defining the coherency function and the site conditions at stations k and l (see Fig. 2.1). Figs. 3.8-3.13 show plots of this function against ω_j for $\zeta_i = \zeta_j = 0.05$, when the two stations have firm or soft soil conditions. Since many parameters are involved, only two values for the incoherence and wave passage parameters and three values for the frequency ω_i are considered, i.e., $\alpha d_{kl}/v_s = 0$ and 0.1, $d_{kl}^L/v_{app} = 0$ and 0.5, and $\omega_i/2\pi = 1$, 2 and 4 Hz. Figs. 3.8-3.10 are for identical soil conditions at the two sites, whereas Figs. 3.11-13 are for dissimilar soil conditions. Furthermore, Figs. 3.8 and 3.11 are for the cases without the wave passage effect, Figs. 3.9 and 3.12 are for the waves arriving first at station k and then at station l, and Figs. 3.10 and 3.13 are for the waves traveling in the opposite direction. In the following, we first investigate the behavior of the coefficient in certain special cases, from which general trends can be deduced. General trends from the plots are then observed.

For $k = l$, i.e., the two oscillators attached at the same support point, $\rho_{s_{ki} s_{kj}}$ represents the modal cross-correlation coefficient for a multi-degree-of-freedom system subjected to a single support excitation. The behavior of this function is well known from earlier studies (Der Kiureghian, 1980, 1991): $\rho_{s_{ki} s_{kj}}$ decays with increasing distance between ω_i and ω_j, particularly for small damping; however,

the decay can be slow or may reverse for modes with frequencies much higher than the dominant range of input frequencies (Der Kiureghian, 1991). These results are equally valid for multiply supported systems that are subjected to perfectly correlated support motions, including the special case of uniform support motions that is often considered in conventional design. With the present formulation, the latter case occurs when there is no effect of incoherence or wave passage, and the soil conditions are identical.

For $i = j$, i.e., for identical oscillators at two different stations, $\rho_{s_{ki}s_{li}}$ is independent of the direction of wave passage, even when the two stations have dissimilar soil conditions. This is because the term $H_i(\mathrm{i}\omega)\,H_j(-\mathrm{i}\omega)$ in Eq. 2.18 is then real valued and the imaginary part of $G_{\ddot{u}_k\ddot{u}_l}(\mathrm{i}\omega)$ does not contribute to the integral. Furthermore, if the two soil conditions are similar, it can be shown that $\rho_{s_{ki}s_{lj}}$ for wave passage in one direction is equal to $\rho_{s_{kj}s_{li}}$ for wave passage in the opposite direction even for $i \neq j$. Finally, in the absence of the wave passage effect, clearly $\rho_{s_{ki}s_{lj}} = \rho_{s_{lj}s_{ki}}$. Other forms of symmetry do not exist.

In Fig. 3.8 for similar soil conditions and no wave passage, it is seen that incoherence uniformly reduces the value of the cross-correlation coefficient, particularly for the firm soil and at higher frequencies. It is interesting to note that $\rho_{s_{ki}s_{lj}}$ for the soft soil condition is relatively large for values of ω_i or ω_j that are higher than 1 Hz. This is because for this soil condition the power in the input excitation is concentrated in the very low frequencies, and hence the above values of the modal frequencies are outside the dominant range of the excitation frequencies. As described by Der Kiureghian (1991), such high-frequency modes essentially respond statically to the low-frequency excitation and, therefore, are closely correlated. For the firm soil condition with the broad-band excitation, the cross-correlation coefficient for the case without the incoherence effect is nearly identical to the coefficients used in the well known CQC combination rule (Der Kiureghian, 1981; Wilson et al., 1981), which is based on the white-noise approximation. It is also worth noting that, except for values of the ω_j near zero, the coefficient $\rho_{s_{ki}s_{lj}}$ is always positive in absence of the wave passage effect.

Figs. 3.9 and 3.10 for the similar soil conditions and including the effect of wave passage in two opposite directions show that $\rho_{s_{ki}s_{lj}}$ is strongly influenced by this effect. The curves now can be oscillatory and take on positive as well as negative values. Furthermore, modes with well spaced frequencies can have significant correlation even on firm soil (e.g., see Fig. 3.10c). It is interesting to observe the influence of the direction of wave passage by comparing the corresponding curves in the two figures. In particular, the symmetry property mentioned earlier can be verified, i.e., $\rho_{s_{ki}s_{lj}}$ for one direction is equal to $\rho_{s_{kj}s_{li}}$ for the opposite direction. The important conclusion here is that the coefficient $\rho_{s_{ki}s_{lj}}$ can be significantly different from zero even for well spaced modes and firm soil conditions due to the wave passage effect. However, this correlation is significantly reduced in presence of the

incoherence effect, particularly on firm soils.

Figs. 3.11-3.13 for dissimilar soil conditions show similar trends, but curves are mostly between the two sets of curves for the uniform firm and uniform soft soil conditions. The only exception is for cases with $\omega_i = \omega_j$, where correlation less than unity is obtained even in the case of zero incoherence and wave passage effect. As explained earlier, this is due to the difference in the shapes of the power spectral densities for the two soil conditions. It is interesting to note that in general $\rho_{s_{ki}s_{lj}} \neq \rho_{s_{lj}s_{ki}}$, except when the wave passage effect is absent.

3.5 Concluding Remarks

From the results in this section, the following general conclusions can be derived:

(1) The cross-correlation coefficient $\rho_{u_k u_l}$ between the ground displacements at stations k and l is generally large, particularly for soft soil conditions, and its contribution to the pseudo-static component of the response cannot be neglected.

(2) The cross-correlation coefficient $\rho_{u_k s_{lj}}$ between the ground displacement at station k and the oscillator response at station l may have a small value, except for frequencies below 0.5 Hz. Thus, the contribution of this coefficient and, therefore, that of the covariance between the pseudo-static and dynamic components of the response may be neglected, if the fundamental frequency of the system is greater than about 0.5 Hz, without a significant loss of accuracy.

(3) The cross-correlation coefficient $\rho_{s_{ki}s_{lj}}$ between the responses of the oscillators at stations k and l depends on the separation between the two frequencies and the soil conditions at the two stations. For firm soil and in absence of the wave passage effect, the correlation is small for well spaced frequencies (as long as they are not far from the range of dominant input frequencies) and tends to further decay as a consequence of the incoherence effect. For soft soils, or in the presence of the wave passage effect, the correlation coefficient can be significant even for well spaced modes if there is not a strong incoherence effect.

Although it is possible to use the above general results to drop some of the terms in Eq. 2.13 and develop simplified combination rules, for reasons of caution it is best to retain all the terms in the combination rule, since the required computations are simple and not demanding of extensive computer time.

Table 3.1 PSD Filter Parameters for Model Soil Types

soil type	$\omega_{fk}, rad/s$	ζ_{fk}	$\omega_{gk}, rad/s$	ζ_{gk}
firm	15.0	0.6	1.5	0.6
medium	10.0	0.4	1.0	0.6
soft	5.0	0.2	0.5	0.6

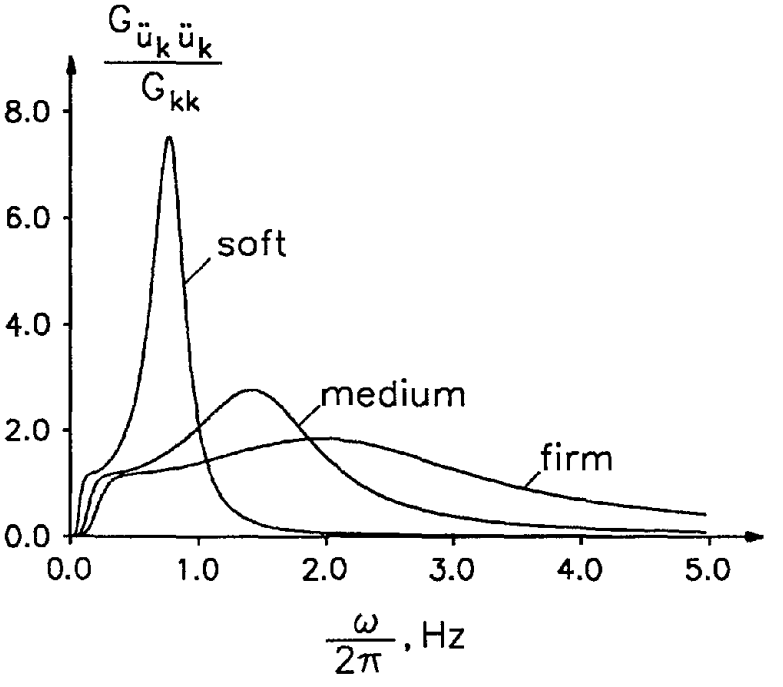

Figure 3.1 PSD's of Ground Acceleration for Three Soil Conditions

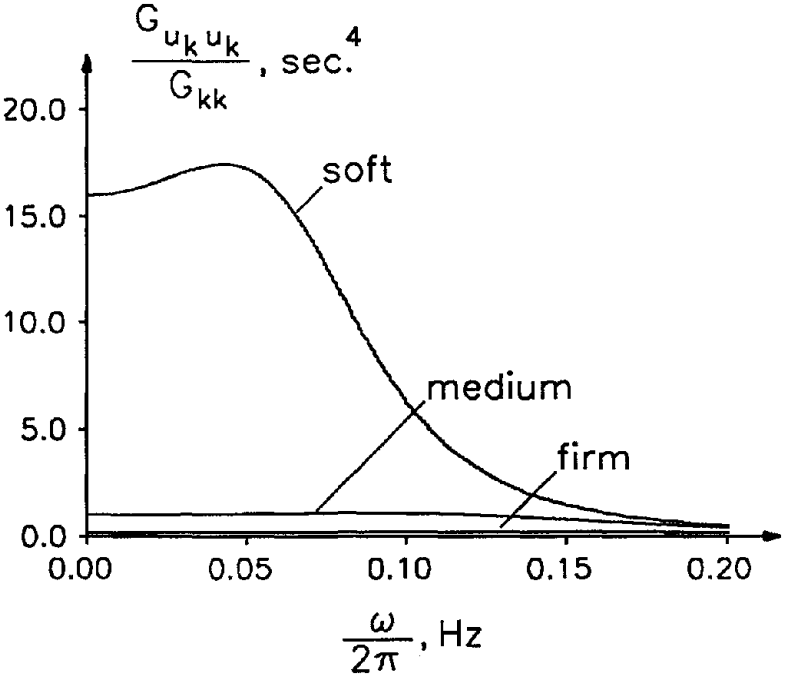

Figure 3.2 PSD's of Ground Displacement for Three Soil Conditions

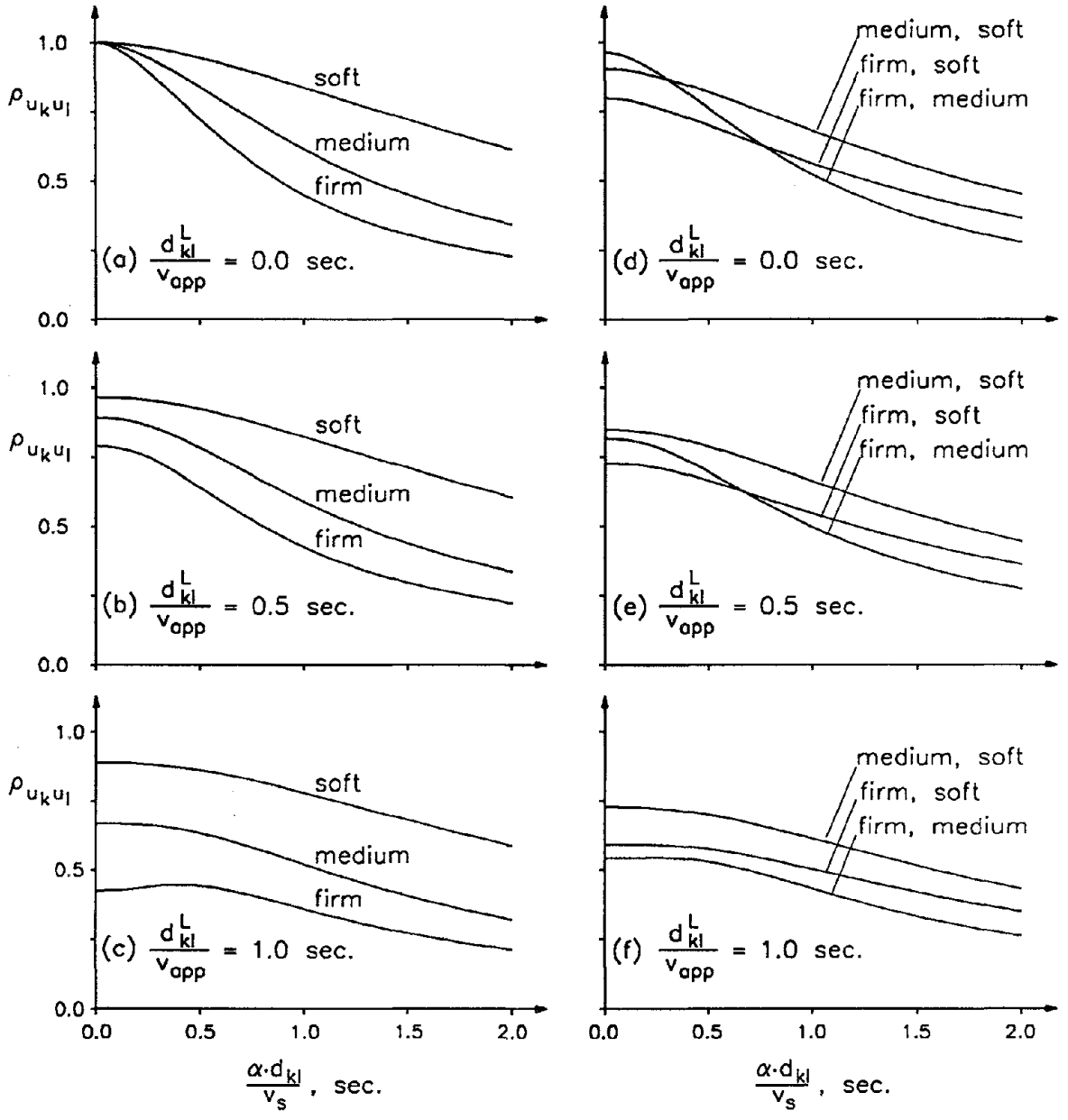

Figure 3.3 Cross-Correlation Coefficient Between Ground Displacements at Stations k and l

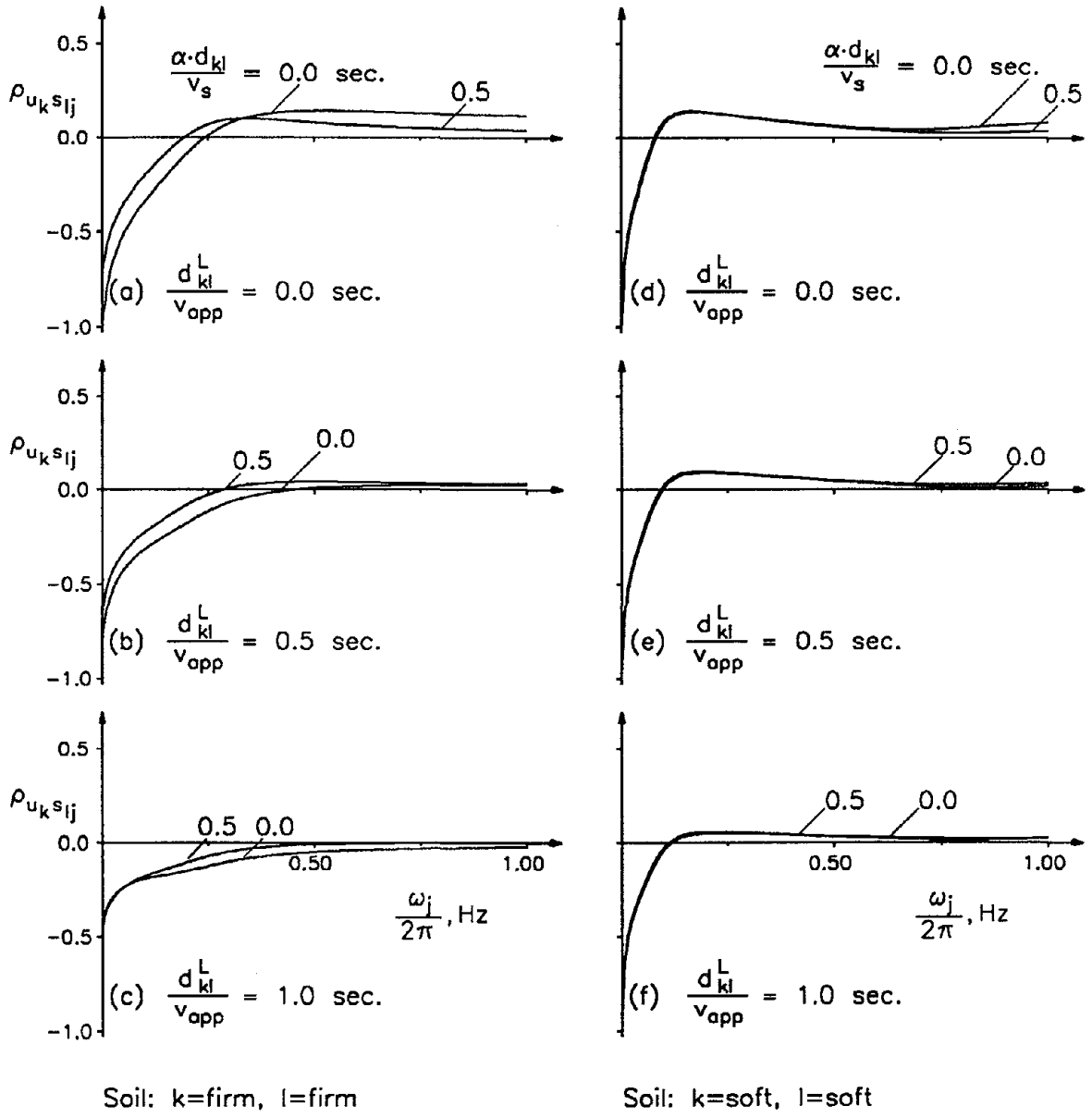

Figure 3.4 Cross-Correlation Coefficient Between Ground Displacement at Station k and Response of Oscillator at Station l for Similar Soil Conditions and Wave Direction k to l

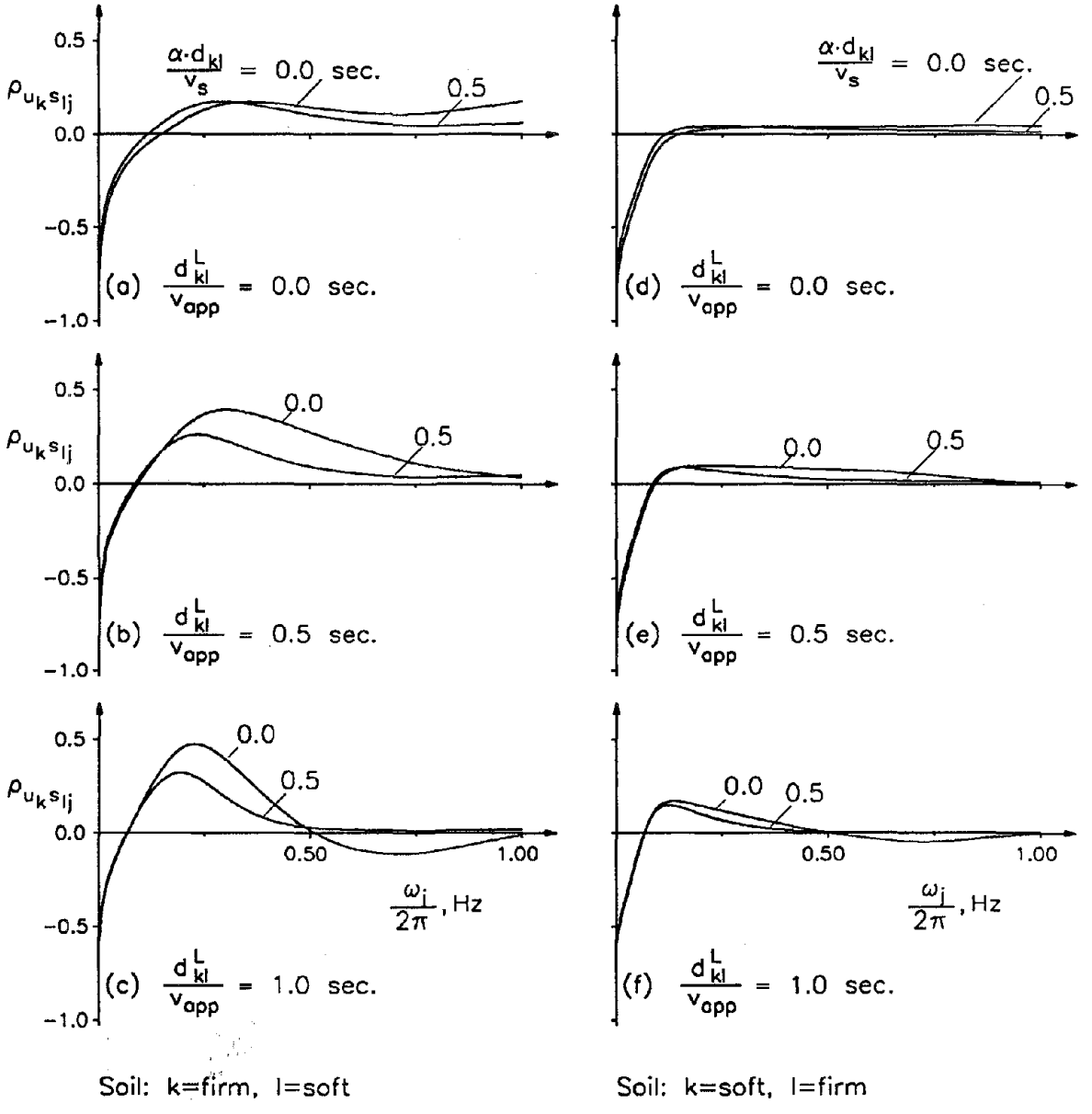

Figure 3.7 Cross-Correlation Coefficient Between Ground Displacement at Station k and Response of Oscillator at Station l for Dissimilar Soil Conditions and Wave Direction l to k

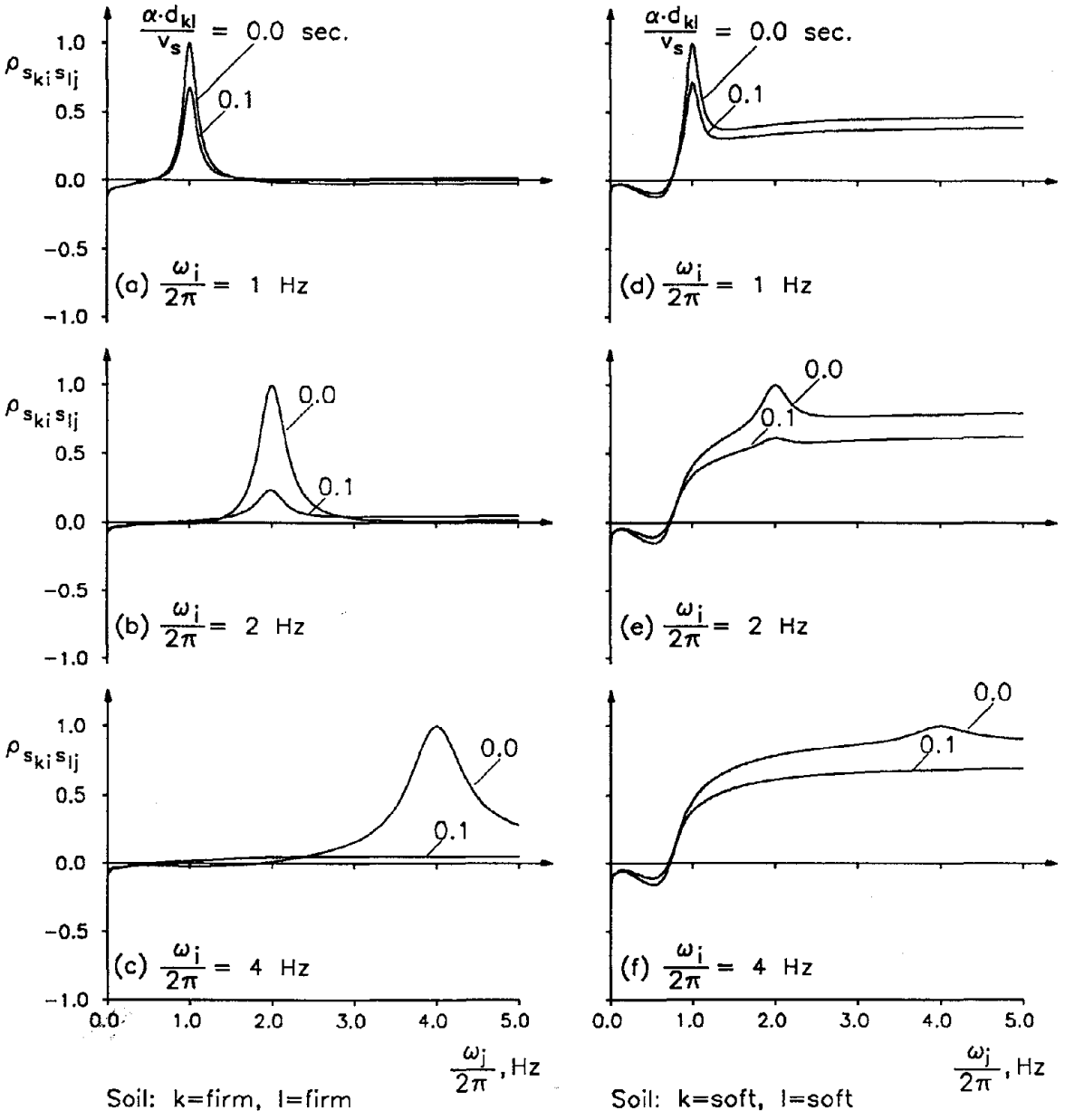

Figure 3.8 Cross-Correlation Coefficient Between Responses of Oscillators at Stations k and l for Similar Soil Conditions and $d_{kl}^{L}/v_{app} = 0\,sec.$

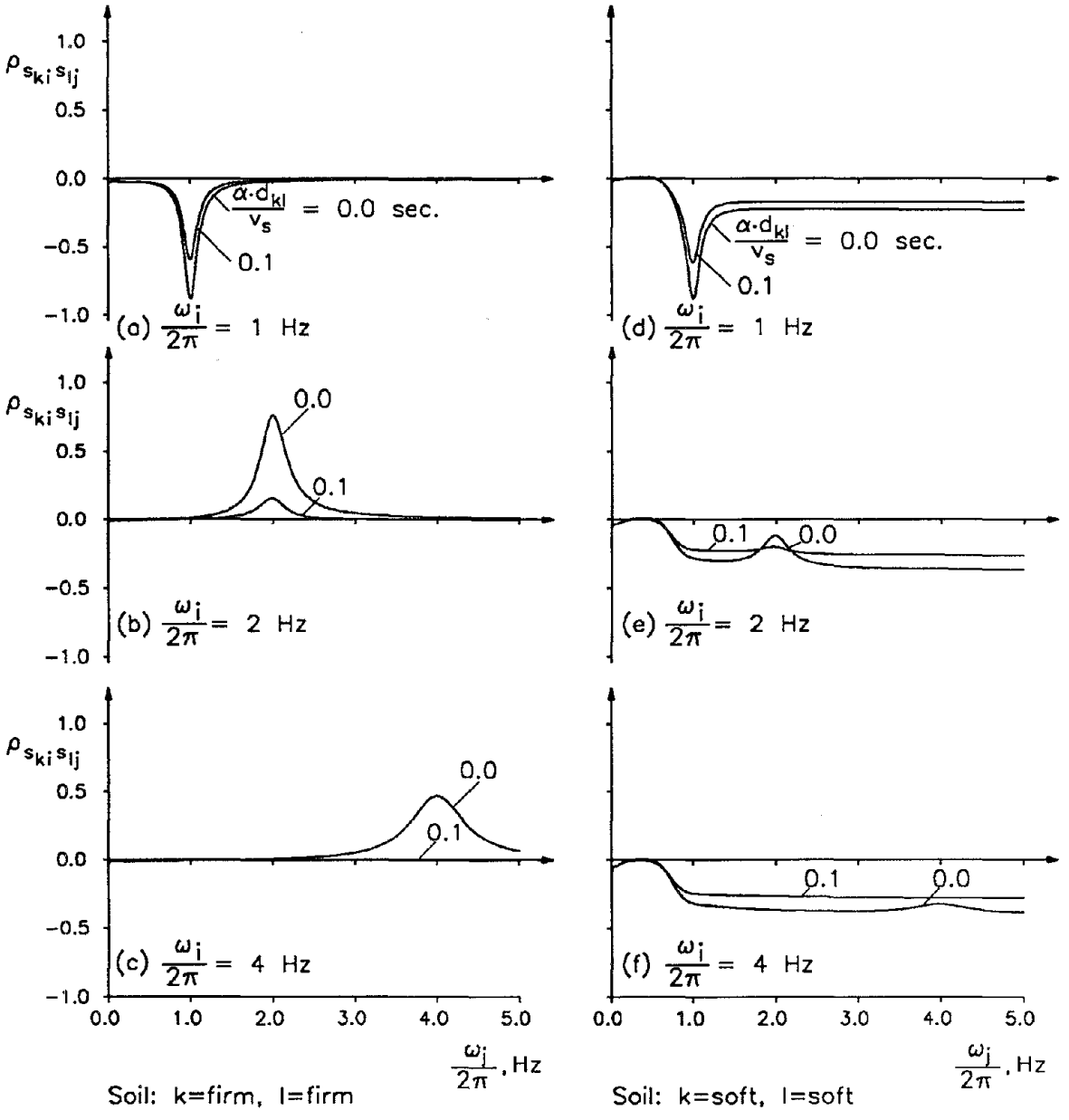

Figure 3.9 Cross-Correlation Coefficient Between Responses of Oscillators at Stations k and l for Similar Soil Conditions and $d_{kl}^{L}/v_{app}=0.5$ *sec.* with Wave Direction from k to l

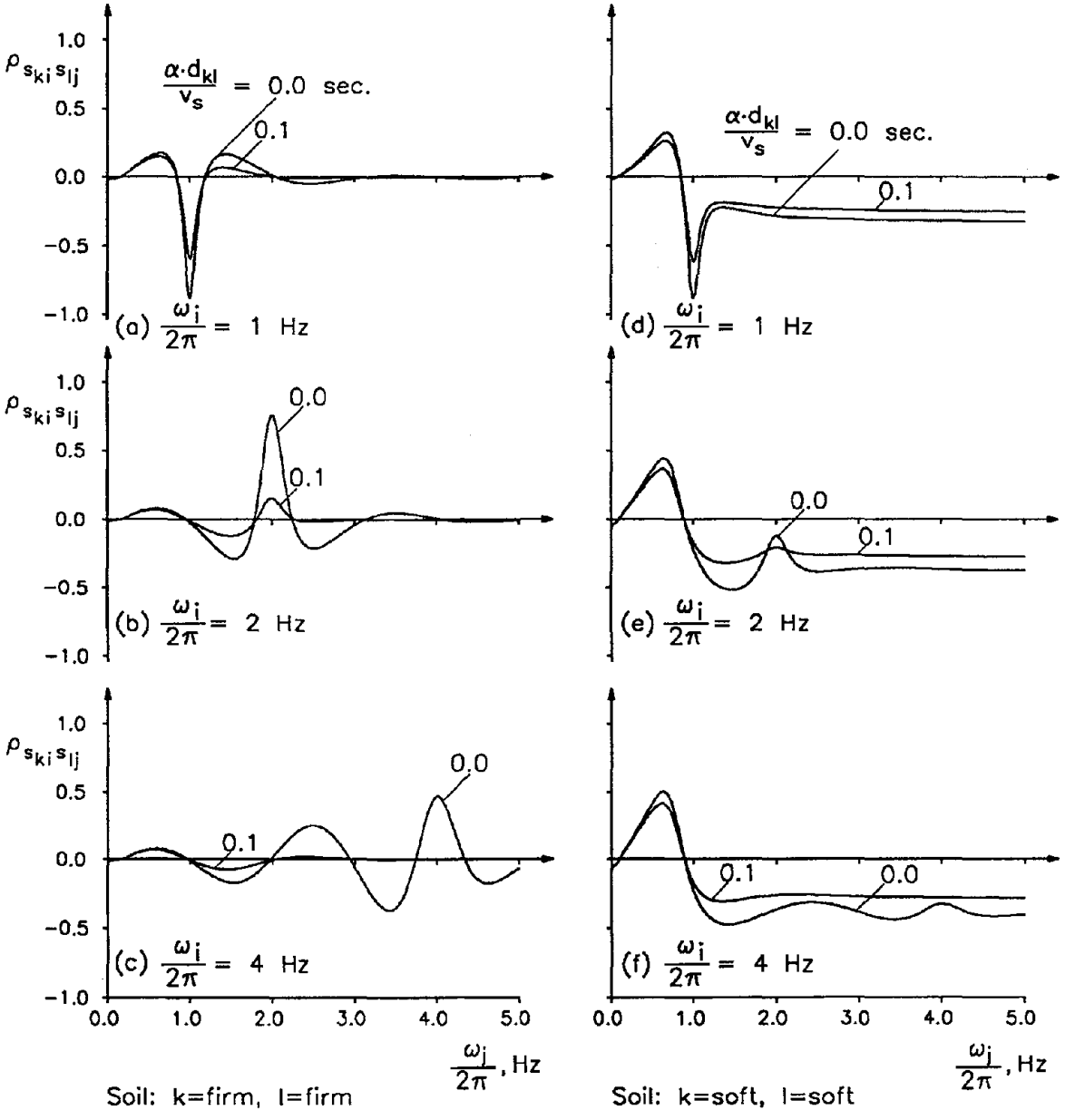

Figure 3.10 Cross-Correlation Coefficient Between Responses of Oscillators at Stations k and l for Similar Soil Conditions and $d_{kl}^{L}/v_{app} = 0.5\ sec.$ with Wave Direction from l to k

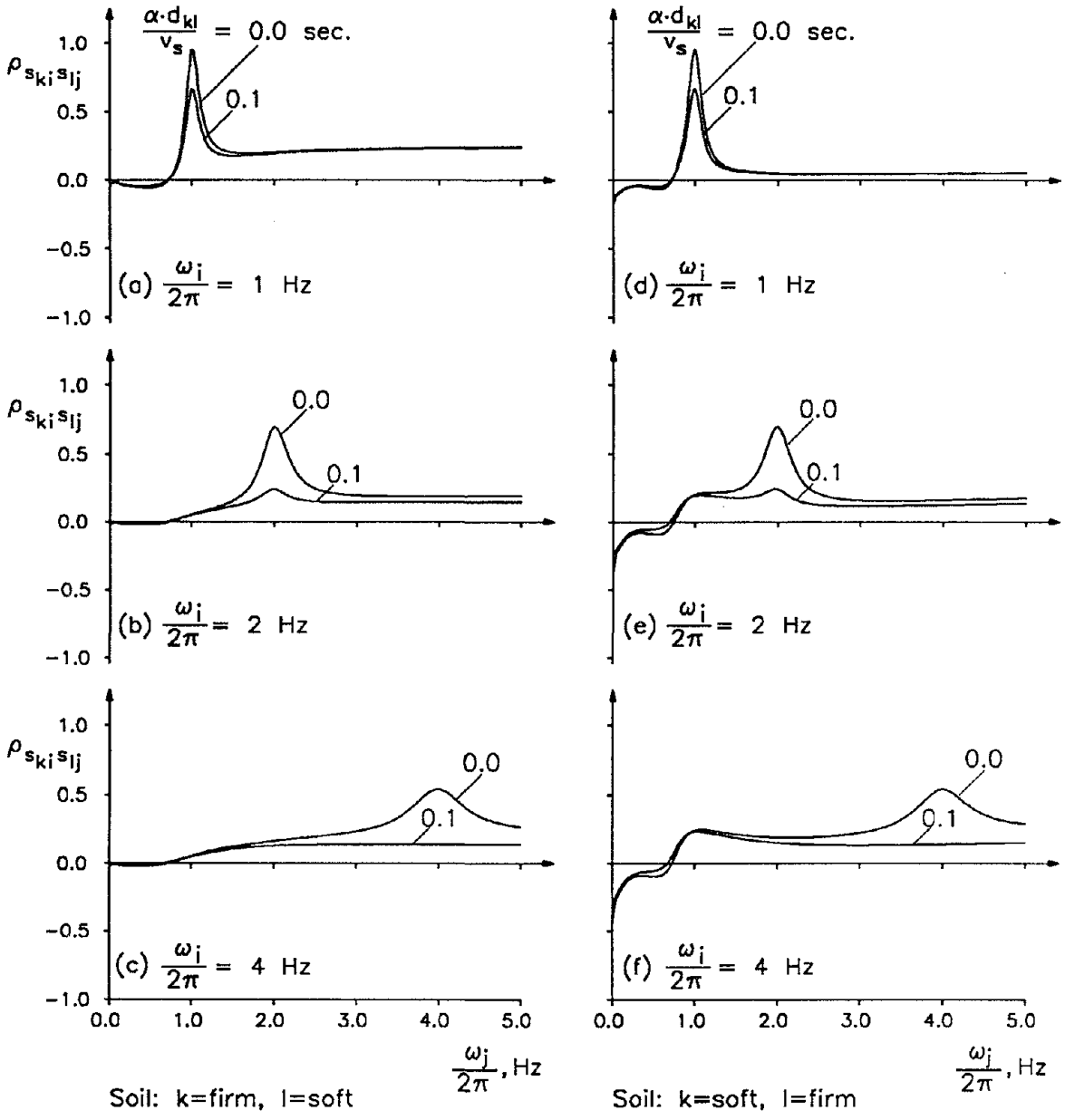

Figure 3.11 Cross-Correlation Coefficient Between Responses of Oscillators at Stations k and l for Dissimilar Soil Conditions and $d_{kl}^{L}/v_{app} = 0\ sec.$

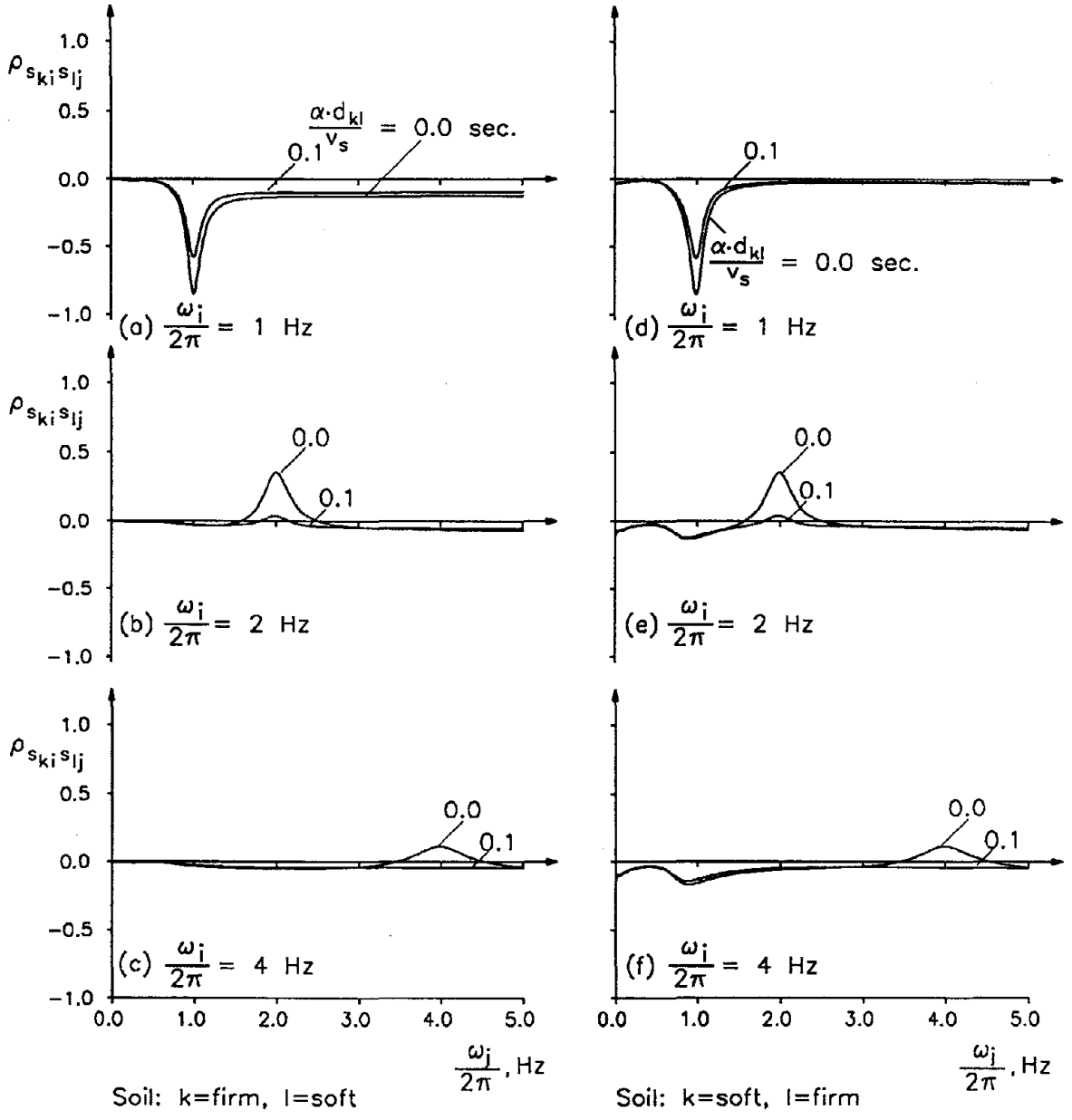

Figure 3.12 Cross-Correlation Coefficient Between Responses of Oscillators at Stations k and l for Dissimilar Soil Conditions and $d_{kl}^{L}/v_{app} = 0.5$ *sec.* with Wave Direction from k to l

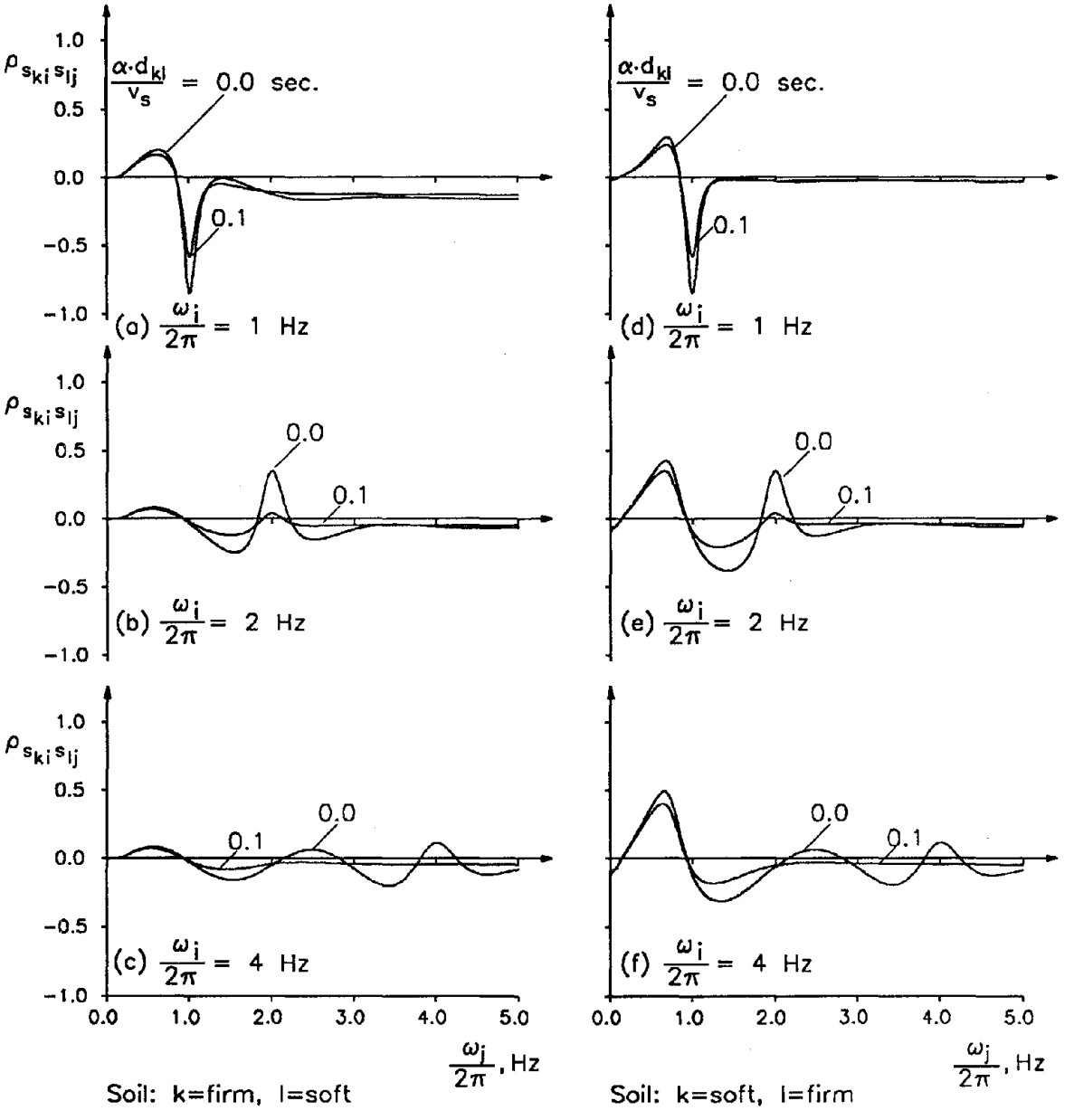

Figure 3.13 Cross-Correlation Coefficient Between Responses of Oscillators at Stations k and l for Dissimilar Soil Conditions and $d_{kl}^{L}/v_{app} = 0.5\ sec.$ with Wave Direction from l to k

CHAPTER 4
DEVELOPMENT OF THE RESPONSE SPECTRUM METHOD

4.1 Introduction

The response spectrum has proven to be a convenient and reliable tool for approximate dynamic analysis of linear structures that are subjected to uniform seismic inputs. Based on the principles of the theory of random vibrations, this method is capable of providing accurate statistical estimates (e.g., mean, standard deviation and distribution) of the peak response, provided care is taken to properly account for the cross-correlation between the modal responses. A series of recent papers have demonstrated the applicability and accuracy of this method for structures (including those with non-classical damping) as well as coupled primary-secondary systems (e.g., Singh and Chu, 1976; Der Kiureghian, 1981, 1991; Igusa and Der Kiureghian, 1983, 1985; Smeby and Der Kiureghian, 1985; Asfura and Der Kiureghian, 1986).

For multiply supported structures subjected to differential support motions, several attempts at developing a response spectrum method have been made. One idea has been to group the support motions into statistically independent subgroups with perfect correlation between the members of each subgroup (Yamamura and Tanaka, 1990). Several ad hoc combination rules have also been investigated by comparison with time-history results (Dong and Wieland, 1988). Recently, a more refined method has been suggested by Berrah and Kausel (1989), where the spectrum at each support point is adjusted in account of the spatial variability effect arising from incoherence alone. However, they do not consider the contribution of the pseudo-static component of the response and its cross-correlation with the dynamic component, nor do they consider the effect of wave passage.

In this chapter, a new formulation of the response spectrum method is presented which properly accounts for the effects of ground motion variability due to incoherence, wave passage and local soil conditions. Based on the random vibration formulation of Chapter 2, the combination rule accurately accounts for the contributions of the cross-correlations between modes, between the support motions, and between the pseudo-static and dynamic components of the response.

It is assumed herein that the set of ground motion components $u_k(t)$, $k = 1, \ldots, m$, at the support degrees of freedom of the structure is specified in terms of a set of mean relative displacement response spectra, $D_k(\omega, \zeta)$, which are expressed as functions of an oscillator frequency ω and damping ζ and incorporate the effects of the local soil conditions; a set of mean peak ground displacements $u_{k,\max}$ associated with each support degree of freedom; a measure of the duration of excitation τ; and a coherency function, $\gamma_{kl}(i\omega)$, describing the effects of incoherency and wave passage for each pair of stations k and l. While the method is capable of employing a different coherency model for each pair of support conditions, in practice one would most probably use a single coherency model for an entire

region regardless of the specific conditions at each support point.

After developing the response spectrum combination rule, the remainder of this chapter deals with the evaluation of the coefficients $\rho_{u_k u_l}$, $\rho_{u_k s_{lj}}$ and $\rho_{s_{ki} s_{lj}}$ in terms of the ground motion specification described above.

4.2 Mode-and-Support Combination Rule

The response spectrum method to be developed is based on Eq. 2.13 of Chapter 2, which is repeated here for convenience

$$\sigma_z^2 = \sum_{k=1}^{m}\sum_{l=1}^{m} a_k a_l \rho_{u_k u_l} \sigma_{u_k} \sigma_{u_l} + 2 \sum_{k=1}^{m}\sum_{l=1}^{m}\sum_{j=1}^{n} a_k b_{lj} \rho_{u_k s_{lj}} \sigma_{u_k} \sigma_{s_{lj}}$$

$$+ \sum_{k=1}^{m}\sum_{l=1}^{m}\sum_{i=1}^{n}\sum_{j=1}^{n} b_{ki} b_{lj} \rho_{s_{ki} s_{lj}} \sigma_{s_{ki}} \sigma_{s_{lj}} \tag{2.13}$$

In order to develop the response spectrum combination rule, we relate the root-mean-squares of the ground displacement and oscillator response, σ_{u_k} and $\sigma_{s_{ki}}$, to the mean peak values of the respective processes. Let $u_{k,\max} = \mathrm{E}[\max |u_k(t)|]$ denote the mean value of the peak displacement at the k-th support degree of freedom, and $D_k(\omega_i, \zeta_i) = \mathrm{E}[\max |s_{ki}(t)|]$ denote the mean response spectrum ordinate for $\omega = \omega_i$ and $\zeta = \zeta_i$, representing the mean peak relative displacement response of an oscillator of frequency ω_i and damping ζ_i to the base motion $u_k(t)$ (i.e., the left oscillator in Fig. 2.1). We note that $D_k(0, \zeta) = u_{k,\max}$, since the relative displacement response of an infinitely flexible oscillator is identical to the base displacement with an opposite sign, and $\lim_{\omega \to \infty} \omega^2 D_k(\omega, \zeta) = \ddot{u}_{k,\max}$, since the pseudo-acceleration response of the oscillator asymptotically approaches the peak ground acceleration as ω approaches infinity.

In general, one may write $u_{k,\max} = p_{u_k} \sigma_{u_k}$ and $D_k(\omega_i, \zeta_i) = p_{s_{ki}} \sigma_{s_{ki}}$, where p_{u_k} and $p_{s_{ki}}$ are known as peak factors (Der Kiureghian 1980). Similarly, for the generic response quantity, $z(t)$, one may write $\mathrm{E}[\max |z(t)|] = p_z \sigma_z$, where p_z is the corresponding peak factor. Using these relations in Eq. 2.13, we obtain

$$\mathrm{E}[\max |z(t)|] = \Bigg[\sum_{k=1}^{m}\sum_{l=1}^{m} a_k a_l \rho_{u_k u_l} \frac{p_z^2}{p_{u_k} p_{u_l}} u_{k,\max} u_{l,\max}$$

$$+ 2 \sum_{k=1}^{m}\sum_{l=1}^{m}\sum_{j=1}^{n} a_k b_{lj} \rho_{u_k s_{lj}} \frac{p_z^2}{p_{u_k} p_{s_{lj}}} u_{k,\max} D_l(\omega_j, \zeta_j)$$

$$+ \sum_{k=1}^{m}\sum_{l=1}^{m}\sum_{i=1}^{n}\sum_{j=1}^{n} b_{ki} b_{lj} \rho_{s_{ki} s_{lj}} \frac{p_z^2}{p_{s_{ki}} p_{s_{lj}}} D_k(\omega_i, \zeta_i) D_l(\omega_j, \zeta_j) \Bigg]^{1/2} \tag{4.1}$$

Since the peak factors are only mildly dependent on the characteristics of each process, their ratios are near unity (Der Kiureghian 1980) and the above equation can be simplified to

$$\mathrm{E}[\max|z(t)|] = \left[\sum_{k=1}^{m}\sum_{l=1}^{m} a_k a_l \rho_{u_k u_l} u_{k,\max} u_{l,\max} + 2\sum_{k=1}^{m}\sum_{l=1}^{m}\sum_{j=1}^{n} a_k b_{lj} \rho_{u_k s_{lj}} u_{k,\max} D_l(\omega_j, \zeta_j) + \sum_{k=1}^{m}\sum_{l=1}^{m}\sum_{i=1}^{n}\sum_{j=1}^{n} b_{ki} b_{lj} \rho_{s_{ki} s_{lj}} D_k(\omega_i, \zeta_i) D_l(\omega_j, \zeta_j) \right]^{1/2} \tag{4.2}$$

The preceding represents the response spectrum combination rule for the mean peak response of the multiply supported structure. It is possible to derive a similar expression for the variance of the peak response or its other statistics that are necessary to compute its probability distribution (see Der Kiureghian, 1980, for the basic idea of the approach). However, usually the variability in the peak response is small in relation to the uncertainties present in the specification of the seismic excitation, and hence this variability is usually ignored in practice. For this reason, these other combination rules will not be developed here.

All terms in the combination rule in Eq. 4.2 are readily available in terms of the properties of the structure or the specified mean response spectra and peak ground displacements, except for the three cross-correlation coefficients $\rho_{u_k u_l}$, $\rho_{u_k s_{lj}}$ and $\rho_{s_{ki} s_{lj}}$. As shown in Eqs. 2.16-2.18 and 2.23-2.25 of Chapter 2, these coefficients are functions of the power spectral densities and the coherency function for each pair of support motions. It is shown in the following section that there exists a unique correspondence between the power spectral density function and the mean response spectrum for a given family of ground motions. Based on this relation and the known coherency function, the three cross-correlation coefficients are computed directly in terms of the given mean response spectra at stations k and l. Numerical examples are given in Section 4.4 and in Chapter 5.

4.3 Power Spectral Density Consistent with Given Mean Response Spectrum

The correspondence between the mean response spectrum and the power spectral density of a ground acceleration process has been investigated by several authors (e.g., Kaul, 1978; Unruh and Kana, 1981; Christian 1989). The following formulation is similar to that proposed by Kaul (1978) and Christian (1989); however, it employs a more refined formulation of the peak factor and extends the analysis to low frequencies. The derivation is based on the concepts of stationary random vibrations and assumes that the seismic motion is a wide-band process and the oscillator damping, ζ, is small. The effect of nonstationarity in the response of low-frequency oscillators is accounted for in an approximate manner. For the purpose of simplifying the notation, the subscript k defining the location

of the support is omitted in this section.

Let $G_{\ddot{u}\ddot{u}}(\omega)_1$ denote a first-order approximation of the unknown power spectral density of the ground acceleration $\ddot{u}(t)$. Assuming the input is wide band, the mean-square response of an oscillator of frequency ω and damping ζ to this excitation can be approximated by $\lambda_0(\omega)_0 = \pi G_{\ddot{u}\ddot{u}}(\omega)_1/(2\zeta\omega^3)$, where the subscript 0 is to indicate that the approximation assumes $G_{\ddot{u}\ddot{u}}(\omega)_1$ to be a constant. Using this approximation in the identity $D(\omega,\zeta) = p_s(\omega)[\lambda_0(\omega)]^{1/2}$, we obtain

$$G_{\ddot{u}\ddot{u}}(\omega)_1 = \frac{2\zeta\omega^3}{\pi}\left[\frac{D(\omega,\zeta)}{p_s(\omega)_0}\right]^2 \qquad \omega \geq 0 \tag{4.3}$$

where $p_s(\omega)$ is the peak factor for the oscillator response (see Appendix I) and the subscript 0 indicates the approximation just mentioned. This expression is valid only for nonnegative frequencies. For negative frequencies, the spectral values are determined by using the symmetry of the function.

It is seen that the first-order approximation in Eq. 4.3 is not a constant but a function of ω. Thus, a second-order approximation can be obtained by replacing the terms $2\zeta\omega^3/\pi$ and $p_s(\omega)_0$ by the corresponding terms based on the above approximation, which are $G_{\ddot{u}\ddot{u}}(\omega)_1/\lambda_0(\omega)_1$ and $p_s(\omega)_1$, respectively. The result is

$$G_{\ddot{u}\ddot{u}}(\omega)_2 = \frac{G_{\ddot{u}\ddot{u}}(\omega)_1}{\lambda_0(\omega)_1}\left[\frac{D(\omega,\zeta)}{p_s(\omega)_1}\right]^2 \qquad \omega \geq 0 \tag{4.4}$$

Repeating this process, the $r+1$-th approximation of the unknown power spectral density is

$$G_{\ddot{u}\ddot{u}}(\omega)_{r+1} = \frac{G_{\ddot{u}\ddot{u}}(\omega)_r}{\lambda_0(\omega)_r}\left[\frac{D(\omega,\zeta)}{p_s(\omega)_r}\right]^2 \qquad \omega \geq 0 \tag{4.5}$$

This is a recursive formula giving the desired power spectral density in terms of the specified mean response spectrum to the $r+1$-th order approximation.

To use the preceding recursive formula, one first computes the first three spectral moments of the oscillator response for the r-th approximation of the input power spectral density

$$\lambda_m(\omega)_r = 2\int_0^\infty w^m\,|H(\mathrm{i}w)|^2\,G_{\ddot{u}\ddot{u}}(w)_r\,dw \qquad m=0,1,2 \tag{4.6}$$

where $H(\mathrm{i}w)=[\omega^2 - w^2 + 2\mathrm{i}\zeta\omega w]^{-1}$ is the frequency response function. The corresponding peak factor is then computed in terms of these three moments and the specified duration, τ, of the excitation from formulas provided in Appendix I. This procedure usually converges rapidly for the range of frequencies that are of engineering interest. An example in the next section will demonstrate this fact.

In the present application we require only a rough approximation of the power spectral density function. This is because the correlation coefficients in Eqs. 2.16-2.18 are expressed as ratios of integrals over the spectral shapes, and hence the coefficients are only mildly dependent on the specific forms of these functions. Thus, for the present purposes, the first-order approximation in Eq. 4.3 is adequate. However, this approximation (as well as the refined approximation obtained by the recursive formula in Eq. 4.5) does not work well for small frequencies. This is because the assumption of stationarity of the oscillator response is not valid for an oscillator whose period is long in relation to the duration of excitation, τ. Based on Rosenblueth and Elorduy (1969), an approximate estimate of the low-frequency oscillator response can be obtained by replacing its damping value, ζ, by an equivalent damping defined by

$$\zeta_{eq} = \zeta + \frac{2}{\omega\tau} \tag{4.7}$$

Replacing the first ζ term in Eq. 4.3 by the above equivalent damping, we obtain

$$G_{\ddot{u}\ddot{u}}(\omega)_1 = \omega^2 \left(\frac{2\zeta\omega}{\pi} + \frac{4}{\pi\tau}\right)\left[\frac{D(\omega,\zeta)}{p_s(\omega)_0}\right]^2 \qquad \omega \geq 0 \tag{4.8}$$

This correction has the effect of amplifying the low-frequency end of the power spectral density shape in account of the nonstationary response to the transient loading.

As mentioned earlier, $D(0, \zeta) = u_{\max}$. Thus, the approximation of the acceleration power spectral density in Eq. 4.8 is of order ω^2 as ω approaches zero. This implies that the corresponding power spectral density of the ground displacement (obtained by dividing Eq. 4.8 by ω^4) will have an infinite amplitude at zero frequency. This is physically impossible. To correct the approximation in Eq. 4.8, we observe that: (1) the spectral density of the ground displacement should approach a finite or zero value as $\omega \to 0$, (2) any adjustment of Eq. 4.8 should not affect the medium and high-frequency regions for which the approximation is sufficiently accurate, and (3) the area underneath the power spectral density of ground displacement should equal $(u_{\max} / p_u)^2$, where p_u is the corresponding peak factor. Based on these considerations, a correction factor of the form $\omega^p/(\omega^p + \omega_f^p)$ is employed, in which ω_f and p denote positive-valued parameters. Obviously, $p \geq 2$ satisfies the first requirement above. For small values of ω_f, this function quickly approaches unity as ω increases, thus satisfying the second requirement. The third requirement is observed by selecting ω_f and p such that the following equation is satisfied:

$$2\int_0^\infty \frac{\omega^{p-2}}{\omega^p + \omega_f^p}\left(\frac{2\zeta\omega}{\pi} + \frac{4}{\pi\tau}\right)\left[\frac{D(\omega,\zeta)}{p_s(\omega)_0}\right]^2 d\omega = \left(\frac{u_{\max}}{p_u}\right)^2 \tag{4.9}$$

Thus, the adjusted first-order approximation of the power spectral density that satisfies the above requirements is

$$G_{\ddot{u}\ddot{u}}(\omega)_1 = \frac{\omega^{p+2}}{\omega^p + \omega_f^p}\left(\frac{2\zeta\omega}{\pi} + \frac{4}{\pi\tau}\right)\left[\frac{D(\omega,\zeta)}{p_s(\omega)_0}\right]^2 \qquad \omega \geq 0 \tag{4.10}$$

The above equation together with the identities in Eqs. 2.23-2.25 are used in Eqs. 2.16-2.18 to numerically compute the desired correlation coefficients $\rho_{u_k u_l}$, $\rho_{u_k s_{lj}}$ and $\rho_{s_{ki} s_{lj}}$. In this study, the Gauss quadrature integration method was employed for this purpose.

Eq. 4.9 provides only one equation for solving for the two unknowns, ω_f and p. However, the coefficients $\rho_{u_k u_l}$, $\rho_{u_k s_{lj}}$ and $\rho_{s_{ki} s_{lj}}$ are not sensitive to the specific values of these parameters and any reasonable pair of values of these parameters that also satisfies the requirements (1) and (3) above can be used. This is further demonstrated by a numerical example in the following section.

It appears in Eq. 4.10 that the estimated power spectral density will depend on the assumed value of the damping ratio, ζ. However, if the spectra for different damping values are properly defined, the quantity $(\zeta + 2/\omega\tau)[D_k(\omega,\zeta)/p_k(\omega)]^2$ must be invariant with respect to ζ. Unfortunately design spectra usually are not perfectly consistent with this rule and some dependence of the estimated spectral density shape on ζ is expected. However, since in the present application the spectral density shapes are needed only for the computation of the cross-correlation coefficients, this dependence is not critical.

4.4 Numerical Example

As an example of the above approach, consider the relative displacement response spectrum in Fig. 4.1, which is the design spectrum recommended by the Structural Engineers Association of California, SEAOC (1990), for 5 percent damping and a peak ground acceleration of $\ddot{u}_{k,\max} = 0.5\,g$ for a site with "type 2" soil, i.e., deep cohesionless or stiff clay soil. The duration of strong shaking is assumed to be $\tau = 10\,s$. Unfortunately this spectrum as well as other recommended spectra in current practice do not specify the shape of the spectrum for long periods (typically above $3\,s$), nor do they specify the associated peak ground displacement. This is a serious shortcoming of the present code provisions for seismic design, which must be overcome in order to ensure a proper design and analysis methodology for multiply supported structures and other seismic design situations (e.g., base-isolated structures) that require knowledge of the low-frequency components of the ground motion. To circumvent this shortcoming in the present work, we use engineering judgment and experience with previous earthquake records in order to make estimates of the peak ground displacement and the low-frequency end of the response spectrum.

To estimate the peak ground displacement, we apply a deamplification factor to the peak spectral displacement, which in the present case is $0.536\,m$ occurring at $3\,s$ period. For 5 percent damping, the deamplification factor recommended by Newmark and Hall (1969) is 1.4. Using this value, we obtain $u_{k,\max}=0.383\,m$. For the spectral values at low frequencies, we assume a displacement spectral shape varying quadratically from $u_{k,\max}$ at $\omega=0$ to $0.536\,m$ at $\omega/2\pi=0.33\,Hz$, i.e., $D(\omega,\zeta)=u_{k,\max}(1+a\omega^2)$ for $0\le\omega/2\pi\le0.33\,Hz$, where $a=0.0912\,s^2$ to match the spectral value at the upper frequency limit. The resulting spectrum is shown in Fig. 4.1 for the frequency range $0\le\omega/2\pi\le5\,Hz$.

Fig. 4.2 shows the first, second, and third-order approximations of the power spectral density function obtained by use of the recursive formula in Eq. 4.5. Clearly, the first-order approximation is sufficiently accurate for the present purpose. Fig. 4.3 shows plots of the first-order approximations of the power spectral densities for the ground acceleration and displacement that are obtained by use of the adjusted formula in Eq. 4.10 for $p=2$, 3 and 4. The corresponding values of ω_f that satisfy Eq. 4.9 are $\omega_f=0.837$, 0.705 and 0.562 *rad/s*, respectively. As can be seen in Fig. 4.3a, the power spectral density of the ground acceleration is unaffected by the choice of p. However, the power spectral density of the ground displacement shown in Fig. 4.3b is strongly influenced by the selection of the parameter p, especially in the range of small frequencies.

Fig. 4.4 shows plots of the cross-correlation coefficient $\rho_{u_k u_l}$ against the incoherence parameter $\alpha d_{kl}/v_s$ (assuming no wave passage effect) for the three displacement power spectral densities in Fig. 4.3b. As can be seen, in spite of the vast difference between the three displacement power spectral density shapes, the cross-correlation coefficient $\rho_{u_k u_l}$ is relatively invariant of the parameter p, particularly for values of the incoherence parameter that are of engineering relevance, i.e., $\alpha d_{kl}/v_s<0.5$. The cross-correlation coefficients $\rho_{u_k s_{lj}}$ and $\rho_{s_{ki} s_{lj}}$ (not shown here) are even less sensitive to the shape of the displacement power spectral density and remain almost entirely unaffected by the choice of p. Further investigations have shown that these coefficients are not sensitive to the other assumptions or parameters used, such as the form of the response spectrum at the lower frequencies (e.g., a linear or exponential function instead of the quadratic function assumed above) and the duration of excitation, τ.

The above numerical example shows that the cross-correlation coefficients $\rho_{u_k u_l}$, $\rho_{u_k s_{lj}}$ and $\rho_{s_{ki} s_{lj}}$ that are required in the response spectrum combination rule can be reliably estimated based on the specified information on the support excitations, i.e., the set of mean relative displacement response spectra, the peak ground displacements, the duration of strong shaking, and the coherency function. The relative invariance of these coefficients with respect to variations in the underlying assumptions or approximations is a key to the stability and accuracy of the proposed response spectrum method.

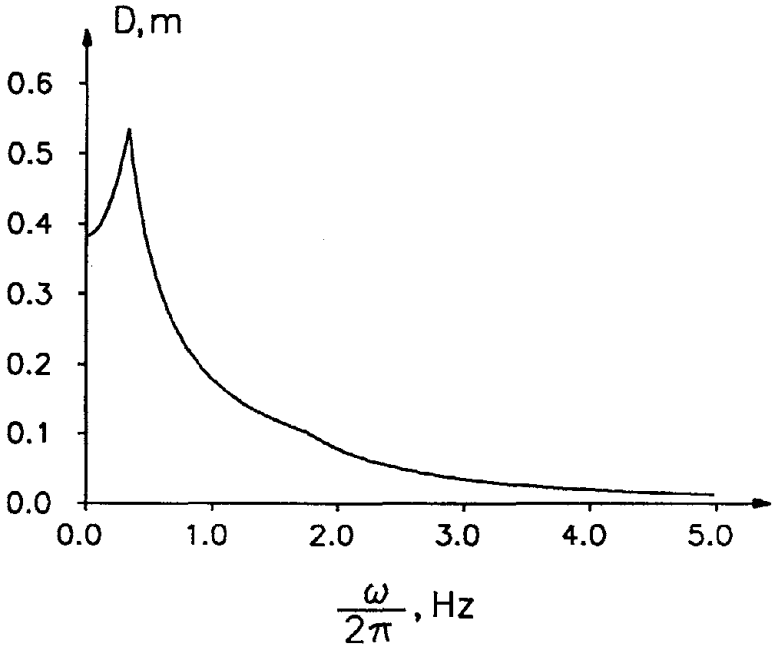

Figure 4.1 Design Relative Displacement Response Spectrum

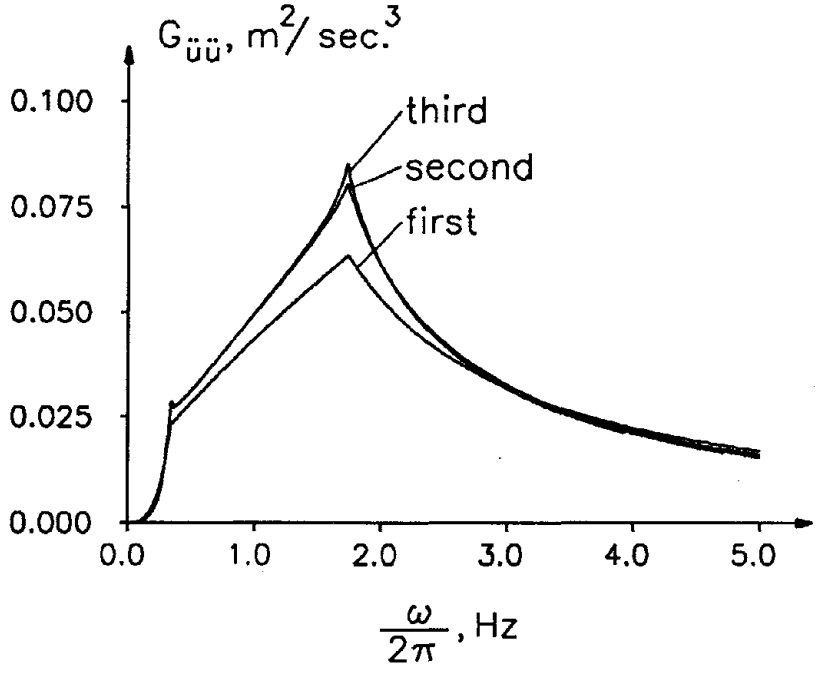

Figure 4.2 Successive Approximations of the Response-Spectrum-Consistent PSD of Ground Acceleration

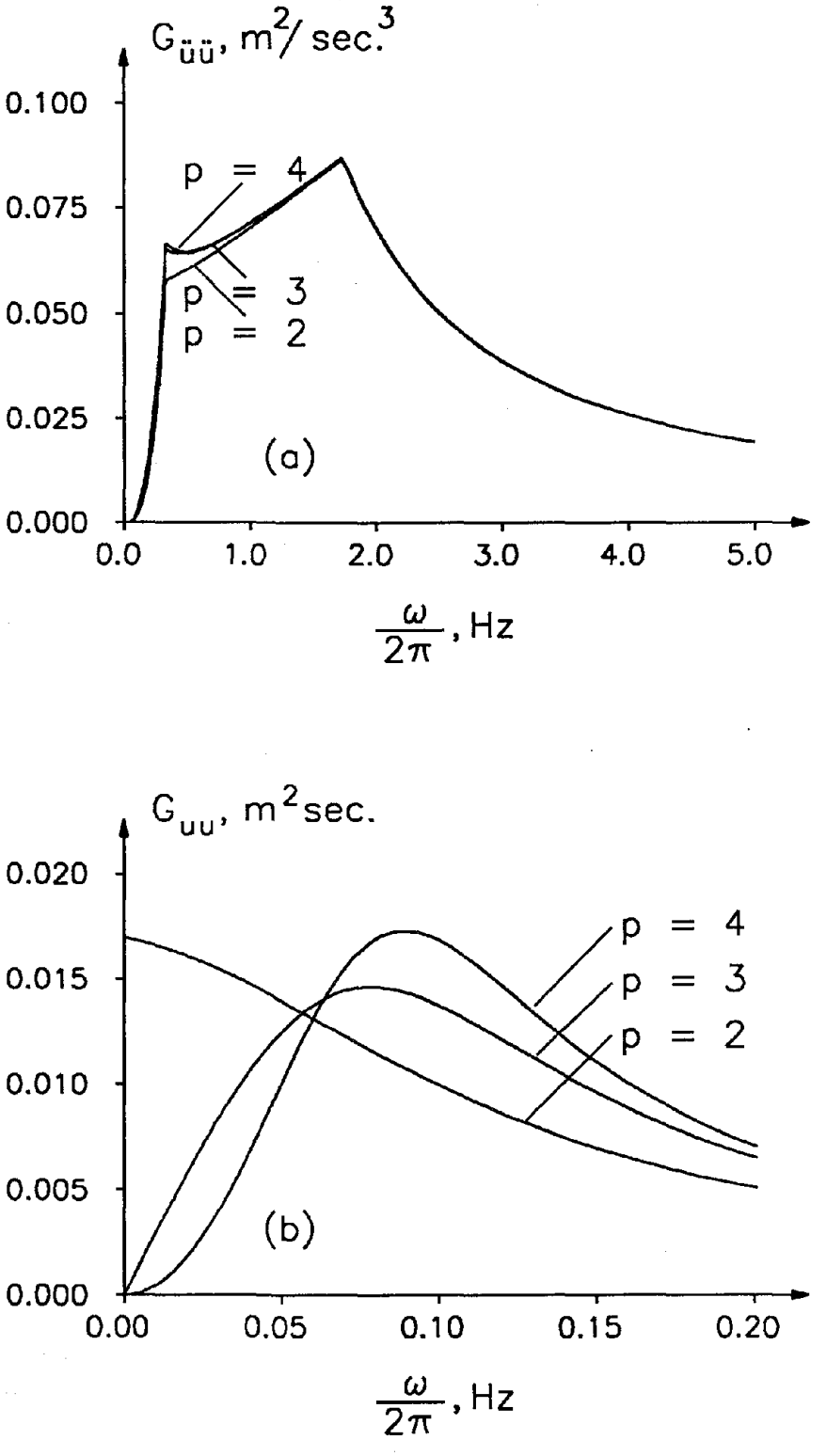

Figure 4.3 First-Order Approximations of the Response-Spectrum-Consistent PSD for Different Values of the Parameter p: (a) Acceleration PSD; (b) Displacement PSD

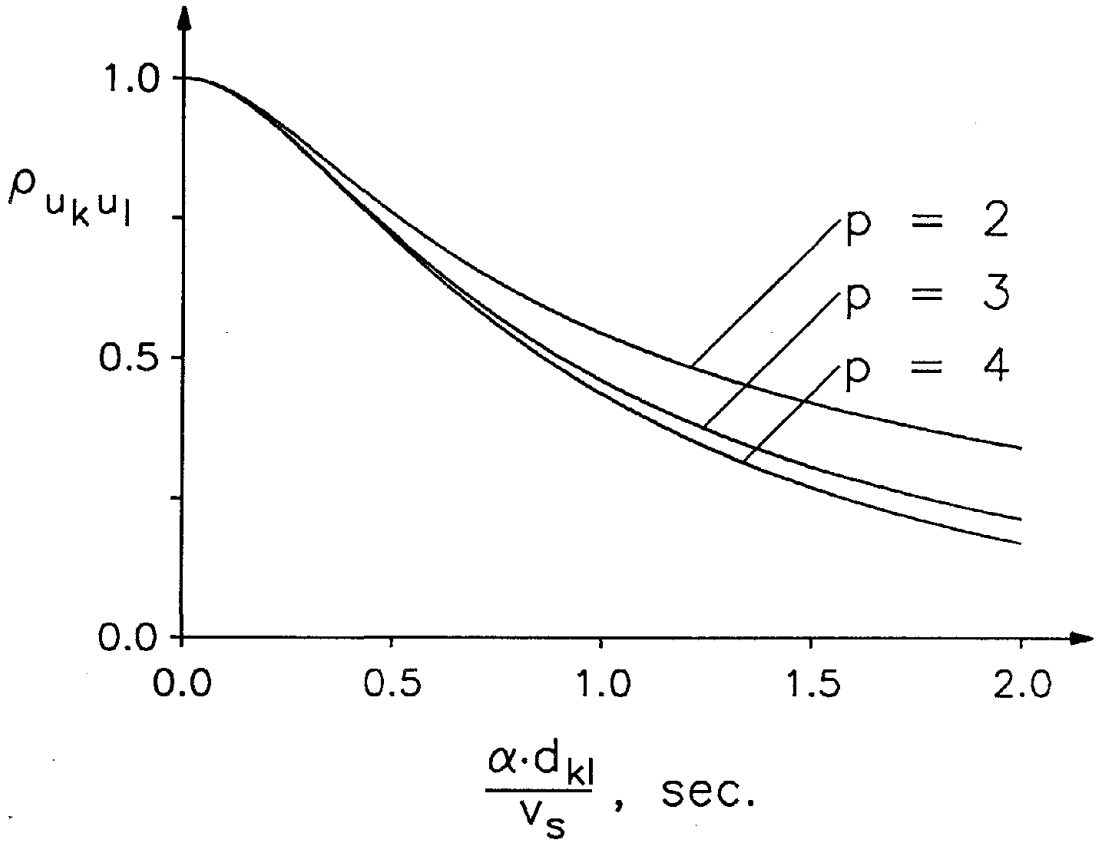

Figure 4.4 Cross-Correlation Coefficient Between Ground Displacements at Stations k and l for Different Values of the Parameter p

CHAPTER 5
EXAMPLE APPLICATION

5.1 Introduction

In this chapter, the proposed response spectrum method is applied to the analysis of an example structure with multiple support excitations. The analysis has two objectives: (a) to demonstrate the application of the method, and (b) to investigate the significances and influences of various factors. Specifically, parametric studies are performed to demonstrate the relative significance of the pseudo-static and dynamic components of the response, to evaluate the effects of wave passage and incoherence, and to determine the importance of the cross-correlation terms. The example structure is purposely taken to be a simple one so as to allow a comprehensive parametric investigation. Application to a more complex bridge structure is now underway and will be reported in a separate study.

5.2 Description of the Example Structure

For the example structure, we consider the two-span continuous beam in Fig. 5.1, which has uniform mass and stiffness properties and simple supports. Although a continuous beam theory may be used to analyze the dynamic response, we employ the finite element method since for a more complex problem this would be the only practical approach. As shown in Fig. 5.1, the beam is discretized into 20 elements along each $L=50\,m$ span and the mass of each element is lumped half at each end of the element. The system, thus, is represented by 38 translational and 41 rotational degrees of freedom (i.e., $n=79$), and 3 translational support degrees of freedom (i.e., $m=3$). Since no mass moments of inertia are associated with the rotational degrees of freedom, the latter are condensed out and the system analyzed has 38 degrees of freedom. The mesh size considered is found to give an accurate representation of the first four modes obtained from the continuous beam theory, which are shown in Fig. 5.2. The higher modes were found to make negligible contributions to the dynamic response.

Two values of the fundamental period of the beam are considered: $T=1\,s$ and $T=1/4\,s$. These are obtained for $EI/m=2.53\times10^6$ and $40.5\times10^6\ m^4/s^2$, respectively, where EI denotes the flexural rigidity and m denotes the mass per unit length of the beam. The resulting frequencies of the first four modes are as listed in Table 5.1. In the following discussion, we refer to the above two cases as the "flexible beam" and the "stiff beam" cases, respectively. The modal damping ratio is assumed to be 5 percent in all modes.

Five response quantities are considered for the analysis: the mid-span deflections u_1 and u_2, the bending moment M at the middle support, and the shear forces V_1 and V_2 at the faces of the middle support. For the convenience of notation, these response quantities are scaled and collected in a dimensionless response vector **z** defined as

$$\mathbf{z} = \begin{Bmatrix} z_1 \\ z_2 \\ z_3 \\ z_4 \\ z_5 \end{Bmatrix} = 10^3 \times \begin{Bmatrix} \frac{u_1}{L} \\ \frac{u_2}{L} \\ \frac{LM}{EI} \\ \frac{L^2 V_1}{EI} \\ \frac{L^2 V_2}{EI} \end{Bmatrix} \tag{5.1}$$

Although the beam is symmetric, the two midspan deflections and the shear forces on both sides of the middle support are considered, because different results are obtained for these pairs of responses when the wave passage effect is considered.

5.3 Description of Support Excitations

The motion at each support is assumed to be vertical, and the corresponding influence vectors, $\mathbf{r}_k$ $k=1$, 2 and 3, are shown in Fig. 5.3. The effective influence coefficients, a_k, and modal participation factors, b_{ki}, respectively defined in Eqs. 2.10 and 2.11, are listed in Tables 5.2 and 5.3, respectively.

It is assumed that the soil conditions at the three supports are identical and that the mean response spectrum is as defined in Fig. 4.1, which is the spectrum specified by SEAOC (1990) with an extension for frequencies below 0.33 Hz. The consistent power spectral density is assumed to be the one in Eq. 4.10 with $p=3$ as the parameter. This power spectral density is only used in determining the cross-correlation coefficients $\rho_{u_k u_l}$, $\rho_{u_k s_{lj}}$ and $\rho_{s_{ki} s_{lj}}$, and as shown in the preceding chapter it is not critical to know its exact shape.

Five different cases are considered for the coherency function $\gamma_{kl}(\mathrm{i}\omega)$ describing the variation between the support motions:

Case 1: Fully coherent motions at all three supports, i.e., $\gamma_{kl}(\mathrm{i}\omega)=1$.

Case 2: Only wave passage effect included (i.e., $\alpha=0$) with $v_{app}=400\,m/s$.

Case 3: Only incoherence effect included (i.e., $v_{app}=\infty$) with $v_s/\alpha=600\,m/s$.

Case 4: Both wave passage and incoherence effects included with $v_{app}=400\,m/s$ and $v_s/\alpha=600\,m/s$.

Case 5: Mutually statistically independent support motions, i.e., $\gamma_{kl}(\mathrm{i}\omega)=0$ for $k\neq l$.

For cases 2 and 4, it is assumed that the waves propagate in the direction from support 1 to support 3; hence, $d_{kl}^L=d_{kl}$ for the present case. The results for the various cases are compared to determine the relative influences of the wave passage and incoherence effects, as well as to determine the consequences of assuming uniform excitations (Case 1) or independent excitations (Case 5). The latter

cases are commonly assumed in the current practice.

5.4 Description of the Results

We first examine the cross-correlation coefficients $\rho_{u_k u_l}$, $\rho_{u_k s_{lj}}$ and $\rho_{s_{ki} s_{lj}}$.

Table 5.4 lists the results for $\rho_{u_k u_l}$, the cross-correlation coefficient between the ground displacements at the various pairs of supports. These coefficients are independent of the direction of wave propagation and hence identical results are obtained for support pairs such as 1,2 and 2,1. The correlation coefficients for Case 1 are unity, because the motions are perfectly correlated, and for Case 5 they are zero, because the motions are statistically independent. The remaining cases correspond to conditions of partial correlation, and $\rho_{u_k u_l}$ is found to be between zero and 1.0. It is interesting to note that the correlation coefficients between the ground displacements for the latter cases are large even for supports 1 and 3 that are $100\,m$ apart.

Table 5.5 lists the cross-correlation coefficients $\rho_{u_k s_{lj}}$ between the displacement at support k and the response of an oscillator at support l. This coefficient is not symmetric with respect to k and l when the wave passage effect is present and, hence, for cases 2 and 4 different values are obtained for each ordered combination of support pairs, e.g., for 1,2 and 2,1. The cross-correlation is found to be relatively small (<0.2) for all cases and modes of both the "flexible" and "stiff" systems. The influences of the wave passage and incoherence effects can be observed separately by comparing the results for Cases 1 and 2 and Cases 1 and 3, respectively, whereas their combined influence can be observed by comparing Cases 1 and 4. It is interesting to note that the results for ordered pairs k, l and l, k are very different for certain modes when the wave passage effect is present, e.g., the first two modes of the "flexible" beam.

Table 5.6 lists the cross-correlation coefficients $\rho_{s_{ki} s_{lj}}$ between the responses of the oscillators at supports k and l. For each case and pair of supports, a 4×4 correlation matrix is given in the table. In Cases 2 and 4 where the wave passage effect is included, the matrix is asymmetric and is given fully. In Cases 1, 3 and 5 the matrix is symmetric and only the upper triangle is given. In Cases 2 and 4, the correlation matrices for support combinations 2,1, 3,2 and 3,1 can be obtained by use of the symmetry rule $\rho_{s_{ki} s_{lj}} = \rho_{s_{lj} s_{ki}}$, as indicated in the footnote to the table. It is found that the cross-correlation between any pair of modes is small when the wave passage effect is not included, except for modes with high frequencies (e.g., modes 3 and 4 of the "stiff" system). However, in presence of the wave passage effect, the cross-correlation coefficient for certain pairs of modes is relatively large (e.g., modes 1 and 2 of the "flexible" beam in Case 2 for the support combination 1,3) and in many cases it is negative. These are due to the oscillatory nature of this coefficient relative to the frequencies of the two modes as was observed in Figs. 3.9 and 3.10.

The mean values of the peak responses z_1-z_5 are listed in Tables 5.7 and 5.8 for the "flexible" and "stiff" beams, respectively. The total response for each case, denoted z_t and representing the result obtained from the combination rule in Eq. 4.2, is listed in the third column. Note that the pair of values for the midspan displacement responses z_1 and z_2, and for the middle support shear forces z_4 and z_5 are identical for Cases 1, 3 and 5 due to the symmetry of the beam and the absence of the wave passage effect. In Cases 2 and 4, these pairs of responses are different, in spite of the symmetry of the beam, due to the directionality of the wave passage effect.

In the fourth columns of Table 5.7 and 5.8 are listed the ratios of the total response to the total response for Case 1. These ratios indicate the influence of the spatial variability on each of the response quantities. By comparing Cases 2 and 3, it is apparent that the influence of the wave passage effect is greater than that of the incoherence effect for both the "flexible" and "stiff" beams (i.e., the ratios for Case 2 are smaller than the corresponding ratios for Case 3), except for responses z_1 and z_4 of the "flexible" beam. For Case 4, which includes both the wave passage and the incoherence effects, the combined influence in some cases is smller (i.e., the ratio is closer to 1.0) than in the individual cases just mentioned. In fact, for response z_3 of the "stiff" beam, the ratio for Case 4 is greater than unity (i.e., the response is amplified due to the spatial variability of the ground motion), whereas in Cases 2 and 3 the ratios are smaller than unity. This is due to the elimination of certain negative cross-correlation terms arising from the wave passage effect by the incoherence effect. All ratios for Cases 2-4 are smaller than unity, except the case just mentioned, indicating that the spatial variability tends to reduce the total response for both systems. This reduction is insignificant for responses z_1 and z_2 (the midspan deflections), but rather significant for the responses z_3-z_5 (the bending moment and shear forces at the middle support). The former is due to the dominance of the pseudo-static component of the displacement response as described below.

As evident from the response z_3 of the "stiff" beam in Case 4, reduction in the response due to the spatial variability effect is not a general rule. One may expect large pseudo-static response to be generated in a stiff structure when there is a rapid loss of coherency in the ground motion. Such pseudo-static response may lead to a larger total response compared with the response for uniform support motions (Case 1). This is evident in Table 5.8 for Case 5 with uncorrelated support motions, where the ratios for the responses z_3-z_5 are greater than unity for the "stiff" beam. Nevertheless, from the results in Tables 5.7 and 5.8, one may conclude that the effect of spatial variability is more likely to reduce the response (compared with the uniform motion case) than to amplify it.

The last three columns of Tables 5.7 and 5.8 list ratios of the three terms inside the square brackets in Eq. 4.2 with respect to the square of the total response. They indicate the relative contributions of the pseudo-static part (the double-sum term), the cross term between the pseudo-static and dynamic parts (the triple-sum term), and the dynamic part (the quadruple-sum term) to the square of the response. Note that the numbers in each row of the three columns add up to 1.0. Also note that for

Case 1 the pseudo-static and cross terms are zero for the force responses z_3-z_5, since rigid body motions of the beam do not generate internal forces.

From the results in the last three columns of Tables 5.7 and 5.8, the displacement responses z_1 and z_2 are found to be dominated by the pseudo-static part, especially for the "stiff" beam. It is interesting to note that for these responses the cross term between the pseudo-static and dynamic parts is negative. The bending moment and shear force responses z_3-z_5 are primarily dominated by the dynamic part of the response, except in Case 5 for the "stiff" beam. The cross term between the pseudo-static and dynamic parts for these responses is positive and in many cases is greater than the contribution of the pseudo-static component alone. However, in most cases the contribution of the cross term can be neglected with little effect on the total response.

5.5 Concluding Remarks

The results for the above example show that the influence of spatial variability of the ground motion on the response of a multiply-supported structure can be significant. In the present case, this influence results in a reduction of the peak response, in some instances by almost 30 percent. However, this trend cannot be generalized since for stiffer structures and in cases of rapid loss of incoherence, the response can be amplified due to the increased contribution of the pseudo-static part of the response.

Table 5.1 Modal Frequencies

mode	ω_i, rad/s	
	"flexible" beam	"stiff" beam
1	6.28	25.13
2	9.82	39.30
3	25.13	100.57
4	31.80	127.26

Table 5.2 Effective Influence Factors a_k

support	response				
	z_1	z_2	z_3	z_4	z_5
1	8.12	−1.88	−30.0	30.0	−30.0
2	13.76	13.76	60.0	−60.0	60.0
3	−1.88	8.12	−30.0	30.0	−30.0

Table 5.3 Effective Modal Participation Factors b_{ki}

response	support	mode 1	2	3	4
z_1	1	−6.35	−5.04	0	1.13
	2	0	−14.7	0	−3.23
	3	6.35	−5.04	0	1.13
z_2	1	6.35	−5.04	0	1.13
	2	0	−14.7	0	−3.23
	3	−6.35	−5.04	0	1.13
z_3	1	0	108	0	−198
	2	0	314	0	566
	3	0	108	0	−198
z_4	1	−197	−423	777	1400
	2	0	−1235	0	−4000
	3	197	−423	−777	1400
z_5	1	−197	423	777	−1400
	2	0	1235	0	4000
	3	197	423	−777	−1400

Table 5.4 Cross-Correlation Coefficients $\rho_{u_k u_l}$

case	supports (k, l) 1,1; 2,2; 3,3	1,2; 2,1; 2,3; 3,2	1,3; 3,1
1	1	1	1
2	1	0.980	0.925
3	1	0.983	0.940
4	1	0.965	0.885
5	1	0	0

Table 5.5 Cross-Correlation Coefficients $\rho_{u_k s_{ij}}$

case	supports	modes of "flexible" beam				modes of "stiff" beam			
		1	2	3	4	1	2	3	4
1 all	any k,l $k=l$	0.140	0.113	0.118	0.121	0.118	0.124	0.165	0.177
2	1,2 and 2,3	0.102	0.080	0.092	0.095	0.091	0.098	0.133	0.143
	2,1 and 3,2	0.176	0.134	0.095	0.094	0.095	0.097	0.134	0.144
	1,3	0.074	0.057	0.062	0.064	0.062	0.067	0.089	0.098
	3,1	0.179	0.097	0.063	0.069	0.063	0.068	0.090	0.098
3	1,2 and 2,3	0.138	0.106	0.101	0.103	0.101	0.105	0.142	0.153
	1,3	0.123	0.086	0.081	0.083	0.081	0.086	0.114	0.123
4	1,2 and 2,3	0.105	0.083	0.089	0.091	0.089	0.094	0.126	0.136
	2,1 and 3,2	0.162	0.112	0.090	0.092	0.090	0.095	0.127	0.137
	1,3	0.080	0.062	0.063	0.065	0.063	0.068	0.089	0.097
	3,1	0.119	0.068	0.064	0.066	0.064	0.068	0.090	0.098
5	any $k \neq l$	0	0	0	0	0	0	0	0

Table 5.6 Cross-Correlation Coefficients $\rho_{s_{ki}s_{lj}}$

case	supports	mode number	modes of "flexible" beam 1	2	3	4	modes of "stiff" beam 1	2	3	4
1	any k, l	1	1	0.020	−0.014	−0.012	1	0.155	0.192	0.204
		2		1	0.011	0.013		1	0.254	0.269
all	$k=l$	3			1	0.242			1	0.523
		4				1				1
2	1,2 and 2,3[a]	1	0.708	0.192	0.095	0.095	−0.776	0.081	0.000	−0.001
		2	−0.154	0.357	0.190	0.181	−0.031	0.050	0.014	0.011
		3	−0.028	−0.044	−0.776	−0.114	0.013	−0.209	0.336	−0.008
		4	−0.021	−0.028	0.059	−0.551	0.015	−0.209	0.056	−0.224
	1,3[b]	1	0.025	0.224	0.147	0.147	0.625	−0.025	−0.037	−0.040
		2	−0.141	−0.688	0.118	0.116	−0.006	−0.542	−0.033	−0.037
		3	−0.009	−0.010	0.625	0.064	−0.047	−0.100	0.125	−0.044
		4	−0.018	−0.028	−0.187	−0.008	−0.051	−0.099	−0.029	0.060
3	1,2 and 2,3	1	0.763	0.022	0.017	0.018	0.087	0.072	0.097	0.102
		2		0.529	0.044	0.045		0.068	0.093	0.098
		3			0.087	0.073			0.126	0.133
		4				0.071				0.142
	1,3	1	0.355	0.031	0.030	0.031	0.025	0.026	0.036	0.038
		2		0.100	0.031	0.031		0.026	0.037	0.039
		3			0.025	0.025			0.051	0.055
		4				0.025				0.059
4	1,2 and 2,3[a]	1	0.548	0.138	0.076	0.076	0.017	0.028	0.040	0.042
		2	−0.084	0.206	0.104	0.101	0.031	0.032	0.045	0.048
		3	−0.013	−0.010	0.017	0.029	0.046	0.047	0.066	0.070
		4	−0.012	−0.008	0.027	0.029	0.049	0.050	0.070	0.075
	1,3[b]	1	0.037	0.073	0.050	0.051	0.008	0.009	0.012	0.013
		2	−0.017	−0.037	0.015	0.016	0.009	0.010	0.013	0.014
		3	−0.002	0.003	0.008	0.009	0.013	0.014	0.019	0.021
		4	−0.002	0.003	0.008	0.009	0.014	0.015	0.021	0.022
5	any $k \neq l$	1	0	0	0	0	0	0	0	0
		2		0	0	0		0	0	0
		3			0	0			0	0
		4				0				0

a The correlation matrix for support combinations 2,1 and 3,2 is the transpose of the matrix for the combinations 1,2 and 2,3.

b The correlation matrix for support combination 3,1 is the transpose of the matrix for the combination 1,3.

Table 5.7 Mean of Peak Responses of the "Flexible" Beam

response	case	z_t	$z_t/z_{t,case\ 1}$	ss/z_t^2	$s\text{-}d/z_t^2$	dd/z_t^2
	1	7.86	1	0.950	−0.080	0.130
	2	7.85	0.999	0.948	−0.090	0.142
z_1	3	7.80	0.993	0.960	−0.080	0.120
	4	7.78	0.990	0.962	−0.090	0.128
	5	6.36	0.809	0.938	−0.088	0.150
	1	7.86	1	0.950	−0.080	0.130
	2	7.71	0.981	0.983	−0.069	0.086
z_2	3	7.80	0.993	0.960	−0.080	0.120
	4	7.73	0.984	0.974	−0.071	0.097
	5	6.36	0.809	0.938	−0.088	0.150
	1	60.6	1	0	0	1
	2	46.3	0.764	0.001	0.015	0.984
z_3	3	51.4	0.848	0.001	0.009	0.990
	4	45.4	0.749	0.003	0.022	0.975
	5	51.2	0.845	0.302	0.066	0.632
	1	238	1	0	0	1
	2	212	0.891	0.000	0.004	0.996
z_4	3	211	0.884	0.000	0.003	0.997
	4	198	0.832	0.000	0.007	0.993
	5	180	0.753	0.025	0.026	0.949
	1	238	1	0	0	1
	2	180	0.753	0.000	0.004	0.996
z_5	3	211	0.884	0.000	0.003	0.997
	4	181	0.760	0.000	0.004	0.995
	5	180	0.753	0.025	0.026	0.949

z_t total value of the peak response

$z_{t,case\ 1}$ total value of the peak response for Case 1

ss pseudo-static part of the squared response (first term inside brackets in Eq. 4.2)

s-d cross term between pseudo-static and dynamic parts of the squared response (second term inside brackets in Eq. 4.2)

dd dynamic part of the squared response (third term inside brackets in Eq. 4.2)

Table 5.8 Mean of Peak Responses of the "Stiff" Beam

response	case	z_t	$z_t/z_{t,case\ 1}$	ss/z_t^2	$s\text{-}d/z_t^2$	dd/z_t^2
	1	7.63	1.000	1.006	−0.006	0.001
	2	7.62	0.998	1.006	−0.007	0.000
z_1	3	7.62	0.999	1.006	−0.007	0.001
	4	7.61	0.997	1.006	−0.007	0.001
	5	6.13	0.804	1.006	−0.008	0.001
	1	7.63	1.000	1.006	−0.006	0.001
	2	7.62	0.998	1.006	−0.006	0.001
z_2	3	7.62	0.999	1.006	−0.007	0.001
	4	7.61	0.997	1.006	−0.006	0.001
	5	6.13	0.804	1.006	−0.008	0.001
	1	4.23	1	0	0	1
	2	3.60	0.853	0.138	0.269	0.594
z_3	3	3.68	0.870	0.184	0.178	0.638
	4	4.34	1.027	0.361	0.198	0.441
	5	28.5	6.739	0.975	0.015	0.010
	1	16.7	1	0	0	1
	2	11.9	0.714	0.013	0.108	0.880
z_4	3	13.4	0.802	0.014	0.057	0.929
	4	13.6	0.817	0.037	0.088	0.875
	5	31.7	1.902	0.787	0.056	0.157
	1	16.7	1	0	0	1
	2	12.7	0.764	0.011	0.088	0.901
z_5	3	13.4	0.802	0.014	0.057	0.929
	4	13.6	0.814	0.037	0.087	0.876
	5	31.7	1.902	0.787	0.056	0.157

z_t total value of the peak response

$z_{t,case\ 1}$ total value of the peak response for Case 1

ss pseudo-static part of the squared response (first term inside brackets in Eq. 4.2)

s-d cross term between pseudo-static and dynamic parts of the squared response (second term inside brackets in Eq. 4.2)

dd dynamic part of the squared response (third term inside brackets in Eq. 4.2)

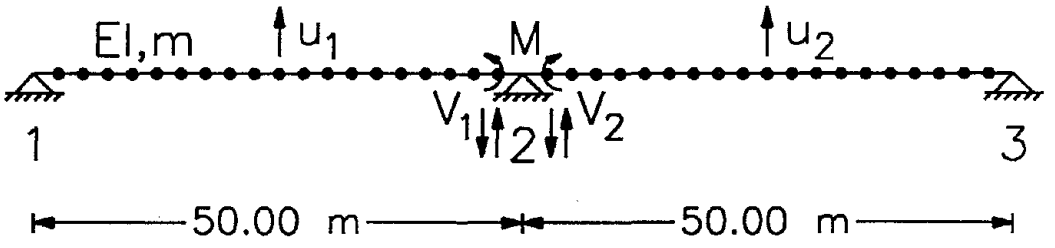

Figure 5.1 Example Structure

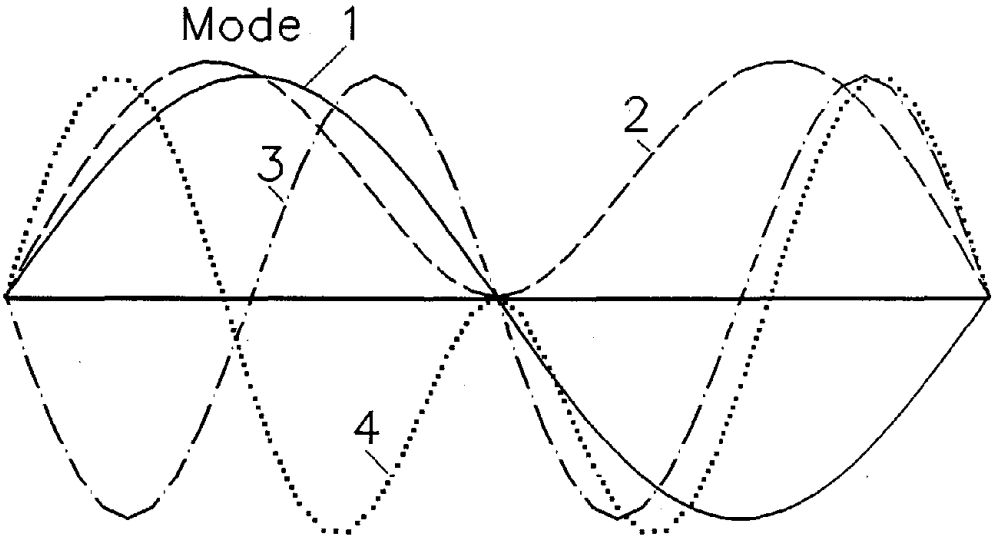

Figure 5.2 First Four Mode Shapes of Example Structure

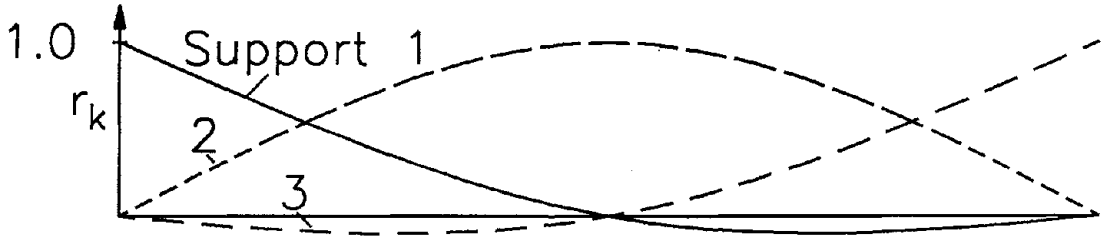

Figure 5.3 Influence Vectors for Vertical Support Motions

CHAPTER 6
SUMMARY AND CONCLUSIONS

6.1 Summary

A new response spectrum method is developed for seismic analysis of linear multi-degree-of-freedom, multiply-supported structures subjected to spatially varying ground motions. Variations of the ground motion due to wave passage, loss of coherency with distance, and variation of local soil conditions are considered. The former two effects are modeled in terms of a coherency function, whereas the local soil effect is considered in terms of its influence on the response spectral shape at each individual support point. The method is based on fundamental principles of random vibration theory and properly accounts for the effects of correlation between the support motions as well as between the modal responses of the structure.

In the proposed method, the peak response is given in terms of a simple combination rule involving a set of structure-dependent coefficients (effective influence factors and effective modal participation factors), the mean peak ground displacement at each support degree of freedom, the mean response spectral ordinate associated with each support degree of freedom and each mode of the structure, and a set of cross-support and cross-mode correlation coefficients that account for the spatial variability of the ground motion and the cross-correlation between the modal responses. The latter coefficients are completely determined in terms of the individual support response spectra and the coherency function describing the nature of the spatial variability of the ground motion. The combination rule explicitly accounts for the contributions of the pseudo-static and dynamic components of the response, as well as for their covariance.

A comprehensive analysis of the required cross-correlation coefficients is carried out to investigate the influences of the wave passage and loss of coherency effects, as well as the effect of local site conditions. It is found that the cross-correlation coefficients involved in the covariance between the pseudo-static and dynamic contributions of the response are generally small, whereas the cross-correlation coefficients involved in the terms representing the pseudo-static and dynamic components can be significant even for distant supports and well spaced modes.

The new method is applied to an example structure with three supports. The example demonstrates the influence of the spatial variability of the ground motion on selected responses of the structure, and examines the relative contributions of the pseudo-static, dynamic, and their covariance terms to the total response. It is found that in most cases the spatial variability tends to reduce the response (in relation to the case with uniform support motions), often by a significant amount (e.g., by close to 30 percent). However, this rule cannot be generalized since, under certain conditions (i.e., stiff structures and rapid loss of coherency) the response may actually amplify due to an increase in the pseudo-

static component of the response. Therefore, a proper accounting of the spatial variability effect in seismic analysis of multiply-supported structures is essential. The response spectrum method developed offers a simple and accurate alternative for this purpose.

6.2 Conclusions

The major conclusions of this study can be summarized as follows:

1. The response spectrum method developed offers a simple and practical alternative for seismic analysis of multiply-supported structures subjected to spatially varying ground motions. The method provides an accurate estimate of the peak response in terms of quantities of the input motions that are usually available to the designer, i.e., peak ground motions and response spectra at the support points, and the coherency function describing the nature of the spatial variability of the ground motion. The effects of wave passage, loss of coherence, and local soil conditions are all included in the analysis. No time-history analysis or specification of power spectral densities is necessary.

2. The response of the multiply-supported structure consists of three components: a pseudo-static component, a dynamic component, and a cross term representing the covariance between the two components. The cross term is usually small in relation to the pseudo-static and dynamic components. The relative contribution of the pseudo-static component is more significant for stiffer structures and for ground motions with more rapid loss of coherency.

3. It is found that the spatial variability of the ground motion may reduce the response, in relation to the case of uniform support motions, by a significant amount, i.e., close to 30 percent for the example structure studied. However, this rule is not general, since the response may actually amplify due to the increased contribution of the pseudo-static response, when the structure is stiff and there is a rapid loss of coherency.

4. The influences of wave passage and incoherency on the modal cross-correlations appear to be fundamentally different. In the presence of wave passage, the cross-support cross-modal correlations tend to oscillate with distance and frequency, whereas in presence of incoherence these correlations tend to uniformly decay with increasing distance and frequency. Generally speaking, the cross-correlation coefficients involved in the covariance term between the pseudo-static and dynamic components of the response are small (e.g., less than about 0.2). However, the cross-correlation coefficients involved in the terms for the pseudo-static and dynamic components of the response can be significant, even for distant supports and well spaced modes.

5. The response spectrum method developed can account for cross-correlations between any pair of ground motion components at any two stations. While recent research has investigated the coherency between similar pairs of components (e.g., both horizontal and in the longitudinal

direction of wave passage), the coherency between dissimilar components, e.g., one longitudinal and one transverse, or one horizontal and one vertical, at two stations has not been investigated. The present work clearly demonstrates the need for such research.

6. The response spectrum method developed can also account for the dependence of the coherency function on the local soil conditions. Such site-dependent coherency functions unfortunately are not available and existing data may not be sufficient to make such refined estimates. However, if and when such data become available, the proposed method provides a framework for incorporating this effect in the analysis.

7. The present work clearly demonstrates the need for a better understanding of ground motions in the low-frequency range. This need arises from the pseudo-static component of the response, which involves terms related to the ground displacement. Specifically, it is necessary to extend existing design response spectra in the range of lower frequencies, and to develop means for the specification of peak ground displacements for design purposes. Development of coherency functions for the components of ground displacement (in addition to the acceleration components) is also desirable.

REFERENCES

1. Abdel-Ghaffar, A., and L.I. Rubin (1982). Suspension bridge response to multiple-support excitations. *J. Eng. Mech*, 108, 419-435.

2. Abrahamson, N. A., and B.A. Bolt (1985). The spatial variation of the phasing of seismic strong ground motion. *Bull. Seism. Soc. America*, 75, 1247-1264.

3. Abrahamson, N. A., and B.A. Bolt (1987). The SMART-1 accelerograph array (1980-1987): a review. *Earthq. Spectra*, 3(2), 263-287.

4. Abrahamson, N.A., J.F. Schneider, and J.C. Stepp (1991). "Empirical spatial coherency functions for application to soil-structure interaction analysis." *Earthq. Spectra*, 7, 1-28.

5. Asfura, A., and A. Der Kiureghian (1986). "Floor response spectrum method for seismic analysis of multiply supported secondary systems." *Earthq. Eng. Struct. Dyn.*, 14, 245-265.

6. Berrah, M., and E. Kausel (1989). "Modified response spectrum model for the design of structures subjected to spatially varying seismic excitations." *Report R90-2, Department of Civil Engineering, MIT, Cambridge, Mass.*

7. Bogdanoff, J.L., J.E. Goldberg and A.J. Schiff (1965). "The effect of ground transmission time on the response of long structures." *Bull. Seism. Soc. America*, 55, 627-640.

8. Bolt, B.A., C.H. Loh, J. Penzien, Y.B. Tsai and Y.T. Yeh (1982a). Preliminary report on the SMART 1 strong motion array in Taiwan. *Report UCB/EERC-82/13*, Earthquake Engineering Research Center, University of California at Berkeley, Berkeley, CA.

9. Bolt, B.A., C.H. Loh, J. Penzien, Y.B. Tsai and Y.T. Yeh (1982b). Earthquake strong motions recorded by a large near-source array of digital seismographs. *Earthq. Eng. Struc. Dynamics*, 10, 561-573.

10. Christian, J.T. (1989). "Generating seismic design power spectral density functions." *Earthq. Spectra*, 5, 351-368.

11. Clough, R.W., and J. Penzien (1975). *Dynamics of structures.* McGraw-Hill Book Co., New York, NY.

12. Der Kiureghian, A. (1980). "Structural response to stationary excitation." *J. Eng. Mechanics Division*, ASCE, 106, 1195-1213.

13. Der Kiureghian, A. (1981). "A response spectrum method for random vibration analysis of MDF systems." *Earthq. Eng. Struct. Dyn.*, 9, 419-435.

14. Der Kiureghian, A. (1991). "CQC modal combination rule for high-frequency modes." *Trans. 11th Int. Conf. on Struct. Mech. in Reactor Technology*, Tokyo, Japan, August, K, .

15. Dong, K.K., and M. Wieland (1988). "Application of response spectrum method to a bridge subjected to multiple support excitation." *Proc. 9th World Conf. Earthq. Eng.*, Tokyo, Japan, VI, 531-536.

16. Hao, H. (1989). Effects of spatial variation of ground motions on large multiply-supported structures. *Report UCB/EERC-89/06*, Earthquake Engineering Research Center, University of California at Berkeley, Berkeley, CA.

17. Hao, H., C.S. Olivera, and J. Penzien (1989). "Multiple-station ground motion processing and simulation based on SMART-1 array data." *Nuclear Eng. and Design*, 111, 293-310.

18. Harichandran, R.S., and E. Vanmarcke (1986). "Stochastic variation of earthquake ground motion in space and time." *J. Eng. Mechanics*, ASCE, 112, 154-174.

19. Harichandran, R.S., and W. Wang (1988a). "Response of simple beam to spatially varying earthquake excitation." *J. Eng. Mechanics*, ASCE, 114, 1526-1541.

20. Harichandran, R.S., and W. Wang (1988b). "Response of indeterminate two-span beams to spatially varying seismic excitation." *Earthq. Eng. Struct. Dyn.*, 19, 173-187.

21. Housner, G., et al. (1990). *Competing against time.* Report to Governor George Deukmejian from The Governor's Board of Inquiry on the 1989 Loma Prieta Earthquake, C.C. Thiel Jr., Ed., Department of General Services, State of California, North Highlands, Cal.

22. Igusa, T., and A. Der Kiureghian (1983). Response spectrum method for systems with non-classical damping. *Proceedings of ASCE-EMD Specialty Conference, West Lafayette, Indiana, 380-384.*

23. Igusa, T., and A. Der Kiureghian (1985). "Generation of floor response spectra including oscillator-structure interaction." *Earthq. Eng. Struct. Dyn.*, 13, 661-676.

24. Johnson, N.E., and R.D. Gallety (1972). "The comparison of the response of a highway bridge to uniform ground shock and moving ground excitation." *Shock Vibration Bull.*, 42, 75-85.

25. Kaul, M.K. (1978). "Stochastic characterization of earthquakes through their response spectrum." *Earthq. Eng. Struc. Dynamics*, 6, 497-509.

26. Lin, Y.K. (1967). *Probabilistic theory of structural dynamics.* McGraw-Hill, New York, NY.

27. Loh, C.H., J. Penzien, and Y.B. Tsai (1982). Engineering analysis of SMART-1 array accelerograms. *Earthq. Eng. Struc. Dynamics*, 10, 575-591.

28. Loh, C.H., and Y.T. Yeh (1988). Spatial variation and stochastic modeling of seismic differential ground movement. *Earthq. Eng. Struc. Dynamics*, 16, 583-596.

29. Luco, J.E., and H.L. Wong (1986). "Response of a rigid foundation to a spatially random ground motion." *Earthq. Eng. Struc. Dynamics*, 14, 891-908.

30. Masri, S. (1976). "Response of beams to propagating boundary excitation." *Earthq. Eng. Struc. Dynamics*, 4, 497-509.

31. Newmark, N., and W.J. Hall (1969). "Seismic design criteria for nuclear reactor facilities." *Proc. 4th World Conf. Earthq. Eng.*, Santiago, Chile, II, 37-50.

32. Smeby, W., and A. Der Kiureghian (1985). "Modal combination rules for multicomponent earthquake excitation." *Earthq. Eng. Struct. Dyn.*, 13, 1-12.

33. Penzien, J. and M. Watabe (1975). Characteristics of 3-dimensional earthquake ground motion." *Earthq. Eng. Struct. Dyn.*, 3, 365-374.

34. Rosenblueth, E., and J. Elorduy (1969). "Response of linear systems to certain transient disturbances." *Proc. 4th World Conf. Earthq. Eng.*, Santiago, Chile, I, 185-196.

35. SEAOC (1990). *Recommended lateral force requirements and commentary.* Structural Engineers Association of California, Sacramento, CA.

36. Singh, M.P. and S.L. Chu (1976). "Stochastic considerations in seismic analysis of structures." *Earthq. Eng. Struct. Dyn.*, 4, 295-307.

37. Unruh, J.F., and D.D. Kana (1981). "An alternative procedure for the generation of consistent power/response spectrum." *Nuclear Eng. and Design*, 66, 427-435.

38. Werner, S.D., L.C. Lee, H.L. Wong and M.D. Trifunac (1979). "Structural response to traveling seismic waves." *J. Structural Division*, ASCE, 105, 2547-2564.

39. Wilson, E.L., A. Der Kiureghian and E.P. Bayo (1981). A replacement for the SRSS method in seismic analysis. *Earthq. Eng. Struc. Dynamics*, 9, 187-194.

40. Yamamura, N., and H. Tanaka (1990). "Response analysis of flexible MDF systems for multiple-support seismic excitations." *Earthq. Eng. Struct. Dyn.*, 19, 345-357.

41. Zerva, A. (1990). "Response of multi-span beams to spatially incoherent seismic ground motions." *Earthq. Eng. Struct. Dyn.*, 19, 819-832.

42. Zerva, A. (1991). "Effect of spatial variability and propagation of seismic ground motions on the response of multiply-supported structures." *Probabilistic Eng. Mechanics*, to appear.

43. Zerva, A., A. H-S. Ang and Y.K. Wen (1988). Lifeline response to spatially variable ground motions. *Earthq. Eng. Struc. Dynamics*, 16, 361-379.

APPENDIX A

PEAK FACTORS

Consider a stationary process $X(t)$ having the power spectral density $G(\omega), -\infty < \omega < \infty$. Let

$$\lambda_m = 2\int_0^\infty \omega^m G(\omega)\, d\omega \quad m=0,1,2 \tag{A.1}$$

denote the first three spectral moments. The peak factors p and q relate the mean and standard deviation of the absolute maximum of the process over a duration τ, defined by $X_{\max} = \max_{0\le t\le\tau} |X(t)|$, to the root-mean-square, $\sigma_X = \lambda_0^{1/2}$, of the process through the relations

$$\mu_{X_{\max}} = p\,\sigma_X \quad \text{and} \quad \sigma_{X_{\max}} = q\,\sigma_X \tag{A.2}$$

Approximate expressions for the above peak factors that account for possible narrow bandedness of the process are given by

$$\begin{aligned} p &= 1.253 + 0.209\,\nu_e\tau \qquad 0 \le \nu_e\tau \le 2.1 \\ &= (2\ln\nu_e\tau)^{1/2} + \frac{0.577}{(2\ln\nu_e\tau)^{1/2}} \qquad 2.1 \le \nu_e\tau \le 1000 \end{aligned} \tag{A.3}$$

and

$$\begin{aligned} q &= 0.655 + 0.0016\,\nu_e\tau \qquad 0 \le \nu_e\tau \le 2.1 \\ &= \frac{1.2}{(2\ln\nu_e\tau)^{1/2}} - \frac{5.4}{13+(2\ln\nu_e\tau)^{3.2}} \qquad 2.1 \le \nu_e\tau \le 1000 \end{aligned} \tag{A.4}$$

in which

$$\begin{aligned} \frac{\nu_e}{\nu} &= 2\delta \qquad 0 < \delta \le 0.1 \\ &= (1.63\delta^{0.45} - 0.38) \qquad 0.1 \le \delta \le 0.69 \\ &= 1 \qquad 0.69 \le \delta < 1 \end{aligned} \tag{A.5}$$

with

$$\nu = \frac{1}{\pi}\left(\frac{\lambda_2}{\lambda_0}\right)^{1/2} \quad \text{and} \quad \delta = \left(1 - \frac{\lambda_1^2}{\lambda_0\lambda_2}\right)^{1/2} \tag{A.6}$$

The above expressions for $2.1 \le \nu_e\tau$ were given earlier by Der Kiureghian (1980). The expressions for $\nu_e\tau < 2.1$ are obtained by using a linear interpolation between the value at $\nu_e\tau = 2.1$ and the peak factors relating the mean and standard deviation of $|X(t)|$ to σ_X.

For the response of an oscillator of frequency ω_0 and damping ζ to a white noise base acceleration, $\nu = \omega_0/\pi$ and $\delta \approx 2(\zeta/\pi)^{1/2}$.

EARTHQUAKE ENGINEERING RESEARCH CENTER REPORT SERIES

EERC reports are available from the National Information Service for Earthquake Engineering(NISEE) and from the National Technical Information Service(NTIS). Numbers in parentheses are Accession Numbers assigned by the National Technical Information Service; these are followed by a price code. Contact NTIS, 5285 Port Royal Road, Springfield Virginia, 22161 for more information. Reports without Accession Numbers were not available from NTIS at the time of printing. For a current complete list of EERC reports (from EERC 67-1) and availablity information, please contact University of California, EERC, NISEE, 1301 South 46th Street, Richmond, California 94804.

UCB/EERC-81/01 "Control of Seismic Response of Piping Systems and Other Structures by Base Isolation," by Kelly, J.M., January 1981, (PB81 200 735)A05.

UCB/EERC-81/02 "OPTNSR- An Interactive Software System for Optimal Design of Statically and Dynamically Loaded Structures with Nonlinear Response," by Bhatti, M.A., Ciampi, V. and Pister, K.S., January 1981, (PB81 218 851)A09.

UCB/EERC-81/03 "Analysis of Local Variations in Free Field Seismic Ground Motions," by Chen, J.-C., Lysmer, J. and Seed, H.B., January 1981, (AD-A099508)A13.

UCB/EERC-81/04 "Inelastic Structural Modeling of Braced Offshore Platforms for Seismic Loading," by Zayas, V.A., Shing, P.-S.B., Mahin, S.A. and Popov, E.P., January 1981, INEL4, (PB82 138 777)A07.

UCB/EERC-81/05 "Dynamic Response of Light Equipment in Structures," by Der Kiureghian, A., Sackman, J.L. and Nour-Omid, B., April 1981, (PB81 218 497)A04.

UCB/EERC-81/06 "Preliminary Experimental Investigation of a Broad Base Liquid Storage Tank," by Bouwkamp, J.G., Kollegger, J.P. and Stephen, R.M., May 1981, (PB82 140 385)A03.

UCB/EERC-81/07 "The Seismic Resistant Design of Reinforced Concrete Coupled Structural Walls," by Aktan, A.E. and Bertero, V.V., June 1981, (PB82 113 358)A11.

UCB/EERC-81/08 "Unassigned," by Unassigned, 1981.

UCB/EERC-81/09 "Experimental Behavior of a Spatial Piping System with Steel Energy Absorbers Subjected to a Simulated Differential Seismic Input," by Stiemer, S.F., Godden, W.G. and Kelly, J.M., July 1981, (PB82 201 898)A04.

UCB/EERC-81/10 "Evaluation of Seismic Design Provisions for Masonry in the United States," by Sveinsson, B.I., Mayes, R.L. and McNiven, H.D., August 1981, (PB82 166 075)A08.

UCB/EERC-81/11 "Two-Dimensional Hybrid Modelling of Soil-Structure Interaction," by Tzong, T.-J., Gupta, S. and Penzien, J., August 1981, (PB82 142 118)A04.

UCB/EERC-81/12 "Studies on Effects of Infills in Seismic Resistant R/C Construction," by Brokken, S. and Bertero, V.V., October 1981, (PB82 166 190)A09.

UCB/EERC-81/13 "Linear Models to Predict the Nonlinear Seismic Behavior of a One-Story Steel Frame," by Valdimarsson, H., Shah, A.H. and McNiven, H.D., September 1981, (PB82 138 793)A07.

UCB/EERC-81/14 "TLUSH: A Computer Program for the Three-Dimensional Dynamic Analysis of Earth Dams," by Kagawa, T., Mejia, L.H., Seed, H.B. and Lysmer, J., September 1981, (PB82 139 940)A06.

UCB/EERC-81/15 "Three Dimensional Dynamic Response Analysis of Earth Dams," by Mejia, L.H. and Seed, H.B., September 1981, (PB82 137 274)A12.

UCB/EERC-81/16 "Experimental Study of Lead and Elastomeric Dampers for Base Isolation Systems," by Kelly, J.M. and Hodder, S.B., October 1981, (PB82 166 182)A05.

UCB/EERC-81/17 "The Influence of Base Isolation on the Seismic Response of Light Secondary Equipment," by Kelly, J.M., April 1981, (PB82 255 266)A04.

UCB/EERC-81/18 "Studies on Evaluation of Shaking Table Response Analysis Procedures," by Blondet, J. M., November 1981, (PB82 197 278)A10.

UCB/EERC-81/19 "DELIGHT.STRUCT: A Computer-Aided Design Environment for Structural Engineering," by Balling, R.J., Pister, K.S. and Polak, E., December 1981, (PB82 218 496)A07.

UCB/EERC-81/20 "Optimal Design of Seismic-Resistant Planar Steel Frames," by Balling, R.J., Ciampi, V. and Pister, K.S., December 1981, (PB82 220 179)A07.

UCB/EERC-82/01 "Dynamic Behavior of Ground for Seismic Analysis of Lifeline Systems," by Sato, T. and Der Kiureghian, A., January 1982, (PB82 218 926)A05.

UCB/EERC-82/02 "Shaking Table Tests of a Tubular Steel Frame Model," by Ghanaat, Y. and Clough, R.W., January 1982, (PB82 220 161)A07.

UCB/EERC-82/03 "Behavior of a Piping System under Seismic Excitation: Experimental Investigations of a Spatial Piping System supported by Mechanical Shock Arrestors," by Schneider, S., Lee, H.-M. and Godden, W. G., May 1982, (PB83 172 544)A09.

UCB/EERC-82/04 "New Approaches for the Dynamic Analysis of Large Structural Systems," by Wilson, E.L., June 1982, (PB83 148 080)A05.

UCB/EERC-82/05 "Model Study of Effects of Damage on the Vibration Properties of Steel Offshore Platforms," by Shahrivar, F. and Bouwkamp, J.G., June 1982, (PB83 148 742)A10.

UCB/EERC-82/06 "States of the Art and Pratice in the Optimum Seismic Design and Analytical Response Prediction of R/C Frame Wall Structures," by Aktan, A.E. and Bertero, V.V., July 1982, (PB83 147 736)A05.

UCB/EERC-82/07 "Further Study of the Earthquake Response of a Broad Cylindrical Liquid-Storage Tank Model," by Manos, G.C. and Clough, R.W., July 1982, (PB83 147 744)A11.

UCB/EERC-82/08 "An Evaluation of the Design and Analytical Seismic Response of a Seven Story Reinforced Concrete Frame," by Charney, F.A. and Bertero, V.V., July 1982, (PB83 157 628)A09.

UCB/EERC-82/09 "Fluid-Structure Interactions: Added Mass Computations for Incompressible Fluid," by Kuo, J.S.-H., August 1982, (PB83 156 281)A07.

UCB/EERC-82/10 "Joint-Opening Nonlinear Mechanism: Interface Smeared Crack Model," by Kuo, J.S.-H., August 1982, (PB83 149 195)A05.

UCB/EERC-82/11 "Dynamic Response Analysis of Techi Dam," by Clough, R.W., Stephen, R.M. and Kuo, J.S.-H., August 1982, (PB83 147 496)A06.

UCB/EERC-82/12 "Prediction of the Seismic Response of R/C Frame-Coupled Wall Structures," by Aktan, A.E., Bertero, V.V. and Piazzo, M., August 1982, (PB83 149 203)A09.

UCB/EERC-82/13 "Preliminary Report on the Smart 1 Strong Motion Array in Taiwan," by Bolt, B.A., Loh, C.H., Penzien, J. and Tsai, Y.B., August 1982, (PB83 159 400)A10.

UCB/EERC-82/14 "Seismic Behavior of an Eccentrically X-Braced Steel Structure," by Yang, M.S., September 1982, (PB83 260 778)A12.

UCB/EERC-82/15 "The Performance of Stairways in Earthquakes," by Roha, C., Axley, J.W. and Bertero, V.V., September 1982, (PB83 157 693)A07.

UCB/EERC-82/16 "The Behavior of Submerged Multiple Bodies in Earthquakes," by Liao, W.-G., September 1982, (PB83 158 709)A07.

UCB/EERC-82/17 "Effects of Concrete Types and Loading Conditions on Local Bond-Slip Relationships," by Cowell, A.D., Popov, E.P. and Bertero, V.V., September 1982, (PB83 153 577)A04.

UCB/EERC-82/18 "Mechanical Behavior of Shear Wall Vertical Boundary Members: An Experimental Investigation," by Wagner, M.T. and Bertero, V.V., October 1982, (PB83 159 764)A05.

UCB/EERC-82/19 "Experimental Studies of Multi-support Seismic Loading on Piping Systems," by Kelly, J.M. and Cowell, A.D., November 1982, (PB90 262 684)A07.

UCB/EERC-82/20 "Generalized Plastic Hinge Concepts for 3D Beam-Column Elements," by Chen, P. F.-S. and Powell, G.H., November 1982, (PB83 247 981)A13.

UCB/EERC-82/21 "ANSR-II: General Computer Program for Nonlinear Structural Analysis," by Oughourlian, C.V. and Powell, G.H., November 1982, (PB83 251 330)A12.

UCB/EERC-82/22 "Solution Strategies for Statically Loaded Nonlinear Structures," by Simons, J.W. and Powell, G.H., November 1982, (PB83 197 970)A06.

UCB/EERC-82/23 "Analytical Model of Deformed Bar Anchorages under Generalized Excitations," by Ciampi, V., Eligehausen, R., Bertero, V.V. and Popov, E.P., November 1982, (PB83 169 532)A06.

UCB/EERC-82/24 "A Mathematical Model for the Response of Masonry Walls to Dynamic Excitations," by Sucuoglu, H., Mengi, Y. and McNiven, H.D., November 1982, (PB83 169 011)A07.

UCB/EERC-82/25 "Earthquake Response Considerations of Broad Liquid Storage Tanks," by Cambra, F.J., November 1982, (PB83 251 215)A09.

UCB/EERC-82/26 "Computational Models for Cyclic Plasticity, Rate Dependence and Creep," by Mosaddad, B. and Powell, G.H., November 1982, (PB83 245 829)A08.

UCB/EERC-82/27 "Inelastic Analysis of Piping and Tubular Structures," by Mahasuverachai, M. and Powell, G.H., November 1982, (PB83 249 987)A07.

UCB/EERC-83/01 "The Economic Feasibility of Seismic Rehabilitation of Buildings by Base Isolation," by Kelly, J.M., January 1983, (PB83 197 988)A05.

UCB/EERC-83/02 "Seismic Moment Connections for Moment-Resisting Steel Frames.," by Popov, E.P., January 1983, (PB83 195 412)A04.

UCB/EERC-83/03 "Design of Links and Beam-to-Column Connections for Eccentrically Braced Steel Frames," by Popov, E.P. and Malley, J.O., January 1983, (PB83 194 811)A04.

UCB/EERC-83/04 "Numerical Techniques for the Evaluation of Soil-Structure Interaction Effects in the Time Domain," by Bayo, E. and Wilson, E.L., February 1983, (PB83 245 605)A09.

UCB/EERC-83/05 "A Transducer for Measuring the Internal Forces in the Columns of a Frame-Wall Reinforced Concrete Structure," by Sause, R. and Bertero, V.V., May 1983, (PB84 119 494)A06.

UCB/EERC-83/06 "Dynamic Interactions Between Floating Ice and Offshore Structures," by Croteau, P., May 1983, (PB84 119 486)A16.

UCB/EERC-83/07 "Dynamic Analysis of Multiply Tuned and Arbitrarily Supported Secondary Systems," by Igusa, T. and Der Kiureghian, A., July 1983, (PB84 118 272)A11.

UCB/EERC-83/08 "A Laboratory Study of Submerged Multi-body Systems in Earthquakes," by Ansari, G.R., June 1983, (PB83 261 842)A17.

UCB/EERC-83/09 "Effects of Transient Foundation Uplift on Earthquake Response of Structures," by Yim, C.-S. and Chopra, A.K., June 1983, (PB83 261 396)A07.

UCB/EERC-83/10 "Optimal Design of Friction-Braced Frames under Seismic Loading," by Austin, M.A. and Pister, K.S., June 1983, (PB84 119 288)A06.

UCB/EERC-83/11 "Shaking Table Study of Single-Story Masonry Houses: Dynamic Performance under Three Component Seismic Input and Recommendations," by Manos, G.C., Clough, R.W. and Mayes, R.L., July 1983, (UCB/EERC-83/11)A08.

UCB/EERC-83/12 "Experimental Error Propagation in Pseudodynamic Testing," by Shiing, P.B. and Mahin, S.A., June 1983, (PB84 119 270)A09.

UCB/EERC-83/13 "Experimental and Analytical Predictions of the Mechanical Characteristics of a 1/5-scale Model of a 7-story R/C Frame-Wall Building Structure," by Aktan, A.E., Bertero, V.V., Chowdhury, A.A. and Nagashima, T., June 1983, (PB84 119 213)A07.

UCB/EERC-83/14 "Shaking Table Tests of Large-Panel Precast Concrete Building System Assemblages," by Oliva, M.G. and Clough, R.W., June 1983, (PB86 110 210/AS)A11.

UCB/EERC-83/15 "Seismic Behavior of Active Beam Links in Eccentrically Braced Frames," by Hjelmstad, K.D. and Popov, E.P., July 1983, (PB84 119 676)A09.

UCB/EERC-83/16 "System Identification of Structures with Joint Rotation," by Dimsdale, J.S., July 1983, (PB84 192 210)A06.

UCB/EERC-83/17 "Construction of Inelastic Response Spectra for Single-Degree-of-Freedom Systems," by Mahin, S. and Lin, J., June 1983, (PB84 208 834)A05.

UCB/EERC-83/18 "Interactive Computer Analysis Methods for Predicting the Inelastic Cyclic Behaviour of Structural Sections," by Kaba, S. and Mahin, S., July 1983, (PB84 192 012)A06.

UCB/EERC-83/19 "Effects of Bond Deterioration on Hysteretic Behavior of Reinforced Concrete Joints," by Filippou, F.C., Popov, E.P. and Bertero, V.V., August 1983, (PB84 192 020)A10.

UCB/EERC-83/20 "Correlation of Analytical and Experimental Responses of Large-Panel Precast Building Systems," by Oliva, M.G., Clough, R.W., Velkov, M. and Gavrilovic, P., May 1988, (PB90 262 692)A06.

UCB/EERC-83/21 "Mechanical Characteristics of Materials Used in a 1/5 Scale Model of a 7-Story Reinforced Concrete Test Structure," by Bertero, V.V., Aktan, A.E., Harris, H.G. and Chowdhury, A.A., October 1983, (PB84 193 697)A05.

UCB/EERC-83/22 "Hybrid Modelling of Soil-Structure Interaction in Layered Media," by Tzong, T.-J. and Penzien, J., October 1983, (PB84 192 178)A08.

UCB/EERC-83/23 "Local Bond Stress-Slip Relationships of Deformed Bars under Generalized Excitations," by Eligehausen, R., Popov, E.P. and Bertero, V.V., October 1983, (PB84 192 848)A09.

UCB/EERC-83/24 "Design Considerations for Shear Links in Eccentrically Braced Frames," by Malley, J.O. and Popov, E.P., November 1983, (PB84 192 186)A07.

UCB/EERC-84/01 "Pseudodynamic Test Method for Seismic Performance Evaluation: Theory and Implementation," by Shing, P.-S.B. and Mahin, S.A., January 1984, (PB84 190 644)A08.

UCB/EERC-84/02 "Dynamic Response Behavior of Kiang Hong Dian Dam," by Clough, R.W., Chang, K.-T., Chen, H.-Q. and Stephen, R.M., April 1984, (PB84 209 402)A08.

UCB/EERC-84/03 "Refined Modelling of Reinforced Concrete Columns for Seismic Analysis," by Kaba, S.A. and Mahin, S.A., April 1984, (PB84 234 384)A06.

UCB/EERC-84/04 "A New Floor Response Spectrum Method for Seismic Analysis of Multiply Supported Secondary Systems," by Asfura, A. and Der Kiureghian, A., June 1984, (PB84 239 417)A06.

UCB/EERC-84/05 "Earthquake Simulation Tests and Associated Studies of a 1/5th-scale Model of a 7-Story R/C Frame-Wall Test Structure," by Bertero, V.V., Aktan, A.E., Charney, F.A. and Sause, R., June 1984, (PB84 239 409)A09.

UCB/EERC-84/06 "Unassigned," by Unassigned, 1984.

UCB/EERC-84/07 "Behavior of Interior and Exterior Flat-Plate Connections subjected to Inelastic Load Reversals," by Zee, H.L. and Moehle, J.P., August 1984, (PB86 117 629/AS)A07.

UCB/EERC-84/08 "Experimental Study of the Seismic Behavior of a Two-Story Flat-Plate Structure," by Moehle, J.P. and Diebold, J.W., August 1984, (PB86 122 553/AS)A12.

UCB/EERC-84/09 "Phenomenological Modeling of Steel Braces under Cyclic Loading," by Ikeda, K., Mahin, S.A. and Dermitzakis, S.N., May 1984, (PB86 132 198/AS)A08.

UCB/EERC-84/10 "Earthquake Analysis and Response of Concrete Gravity Dams," by Fenves, G. and Chopra, A.K., August 1984, (PB85 193 902/AS)A11.

UCB/EERC-84/11 "EAGD-84: A Computer Program for Earthquake Analysis of Concrete Gravity Dams," by Fenves, G. and Chopra, A.K., August 1984, (PB85 193 613/AS)A05.

UCB/EERC-84/12 "A Refined Physical Theory Model for Predicting the Seismic Behavior of Braced Steel Frames," by Ikeda, K. and Mahin, S.A., July 1984, (PB85 191 450/AS)A09.

UCB/EERC-84/13 "Earthquake Engineering Research at Berkeley - 1984," by EERC, August 1984, (PB85 197 341/AS)A10.

UCB/EERC-84/14 "Moduli and Damping Factors for Dynamic Analyses of Cohesionless Soils," by Seed, H.B., Wong, R.T., Idriss, I.M. and Tokimatsu, K., September 1984, (PB85 191 468/AS)A04.

UCB/EERC-84/15 "The Influence of SPT Procedures in Soil Liquefaction Resistance Evaluations," by Seed, H.B., Tokimatsu, K., Harder, L.F. and Chung, R.M., October 1984, (PB85 191 732/AS)A04.

UCB/EERC-84/16 "Simplified Procedures for the Evaluation of Settlements in Sands Due to Earthquake Shaking," by Tokimatsu, K. and Seed, H.B., October 1984, (PB85 197 887/AS)A03.

UCB/EERC-84/17 "Evaluation of Energy Absorption Characteristics of Highway Bridges Under Seismic Conditions - Volume I (PB90 262 627)A16 and Volume II (Appendices) (PB90 262 635)A13," by Imbsen, R.A. and Penzien, J., September 1986.

UCB/EERC-84/18 "Structure-Foundation Interactions under Dynamic Loads," by Liu, W.D. and Penzien, J., November 1984, (PB87 124 889/AS)A11.

UCB/EERC-84/19 "Seismic Modelling of Deep Foundations," by Chen, C.-H. and Penzien, J., November 1984, (PB87 124 798/AS)A07.

UCB/EERC-84/20 "Dynamic Response Behavior of Quan Shui Dam," by Clough, R.W., Chang, K.-T., Chen, H.-Q., Stephen, R.M., Ghanaat, Y. and Qi, J.-H., November 1984, (PB86 115177/AS)A07.

UCB/EERC-85/01 "Simplified Methods of Analysis for Earthquake Resistant Design of Buildings," by Cruz, E.F. and Chopra, A.K., February 1985, (PB86 112299/AS)A12.

UCB/EERC-85/02 "Estimation of Seismic Wave Coherency and Rupture Velocity using the SMART 1 Strong-Motion Array Recordings," by Abrahamson, N.A., March 1985, (PB86 214 343)A07.

UCB/EERC-85/03 "Dynamic Properties of a Thirty Story Condominium Tower Building," by Stephen, R.M., Wilson, E.L. and Stander, N., April 1985, (PB86 118965/AS)A06.

UCB/EERC-85/04 "Development of Substructuring Techniques for On-Line Computer Controlled Seismic Performance Testing," by Dermitzakis, S. and Mahin, S., February 1985, (PB86 132941/AS)A08.

UCB/EERC-85/05 "A Simple Model for Reinforcing Bar Anchorages under Cyclic Excitations," by Filippou, F.C., March 1985, (PB86 112 919/AS)A05.

UCB/EERC-85/06 "Racking Behavior of Wood-framed Gypsum Panels under Dynamic Load," by Oliva, M.G., June 1985, (PB90 262 643)A04.

UCB/EERC-85/07 "Earthquake Analysis and Response of Concrete Arch Dams," by Fok, K.-L. and Chopra, A.K., June 1985, (PB86 139672/AS)A10.

UCB/EERC-85/08 "Effect of Inelastic Behavior on the Analysis and Design of Earthquake Resistant Structures," by Lin, J.P. and Mahin, S.A., June 1985, (PB86 135340/AS)A08.

UCB/EERC-85/09 "Earthquake Simulator Testing of a Base-Isolated Bridge Deck," by Kelly, J.M., Buckle, I.G. and Tsai, H.-C., January 1986, (PB87 124 152/AS)A06.

UCB/EERC-85/10 "Simplified Analysis for Earthquake Resistant Design of Concrete Gravity Dams," by Fenves, G. and Chopra, A.K., June 1986, (PB87 124 160/AS)A08.

UCB/EERC-85/11 "Dynamic Interaction Effects in Arch Dams," by Clough, R.W., Chang, K.-T., Chen, H.-Q. and Ghanaat, Y., October 1985, (PB86 135027/AS)A05.

UCB/EERC-85/12 "Dynamic Response of Long Valley Dam in the Mammoth Lake Earthquake Series of May 25-27, 1980," by Lai, S. and Seed, H.B., November 1985, (PB86 142304/AS)A05.

UCB/EERC-85/13 "A Methodology for Computer-Aided Design of Earthquake-Resistant Steel Structures," by Austin, M.A., Pister, K.S. and Mahin, S.A., December 1985, (PB86 159480/AS)A10 .

UCB/EERC-85/14 "Response of Tension-Leg Platforms to Vertical Seismic Excitations," by Liou, G.-S., Penzien, J. and Yeung, R.W., December 1985, (PB87 124 871/AS)A08.

UCB/EERC-85/15 "Cyclic Loading Tests of Masonry Single Piers: Volume 4 - Additional Tests with Height to Width Ratio of 1," by Sveinsson, B., McNiven, H.D. and Sucuoglu, H., December 1985.

UCB/EERC-85/16 "An Experimental Program for Studying the Dynamic Response of a Steel Frame with a Variety of Infill Partitions," by Yanev, B. and McNiven, H.D., December 1985, (PB90 262 676)A05.

UCB/EERC-86/01 "A Study of Seismically Resistant Eccentrically Braced Steel Frame Systems," by Kasai, K. and Popov, E.P., January 1986, (PB87 124 178/AS)A14.

UCB/EERC-86/02 "Design Problems in Soil Liquefaction," by Seed, H.B., February 1986, (PB87 124 186/AS)A03.

UCB/EERC-86/03 "Implications of Recent Earthquakes and Research on Earthquake-Resistant Design and Construction of Buildings," by Bertero, V.V., March 1986, (PB87 124 194/AS)A05.

UCB/EERC-86/04 "The Use of Load Dependent Vectors for Dynamic and Earthquake Analyses," by Leger, P., Wilson, E.L. and Clough, R.W., March 1986, (PB87 124 202/AS)A12.

UCB/EERC-86/05 "Two Beam-To-Column Web Connections," by Tsai, K.-C. and Popov, E.P., April 1986, (PB87 124 301/AS)A04.

UCB/EERC-86/06 "Determination of Penetration Resistance for Coarse-Grained Soils using the Becker Hammer Drill," by Harder, L.F. and Seed, H.B., May 1986, (PB87 124 210/AS)A07.

UCB/EERC-86/07 "A Mathematical Model for Predicting the Nonlinear Response of Unreinforced Masonry Walls to In-Plane Earthquake Excitations," by Mengi, Y. and McNiven, H.D., May 1986, (PB87 124 780/AS)A06.

UCB/EERC-86/08 "The 19 September 1985 Mexico Earthquake: Building Behavior," by Bertero, V.V., July 1986.

UCB/EERC-86/09 "EACD-3D: A Computer Program for Three-Dimensional Earthquake Analysis of Concrete Dams," by Fok, K.-L., Hall, J.F. and Chopra, A.K., July 1986, (PB87 124 228/AS)A08.

UCB/EERC-86/10 "Earthquake Simulation Tests and Associated Studies of a 0.3-Scale Model of a Six-Story Concentrically Braced Steel Structure," by Uang, C.-M. and Bertero, V.V., December 1986, (PB87 163 564/AS)A17.

UCB/EERC-86/11 "Mechanical Characteristics of Base Isolation Bearings for a Bridge Deck Model Test," by Kelly, J.M., Buckle, I.G. and Koh, C.-G., November 1987, (PB90 262 668)A04.

UCB/EERC-86/12 "Effects of Axial Load on Elastomeric Isolation Bearings," by Koh, C.-G. and Kelly, J.M., November 1987.

UCB/EERC-87/01 "The FPS Earthquake Resisting System: Experimental Report," by Zayas, V.A., Low, S.S. and Mahin, S.A., June 1987.

UCB/EERC-87/02 "Earthquake Simulator Tests and Associated Studies of a 0.3-Scale Model of a Six-Story Eccentrically Braced Steel Structure," by Whittaker, A., Uang, C.-M. and Bertero, V.V., July 1987.

UCB/EERC-87/03 "A Displacement Control and Uplift Restraint Device for Base-Isolated Structures," by Kelly, J.M., Griffith, M.C. and Aiken, I.D., April 1987.

UCB/EERC-87/04 "Earthquake Simulator Testing of a Combined Sliding Bearing and Rubber Bearing Isolation System," by Kelly, J.M. and Chalhoub, M.S., 1987.

UCB/EERC-87/05 "Three-Dimensional Inelastic Analysis of Reinforced Concrete Frame-Wall Structures," by Moazzami, S. and Bertero, V.V., May 1987.

UCB/EERC-87/06 "Experiments on Eccentrically Braced Frames with Composite Floors," by Ricles, J. and Popov, E., June 1987.

UCB/EERC-87/07 "Dynamic Analysis of Seismically Resistant Eccentrically Braced Frames," by Ricles, J. and Popov, E., June 1987.

UCB/EERC-87/08 "Undrained Cyclic Triaxial Testing of Gravels-The Effect of Membrane Compliance," by Evans, M.D. and Seed, H.B., July 1987.

UCB/EERC-87/09 "Hybrid Solution Techniques for Generalized Pseudo-Dynamic Testing," by Thewalt, C. and Mahin, S.A., July 1987.

UCB/EERC-87/10 "Ultimate Behavior of Butt Welded Splices in Heavy Rolled Steel Sections," by Bruneau, M., Mahin, S.A. and Popov, E.P., September 1987.

UCB/EERC-87/11 "Residual Strength of Sand from Dam Failures in the Chilean Earthquake of March 3, 1985," by De Alba, P., Seed, H.B., Retamal, E. and Seed, R.B., September 1987.

UCB/EERC-87/12 "Inelastic Seismic Response of Structures with Mass or Stiffness Eccentricities in Plan," by Bruneau, M. and Mahin, S.A., September 1987, (PB90 262 650)A14.

UCB/EERC-87/13 "CSTRUCT: An Interactive Computer Environment for the Design and Analysis of Earthquake Resistant Steel Structures," by Austin, M.A., Mahin, S.A. and Pister, K.S., September 1987.

UCB/EERC-87/14 "Experimental Study of Reinforced Concrete Columns Subjected to Multi-Axial Loading," by Low, S.S. and Moehle, J.P., September 1987.

UCB/EERC-87/15 "Relationships between Soil Conditions and Earthquake Ground Motions in Mexico City in the Earthquake of Sept. 19, 1985," by Seed, H.B., Romo, M.P., Sun, J., Jaime, A. and Lysmer, J., October 1987.

UCB/EERC-87/16 "Experimental Study of Seismic Response of R. C. Setback Buildings," by Shahrooz, B.M. and Moehle, J.P., October 1987.

UCB/EERC-87/17 "The Effect of Slabs on the Flexural Behavior of Beams," by Pantazopoulou, S.J. and Moehle, J.P., October 1987, (PB90 262 700)A07.

UCB/EERC-87/18 "Design Procedure for R-FBI Bearings," by Mostaghel, N. and Kelly, J.M., November 1987, (PB90 262 718)A04.

UCB/EERC-87/19 "Analytical Models for Predicting the Lateral Response of R C Shear Walls: Evaluation of their Reliability," by Vulcano, A. and Bertero, V.V., November 1987.

UCB/EERC-87/20 "Earthquake Response of Torsionally-Coupled Buildings," by Hejal, R. and Chopra, A.K., December 1987.

UCB/EERC-87/21 "Dynamic Reservoir Interaction with Monticello Dam," by Clough, R.W., Ghanaat, Y. and Qiu, X-F., December 1987.

UCB/EERC-87/22 "Strength Evaluation of Coarse-Grained Soils," by Siddiqi, F.H., Seed, R.B., Chan, C.K., Seed, H.B. and Pyke, R.M., December 1987.

UCB/EERC-88/01 "Seismic Behavior of Concentrically Braced Steel Frames," by Khatib, I., Mahin, S.A. and Pister, K.S., January 1988.

UCB/EERC-88/02 "Experimental Evaluation of Seismic Isolation of Medium-Rise Structures Subject to Uplift," by Griffith, M.C., Kelly, J.M., Coveney, V.A. and Koh, C.G., January 1988.

UCB/EERC-88/03 "Cyclic Behavior of Steel Double Angle Connections," by Astaneh-Asl, A. and Nader, M.N., January 1988.

UCB/EERC-88/04 "Re-evaluation of the Slide in the Lower San Fernando Dam in the Earthquake of Feb. 9, 1971," by Seed, H.B., Seed, R.B., Harder, L.F. and Jong, H.-L., April 1988.

UCB/EERC-88/05 "Experimental Evaluation of Seismic Isolation of a Nine-Story Braced Steel Frame Subject to Uplift," by Griffith, M.C., Kelly, J.M. and Aiken, I.D., May 1988.

UCB/EERC-88/06 "DRAIN-2DX User Guide.," by Allahabadi, R. and Powell, G.H., March 1988.

UCB/EERC-88/07 "Theoretical and Experimental Studies of Cylindrical Water Tanks in Base-Isolated Structures," by Chalhoub, M.S. and Kelly, J.M., April 1988.

UCB/EERC-88/08 "Analysis of Near-Source Waves: Separation of Wave Types using Strong Motion Array Recordings," by Darragh, R.B., June 1988.

UCB/EERC-88/09 "Alternatives to Standard Mode Superposition for Analysis of Non-Classically Damped Systems," by Kusainov, A.A. and Clough, R.W., June 1988.

UCB/EERC-88/10 "The Landslide at the Port of Nice on October 16, 1979," by Seed, H.B., Seed, R.B., Schlosser, F., Blondeau, F. and Juran, I., June 1988.

UCB/EERC-88/11 "Liquefaction Potential of Sand Deposits Under Low Levels of Excitation," by Carter, D.P. and Seed, H.B., August 1988.

UCB/EERC-88/12 "Nonlinear Analysis of Reinforced Concrete Frames Under Cyclic Load Reversals," by Filippou, F.C. and Issa, A., September 1988.

UCB/EERC-88/13 "Implications of Recorded Earthquake Ground Motions on Seismic Design of Building Structures," by Uang, C.-M. and Bertero, V.V., November 1988.

UCB/EERC-88/14 "An Experimental Study of the Behavior of Dual Steel Systems," by Whittaker, A.S. , Uang, C.-M. and Bertero, V.V., September 1988.

UCB/EERC-88/15 "Dynamic Moduli and Damping Ratios for Cohesive Soils," by Sun, J.I., Golesorkhi, R. and Seed, H.B., August 1988.

UCB/EERC-88/16 "Reinforced Concrete Flat Plates Under Lateral Load: An Experimental Study Including Biaxial Effects," by Pan, A. and Moehle, J., October 1988.

UCB/EERC-88/17 "Earthquake Engineering Research at Berkeley - 1988," by EERC, November 1988.

UCB/EERC-88/18 "Use of Energy as a Design Criterion in Earthquake-Resistant Design," by Uang, C.-M. and Bertero, V.V., November 1988.

UCB/EERC-88/19 "Steel Beam-Column Joints in Seismic Moment Resisting Frames," by Tsai, K.-C. and Popov, E.P., November 1988.

UCB/EERC-88/20 "Base Isolation in Japan, 1988," by Kelly, J.M., December 1988.

UCB/EERC-89/01 "Behavior of Long Links in Eccentrically Braced Frames," by Engelhardt, M.D. and Popov, E.P., January 1989.

UCB/EERC-89/02 "Earthquake Simulator Testing of Steel Plate Added Damping and Stiffness Elements," by Whittaker, A., Bertero, V.V., Alonso, J. and Thompson, C., January 1989.

UCB/EERC-89/03 "Implications of Site Effects in the Mexico City Earthquake of Sept. 19, 1985 for Earthquake-Resistant Design Criteria in the San Francisco Bay Area of California," by Seed, H.B. and Sun, J.I., March 1989.

UCB/EERC-89/04 "Earthquake Analysis and Response of Intake-Outlet Towers," by Goyal, A. and Chopra, A.K., July 1989.

UCB/EERC-89/05 "The 1985 Chile Earthquake: An Evaluation of Structural Requirements for Bearing Wall Buildings," by Wallace, J.W. and Moehle, J.P., July 1989.

UCB/EERC-89/06 "Effects of Spatial Variation of Ground Motions on Large Multiply-Supported Structures," by Hao, H., July 1989.

UCB/EERC-89/07 "EADAP - Enhanced Arch Dam Analysis Program: Users's Manual," by Ghanaat, Y. and Clough, R.W., August 1989.

UCB/EERC-89/08 "Seismic Performance of Steel Moment Frames Plastically Designed by Least Squares Stress Fields," by Ohi, K. and Mahin, S.A., August 1989.

UCB/EERC-89/09 "Feasibility and Performance Studies on Improving the Earthquake Resistance of New and Existing Buildings Using the Friction Pendulum System," by Zayas, V., Low, S., Mahin, S.A. and Bozzo, L., July 1989.

UCB/EERC-89/10 "Measurement and Elimination of Membrane Compliance Effects in Undrained Triaxial Testing," by Nicholson, P.G., Seed, R.B. and Anwar, H., September 1989.

UCB/EERC-89/11 "Static Tilt Behavior of Unanchored Cylindrical Tanks," by Lau, D.T. and Clough, R.W., September 1989.

UCB/EERC-89/12 "ADAP-88: A Computer Program for Nonlinear Earthquake Analysis of Concrete Arch Dams," by Fenves, G.L., Mojtahedi, S. and Reimer, R.B., September 1989.

UCB/EERC-89/13 "Mechanics of Low Shape Factor Elastomeric Seismic Isolation Bearings," by Aiken, I.D., Kelly, J.M. and Tajirian, F.F., November 1989.

UCB/EERC-89/14 "Preliminary Report on the Seismological and Engineering Aspects of the October 17, 1989 Santa Cruz (Loma Prieta) Earthquake," by EERC, October 1989.

UCB/EERC-89/15 "Experimental Studies of a Single Story Steel Structure Tested with Fixed, Semi-Rigid and Flexible Connections," by Nader, M.N. and Astaneh-Asl, A., August 1989.

UCB/EERC-89/16 "Collapse of the Cypress Street Viaduct as a Result of the Loma Prieta Earthquake," by Nims, D.K., Miranda, E., Aiken, I.D., Whittaker, A.S. and Bertero, V.V., November 1989.

UCB/EERC-90/01 "Mechanics of High-Shape Factor Elastomeric Seismic Isolation Bearings," by Kelly, J.M., Aiken, I.D. and Tajirian, F.F., March 1990.

UCB/EERC-90/02 "Javid's Paradox: The Influence of Preform on the Modes of Vibrating Beams," by Kelly, J.M., Sackman, J.L. and Javid, A., May 1990.

UCB/EERC-90/03 "Earthquake Simulator Testing and Analytical Studies of Two Energy-Absorbing Systems for Multistory Structures," by Aiken, I.D. and Kelly, J.M., October 1990.

UCB/EERC-90/04 "Damage to the San Francisco-Oakland Bay Bridge During the October 17, 1989 Earthquake," by Astaneh, A., June 1990.

UCB/EERC-90/05 "Preliminary Report on the Principal Geotechnical Aspects of the October 17, 1989 Loma Prieta Earthquake," by Seed, R.B., Dickenson, S.E., Riemer, M.F., Bray, J.D., Sitar, N., Mitchell, J.K., Idriss, I.M., Kayen, R.E., Kropp, A., Harder, L.F., Jr. and Power, M.S., April 1990.

UCB/EERC-90/06 "Models of Critical Regions in Reinforced Concrete Frames Under Seismic Excitations," by Zulfiqar, N. and Filippou, F., May 1990.

UCB/EERC-90/07 "A Unified Earthquake-Resistant Design Method for Steel Frames Using ARMA Models," by Takewaki, I., Conte, J.P., Mahin, S.A. and Pister, K.S., June 1990.

UCB/EERC-90/08 "Soil Conditions and Earthquake Hazard Mitigation in the Marina District of San Francisco," by Mitchell, J.K., Masood, T., Kayen, R.E. and Seed, R.B., May 1990.

UCB/EERC-90/09 "Influence of the Earthquake Ground Motion Process and Structural Properties on Response Characteristics of Simple Structures," by Conte, J.P., Pister, K.S. and Mahin, S.A., July 1990.

UCB/EERC-90/10 "Experimental Testing of the Resilient-Friction Base Isolation System," by Clark, P.W. and Kelly, J.M., July 1990.

UCB/EERC-90/11 "Seismic Hazard Analysis: Improved Models, Uncertainties and Sensitivities," by Araya, R. and Der Kiureghian, A., March 1988.

UCB/EERC-90/12 "Effects of Torsion on the Linear and Nonlinear Seismic Response of Structures," by Sedarat, H. and Bertero, V.V., September 1989.

UCB/EERC-90/13 "The Effects of Tectonic Movements on Stresses and Deformations in Earth Embankments," by Bray, J. D., Seed, R. B. and Seed, H. B., September 1989.

UCB/EERC-90/14 "Inelastic Seismic Response of One-Story, Asymmetric-Plan Systems," by Goel, R.K. and Chopra, A.K., October 1990.

UCB/EERC-90/15 "Dynamic Crack Propagation: A Model for Near-Field Ground Motion.," by Seyyedian, H. and Kelly, J.M., 1990.

UCB/EERC-90/16 "Sensitivity of Long-Period Response Spectra to System Initial Conditions," by Blasquez, R., Ventura, C. and Kelly, J.M., 1990.

UCB/EERC-90/17 "Behavior of Peak Values and Spectral Ordinates of Near-Source Strong Ground-Motion over a Dense Array," by Niazi, M., June 1990.

UCB/EERC-90/18 "Material Characterization of Elastomers used in Earthquake Base Isolation," by Papoulia, K.D. and Kelly, J.M., 1990.

UCB/EERC-90/19 "Cyclic Behavior of Steel Top-and-Bottom Plate Moment Connections," by Harriott, J.D. and Astaneh, A., August 1990.

UCB/EERC-90/20 "Seismic Response Evaluation of an Instrumented Six Story Steel Building," by Shen, J.-H. and Astaneh, A., December 1990.

UCB/EERC-90/21 "Observations and Implications of Tests on the Cypress Street Viaduct Test Structure," by Bollo, M., Mahin, S.A., Moehle, J.P., Stephen, R.M. and Qi, X., December 1990.

UCB/EERC-91/01 "Experimental Evaluation of Nitinol for Energy Dissipation in Structures," by Nims, D.K., Sasaki, K.K. and Kelly, J.M., 1991.

UCB/EERC-91/02 "Displacement Design Approach for Reinforced Concrete Structures Subjected to Earthquakes," by Qi, X. and Moehle, J.P., January 1991.

UCB/EERC-91/03 "Shake Table Tests of Long Period Isolation System for Nuclear Facilities at Soft Soil Sites," by Kelly, J.M., March 1991.

UCB/EERC-91/04 "Dynamic and Failure Characteristics of Bridgestone Isolation Bearings," by Kelly, J.M., April 1991.

UCB/EERC-91/05 "Base Sliding Response of Concrete Gravity Dams to Earthquakes," by Chopra, A.K. and Zhang, L., May 1991.

UCB/EERC-91/06 "Computation of Spatially Varying Ground Motion and Foundation-Rock Impedance Matrices for Seismic Analysis of Arch Dams," by Zhang, L. and Chopra, A.K., May 1991.

UCB/EERC-91/07 "Estimation of Seismic Source Processes Using Strong Motion Array Data," by Chiou, S.-J., July 1991.

UCB/EERC-91/08 "A Response Spectrum Method for Multiple-Support Seismic Excitations," by Der Kiureghian, A. and Neuenhofer, A., August 1991